

**Effects of Axial Ligands on the Photosensitising
Properties of Silicon
Octaphenoxyphthalocyanines**

A thesis submitted in fulfilment of the requirements for the degree

Doctor of Philosophy

of

Rhodes University

by

Machiel David Maree

November 2001

Acknowledgments

I would firstly like to thank my supervisor, Prof. Tebello Nyokong for her leadership during this study and also for her efforts in the preparation of this manuscript.

Collectively to the postgraduate students for their friendship and advice over the last 3 years.

Thanks are also due to family, my mother and grandparents, as well as my wife, Suzanne, to which this thesis is dedicated in appreciation for all the support moral and otherwise.

Financial assistance came in the form of an NRF scholarship as well as an EPSRC grant.

David Maree
2001

Abstract

Various axially substituted Silicon octaphenoxypthalocyanines were synthesised as potential photosensitisers in the photodynamic therapy of cancer. Conventional reflux reactions were used for synthesis as well as new microwave irradiation reactions, wherein the reaction times were decreased tenfold with a marginal increase in reaction yield and product purity. An interesting series of oligomeric (dimer to a nonamer) silicon octaphenoxypthalocyanines were also successfully synthesised in a reaction similar to polymerisation reactions.

These compounds were found to undergo an axial ligand transformation upon irradiation with red light (> 600 nm) in dimethylsulphoxide solution. All the ligands were transformed into the dihydroxy silicon octaphenoxypthalocyanine with varying degrees of phototransformation quantum yields ranging in order from 10^{-3} to 10^{-5} depending on the axial ligand involved. During and after axial ligand transformations a photodegradation of the dihydroxy silicon octaphenoxypthalocyanine was observed upon continued irradiation. The oligomers were found to undergo the same axial ligand transformation process with a phototransformation quantum yield of 10^{-5} .

The singlet oxygen quantum yields of the unaggregated monomeric silicon octaphenoxypthalocyanines were all found to be approximately 0.2 with the exception of a compound with two (trihexyl)siloxy axial substituents that had a singlet oxygen quantum yield of approximately 0.4 in dimethylsulphoxide

solutions. The oligomers showed a surprising trend of an increase in singlet oxygen quantum yield with an increase in phthalocyanine ring number up to the pentamer and then a dramatic decrease to the nonamer.

The triplet quantum yield and triplet lifetime were determined by laser flash photolysis for selected compounds and no correlation was observed with any of these properties and the singlet oxygen quantum yields. These selected compounds all fluoresce and a very good correlation was found between the fluorescence lifetimes determined experimentally by laser photolysis and the Strickler-Berg equation for the non-aggregated compounds.

Electrochemical measurements also indicate the importance of the axial ligands upon the behaviour of the phthalocyanines as cyclic voltammetric behaviour was determined by the nature of the axial ligand.

Table of contents

List of Symbols and Abbreviations	ix
List of Figures	xi
List of Schemes	xiv
List of Tables	xvi
General introduction	1
Chapter 1 Introduction	3
1.1 General phthalocyanine synthesis	3
1.2 Synthesis of silicon phthalocyanines	5
1.3 Peripheral phthalocyanine substitution	8
1.3.1 Phthalonitrile derivitization	8
1.4 Axial modification of phthalocyanines	13
1.4.1 Coordinative axially substituted phthalocyanines	13
1.4.2 Axially substituted silicon phthalocyanines	14
1.4.3 Alcohols and phenols as ligands	15
1.4.4 Silanols as ligands	16
1.4.5 Organic acids as ligands	17
1.4.6 Miscellaneous ligands	19
1.5 Microwave synthesis	24
1.5.1 Microwave synthesis of phthalocyanines	24
1.6 Photodynamic therapy (PDT)	25
1.6.1 Localization of drugs	27
1.7 Phthalocyanines in photodynamic therapy	29

1.7.1 Photochemistry involved in photodynamic therapy	30
1.8 Photochemical Processes	33
1.8.1 Singlet oxygen generation	33
1.8.2 Photobleaching	38
1.9 Photophysical processes	39
1.9.1 Fluorescence lifetimes	40
1.9.2 Fluorescence quantum yields	43
1.9.3 Triplet lifetimes and quantum yields	44
1.10 Electrochemistry of phthalocyanines	46
1.11 Characterisation of phthalocyanines	51
1.11.1 ¹ H-NMR spectroscopy of phthalocyanines	51
1.11.2 UV-spectroscopy of phthalocyanines	51
1.11.3 IR spectroscopy	53
1.12 Summary of aims	54
Chapter 2 Results and Discussion	55
2.1 Introduction	55
2.2 Synthesis	56
2.2.1 Synthesis of 4,5-diphenoxyphthalonitrile	57
2.2.2 Synthesis of octaphenoxy silicon phthalocyanine	60
2.2.3 Synthesis of axially substituted phthalocyanines	67
2.2.4 Synthesis by microwave irradiation	74
2.2.5 Synthesis of oligomers	77

2.3 Spectroscopic characterization	80
2.3.1 ¹ H NMR spectroscopy	80
2.3.2 UV visible spectra	95
2.3.3 Infrared spectra	100
2.4 Photochemistry	103
2.4.1 Phototransformation involving axial substituents	105
2.4.2 Photobleaching studies	113
2.4.3 Singlet oxygen quantum yields	117
2.5 Photophysical properties	122
2.5.1 Triplet lifetimes and quantum yields	123
2.5.2 Fluorescence quantum yields	125
2.5.3 Fluorescence lifetimes	125
2.6 Cyclic Voltammetry	126
Chapter 3 Experimental	137
3.1 Equipment	137
3.2 Materials	137
3.3 Electrochemical methods	138
3.4 Photochemical methods	138
3.4.1 Singlet oxygen quantum yields determination	140
3.5 Photophysical determinations	141
3.5.1 Geometry optimization	142
3.6 Synthesis	143

3.6.1 Phthalonitriles synthesis	143
3.6.2 Silicon phthalocyanines synthesis	145
3.6.3 Microwave synthesis	159
Chapter 4 Conclusions and Future perspectives	161
References	163

List of Symbols and Abbreviations

A_s	-	area of the sample under an emission band
A_{st}	-	area of the standard under an emission band
C_0	-	DPBF concentration at time 0
C_t	-	DPBF concentration at time t
DABCO	-	diazabicyclooctane
DBU	-	1,8,-diazabicyclo[5.4.0]undec-7-ene
DBN	-	1,5-diazabicyclo[4.3.0]non-5-ene
$(Cl)_2SiPc$	-	Dichloro silicon phthalocyanine
$(OH)_2SiPc$	-	Dihydroxy silicon phthalocyanine
DMAE	-	2-N,N-dimethylaminoethanol
DMF	-	dimethylformamide
DMSO	-	dimethylsulphoxide
DNA	-	deoxyribonucleic acid
DPBF	-	1,3-diphenylisobenzofuran
$E_{1/2}$	-	half wave potential
E_a	-	activation energy
E_{pa}	-	anodic peak potential
E_{pc}	-	cathodic peak potential
Et	-	ethyl
Fc	-	ferrocene
HPD	-	haematoporphyrin derivatives
HDL	-	high density lipoprotein
HOMO	-	highest occupied molecular orbital
I	-	light intensity
I_{abs}	-	amount of light absorbed by a photon
i_{pa}	-	anodic peak current
i_{pc}	-	cathodic peak current
LDL	-	low density lipoprotein
LUMO	-	lowest unoccupied molecular orbital
MPc	-	metallated phthalocyanines
NDA	-	<i>p</i> -nitroso- <i>N,N'</i> -dimethylaniline
ns	-	nanosecond
Pc	-	Phthalocyanines
PDT	-	photodynamic therapy
Ph	-	phenyl
ps	-	picosecond
RNA	-	ribonucleic acids
SCE	-	saturated calomel electrode
SiPc	-	Silicon phthalocyanines
TBAHP	-	tetrabutylammonium hexafluorophosphate
TLC	-	thin layer chromatography
Φ_Δ	-	singlet oxygen quantum yield
Φ_F	-	fluorescence quantum yield
Φ_P	-	phototransformation quantum yield

$\Phi_{\text{Photobleaching}}$	-	photobleaching quantum yield
Φ_{T}	-	triplet quantum yield
τ_0	-	natural radiative lifetime
τ_{F}	-	fluorescence lifetime
τ_{T}	-	triplet lifetime
$^1\text{O}_2$	-	singlet oxygen
η_{s}	-	refractive index of a solvent

List of Figures

Fig. 1 Notations for substitution of phthalocyanine molecules	3
Fig. 2 The structure of Pc-4	17
Fig. 3 A series of polyhydroxy silicon phthalocyanines used for polymer crosslinking	20
Fig. 4 A phthalocyanine trimer with silicon phthalocyanine in the centre	22
Fig. 5 Structure of hematoporphyrin 43	26
Fig. 6 Structure of dihematoporphyrin ether 44	27
Fig. 7 Disulphonated aluminium phthalocyanine 45	30
Fig. 8 Dissipation of electronic energy in an excited molecule	40
Fig. 9. The origin of the so-called Q and B bands in the UV-Visible spectrum of phthalocyanines	48
Fig. 10 Cyclic voltammogram of cobalt tetrasulfonated phthalocyanine with the structure inserted	49
Fig. 11 A typical UV-visible for metallated phthalocyanines showing the Q-band and the B-band (or Soret Band)	52
Fig. 12 Infrared spectra of phthalocyanines	53
Fig. 13 Hydrogen bonding in compound 55	64
Fig. 14 The IR spectra of compounds 54 and 55 overlain	65
Fig. 15 The UV-Visible spectrum of compound 54	66
Fig. 16 Axially substituted octaphenoxy silicon phthalocyanines made in this study	70
Fig. 17 Structures of the oligomers 74 to 78 synthesised	78
Fig. 18 The $^1\text{H-NMR}$ spectrum of compounds 52 and 54 in CDCl_3 overlain	84
Fig. 19 $^1\text{H-NMR}$ assignments for the phenoxy group on the octasubstituted phthalocyanine	86

Fig. 20 $^1\text{H-NMR}$ spectrum of compound 60 in CDCl_3 with aromatic protons at 2.44 ppm	88
Fig. 21 Aliphatic negative resonances of compound 61 in CDCl_3	90
Fig. 22 Axial ligands of compounds 57 to 73 with their chemical shifts	91
Fig. 23 Fragments of the $^1\text{H-NMR}$ spectrum of oligomer 75	94
Fig. 24 UV-Visible spectra of compounds 54 , 57 and 69 in DMF	96
Fig. 25 Beers law deviation for the oligomers 74 to 78 in DMF	97
Fig. 26 UV-Visible spectrum of compound 76 in DMF	98
Fig. 27 Phototransformation of compound 58 to the dihydroxyl 55 in DMSO	106
Fig. 28 The photobleaching process as witnessed by UV spectroscopy	114
Fig. 29 Photobleaching kinetic curves for compound 55 in DMSO saturated with air, nitrogen or oxygen or in aerated $\text{d}^6\text{-DMSO}$ and in aerated DMSO in the presence of 0.02 mol l^{-1} DABCO	115
Fig. 30 Suggested photobleaching mechanism	116
Fig. 31 UV-visible spectra of DPBF degradation by singlet oxygen in DMSO	118
Fig. 32 Geometry optimized structure of hexyl substituents on compound 73	119
Fig. 33 Relationship of degree of oligomerization with singlet oxygen quantum yield (ϕ_Δ)	121
Fig. 34 Transient absorption spectrum of compound 72 in DMSO	123
Fig. 35 Triplet decay observed at 500 nm for compound 72 in DMSO	124
Fig. 36 Cyclic voltammograms (2^{nd} scans) of complex 61 in A) CH_2Cl_2 and B) DMF. Electrolyte = 0.1 m dm^{-3} TBAHP. Scan rate = 100 mV s^{-1}	128

Fig. 37 The dependance of currents on the square root of scan rate for compounds 57 to 61 in a) DMF and b) CH ₂ Cl ₂ . The currents plotted are for the first reduction couple (cathodic currents). Electrolyte = 0.1 mol dm ⁻³ TBAHP	129
Fig. 38 Repetitive scanning of a solution of 61 in DMF. Electrolyte = 0.1 mol dm ⁻³ TBAHP. Scan rate = 100 mV s ⁻¹	130
Fig. 39 Repetitive scanning of a solution of 59 in DMF. Electrolyte = 0.1 mol dm ⁻³ TBAHP. Scan rate = 100 mV s ⁻¹	132
Fig. 40 The variation of current with scan number for 54 dissolved in DMF. Electrolyte = 0.1 mol dm ⁻³ TBAHP. Scan rate = 100 mV s ⁻¹	133
Fig. 41 Equipment setup for photochemical experiments	141
Fig. 42 The laser flash photolysis system for photophysical determinations	142

List of Schemes

Scheme 1 First metal free phthalocyanine synthesis	4
Scheme 2 Synthesis of dichloro silicon phthalocyanine	6
Scheme 3 The synthesis of a silicon phthalocyanine with two different axial ligands	7
Scheme 4 Polymerization of dihydroxy silicon phthalocyanine	7
Scheme 5 Synthesis of disubstituted phthalonitriles	9
Scheme 6 Synthesis of a disubstituted phthalonitrile	9
Scheme 7 Phthalonitriles in phthalocyanine synthesis	10
Scheme 8 Diiminoisoidolines in phthalocyanine synthesis, where Et = ethyl and Ph = phenyl	11
Scheme 9 Non-peripherally substituted phthalonitrile synthesis from Furan	12
Scheme 10 Coordinative bonding in iron phthalocyanine with pyridine and cyanide	14
Scheme 11 Axial ligand substitution in dihydroxy silicon phthalocyanine	15
Scheme 12 Axial ligand substitution of dihydroxy silicon phthalocyanine	16
Scheme 13 Axial ligation of ferrocene carboxylic acid to silicon phthalocyanine	18
Scheme 14 An oligomeric silicon phthalocyanine	19
Scheme 15 A crosslinked polymer containing silicon phthalocyanine units	21
Scheme 16 Synthesis of a silicon phthalocyanine with two different axial ligands using trifluoroacetic acid	23
Scheme 17 Photochemical processes in PDT	31
Scheme 18 Type II mechanism wherein S represents a metallated phthalocyanine	32
Scheme 19 Processes involved in DPBF photodegradation	35

Scheme 20	The synthesis of 4,5-diphenoxyphthalonitrile 52 , Ac = acetyl.	57
Scheme 21	The synthesis of diphenoxy diiminoisoindoline 53	59
Scheme 22	Synthesis of dichloro silicon octaphenoxypthalocyanine 54	61
Scheme 23	Synthesis of the dihydroxy silicon phthalocyanine 55	63
Scheme 24	Axial substitution of phthalocyanine 54	67
Scheme 25	Silver triflate activated axial ligand substitution, Tf = triflate, r.t. = room temperature	68
Scheme 26	Summary of the workup procedures followed prep. = preparative	73
Scheme 27	The 8 non-peripheral (or 1,4) protons on the macrocycle	85
Scheme 28	A possible mechanism of axial ligand phototransformation	110
Scheme 29	An alternative mechanism of phototransformation where A is an electron acceptor and RH is the solvent	112

List of Tables

Table 1 Reduction couples of zinc(II)tetraneopentoxyphthalocyanine	49
Table 2 $E_{1/2}$ values for SiPc(OR) ₂ and SiNc(OR) ₂ in CH ₂ Cl ₂	50
Table 3 Reaction details for axial modifications	75
Table 4 ¹ H-NMR (number of protons in brackets) data for the (X) ₂ SiOPPc compounds	80
Table 5 The UV-Visible spectral data of all the phthalocyanines synthesized	99
Table 6 Distinguishing IR bands for all the compounds made	102
Table 7 Calculation of the alpha coefficient for photochemical quantum yields	104
Table 8 The quantum yields of phototransformation (Φ_p)	107
Table 9 Singlet oxygen quantum yields of compounds 54 to 73	117
Table 10 Photophysical data of compounds 54 , 55 , 62 , 65 , 72 and 73	122
Table 11 Cyclic voltammetric data for all the silicon phthalocyanines containing 0.1M TBAHFP (all data represents $E_{1/2}$ /mV (vs Fc ⁺ /Fc)	135

General Introduction

This study was undertaken with the intention of discerning the requirements for useful sensitisers for photodynamic therapy. The sensitisers were to be variants of the silicon phthalocyanine parent structure. The first aim of this study was to modify the phthalocyanine macrocycle with electron donating groups in the peripheral position in order to achieve greater red-absorbing ability. The structure-activity relationship was established by the variation of the axial ligands of the silicon phthalocyanine structure with various phenols, alcohols, organic carboxylic acids and sulphonic acids. The second aim thus was to synthesise many axially ligated silicon phthalocyanines and obtain the products in high yield and high isomeric purity. The currently used drugs for photodynamic therapy are a mixture of isomers and it seems that the oligomers are the active components in the drugs photodynamic action, thus the third aim of this thesis was to produce oligomeric silicon phthalocyanines wherein the oligomerisation is perpetuated on the silicon central metal.

Of central importance to photodynamic therapy is the ability of the sensitiser to generate singlet oxygen and also its stability in this environment. It was thus the fourth aim of this thesis to study the singlet oxygen quantum yield of all the compounds synthesised as well as their photodegradation properties when subjected to the intense light required for photodynamic therapy.

The ability of a sensitiser to generate the toxic singlet oxygen species is determined by the triplet properties of the sensitiser therefore the fifth aim was to study the triplet quantum yields as well as the triplet lifetimes of various sensitisers to determine the necessary structural qualities required for efficient triplet generation.

The fluorescence properties of a molecule have no direct bearing on its ability to generate singlet oxygen but a fluorescent compound may be used for tumour imaging, and a compound that is selectively retained in a tumour with both these properties will be an ideal sensitiser. The sixth aim was thus to study the fluorescence properties of selected compounds in order to determine a structure-fluorescence relationship.

The final aim of this work was to study the electrochemical behaviour of selected compounds to establish the influence of the axial ligands on the redox potentials as this may be important in any oxidative mechanism of photodynamic behaviour.

Introduction

1.1 General phthalocyanine synthesis

Phthalocyanines (Pc's) have generated much interest since their characterization and laboratory synthesis in the 1930's. The unusual optical properties and relative thermal stability of these organic compounds have led to applications in dye, medical, optical recording, infra-red detection, organic solar cell and gas sensing industries. The Pc macrocycle consists of 4 pyrrole moieties bridged by nitrogen atoms (Fig. 1). The generally accepted notation for naming phthalocyanines is roughly shown in Fig. 1 where peripheral refers to the 2, 3 positions and non-peripheral refers to the 1, 4 positions. This notation will be used throughout this thesis. When dealing with tetrasubstituted isomers that are monosubstituted in four peripheral positions the 2, 9, 16, 23 prefix is used whereas non-peripheral monosubstitution is prefixed by 1, 8, 15, 22.

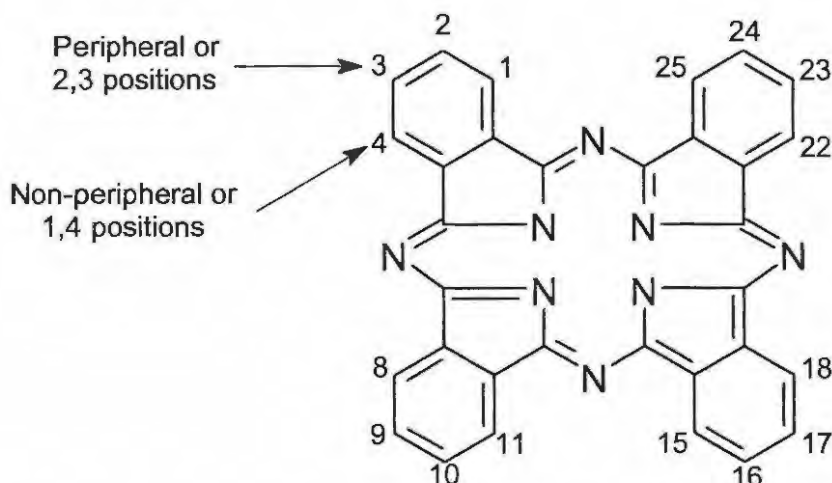
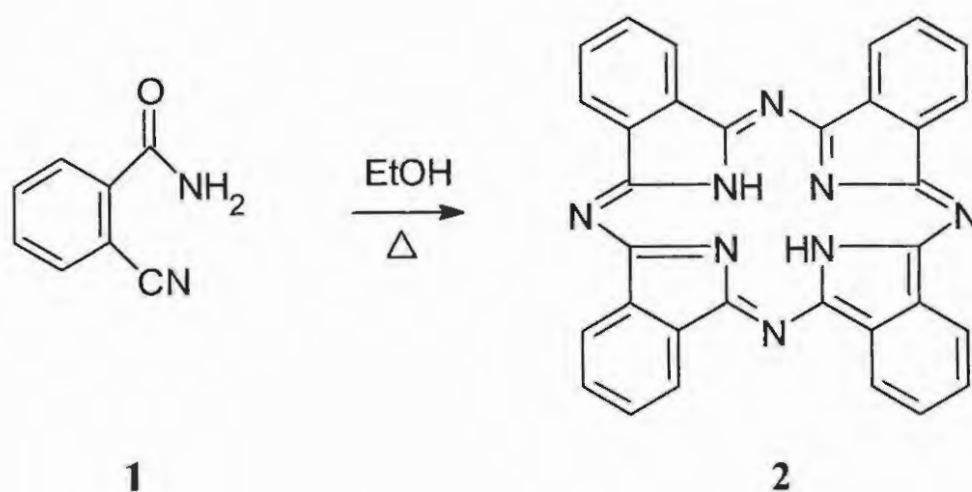


Fig. 1. Notations for substitution of phthalocyanine molecules.

- Chapter 1 -

Some good reviews are available that describe a variety of phthalocyanine syntheses in detail.^{1,2,3} In this section the basics of phthalocyanine synthesis will be described. Phthalocyanine complexes may be produced from a small variety of starting materials and the materials used depend on price, possible yields and availability. Scheme 1 shows the reaction of *o*-cyanobenzamide **1** that led to the accidental discovery of the useful phthalocyanine materials in 1907.⁴

This metal-free phthalocyanine **2** was only characterised 27 years later after a Scottish dyes company reported a similar compound that turned out to be iron phthalocyanine.⁵



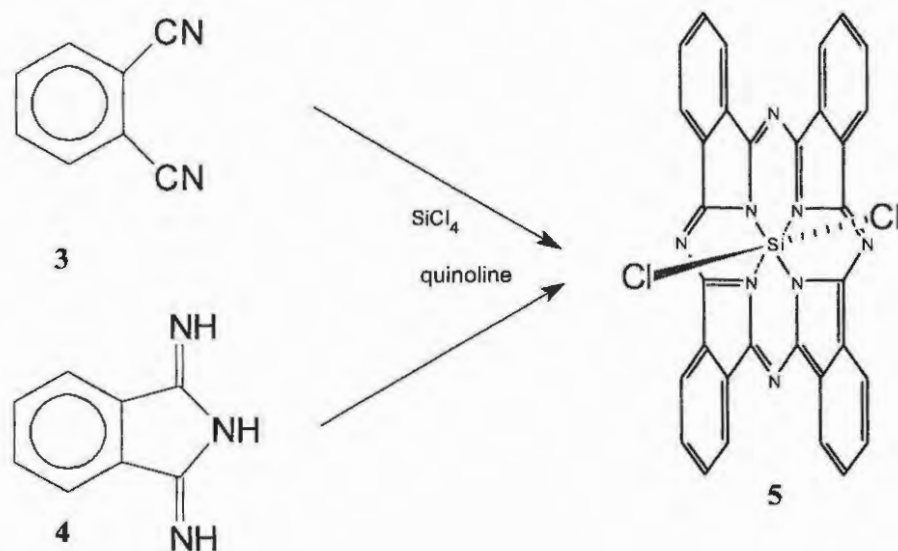
Scheme 1. First metal free phthalocyanine synthesis.

- Chapter 1 -

This discovery led to the utilization of variants of the benzamide **1** for the synthesis of many different phthalocyanine molecules. The most prominent among these is the phthalonitrile (or dicyanobenzene) molecule **3** (Scheme 2), which in modern times has been extremely useful in producing many peripherally and some non-peripherally substituted molecules. Generally, phthalonitriles form phthalocyanines under various conditions. Both metallated and metal-free phthalocyanines may be produced with ease. Linstead and Lowe⁶ treated phthalonitrile with sodium or lithium pentoxide in pentanol at 140°C to yield, after acid treatment, the metal free phthalocyanine.

1.2 Synthesis of silicon phthalocyanines

Silicon phthalocyanines (SiPc) were elusive compounds until the groundbreaking work of Joyner and co-workers.⁷ The first silicon phthalocyanines were made by the reflux reaction of phthalonitrile **3** and SiCl₄ or hexachlorodisiloxane in quinoline (Scheme 2), giving dichloro silicon phthalocyanine **5**. Soon after, however, Lowery and co-workers⁸ reported an improved method based upon the use of 1,3-diiminoisoindoline **4** instead of phthalonitrile.



Scheme 2. Synthesis of dichloro silicon phthalocyanine.

The dichloro silicon phthalocyanine **5** may then be hydrolyzed to dihydroxy silicon phthalocyanine ($\text{SiPc}(\text{OH})_2$), by reflux in equal volumes of pyridine and aqueous ammonia⁹ or by reflux in a sodium methoxide solution in aqueous ethanol.⁸

These methods have been the standard ways of preparing silicon phthalocyanines for many years. Organic solvent soluble silicon phthalocyanines **6** with two different axial ligands may be synthesised by using an alkyl or aryl substituted trichlorosilane.^{10,11,12} These compounds, however, suffer from quick decomposition in solution due to the Si-C bond formed, which are stable as solids but are light sensitive in solution. Li et. al.¹³ isolated various of these compounds such as the methylchlorosilane adduct shown in Scheme 3.

- Chapter 1 -

A rough estimate of the degree of polymerisation places x between 10 and 100 and this was done by a determination of the amount of water released in the reaction.

1.3 Peripheral phthalocyanine substitution

There are now many ways in which peripherally and non-peripherally substituted phthalocyanines may be produced. Direct substitution of halogenated copper phthalocyanines with phenols and thiophenols is used in the dye industry.³ More often, however, substituted phthalonitriles are used due to their general availability and ease of synthesis.

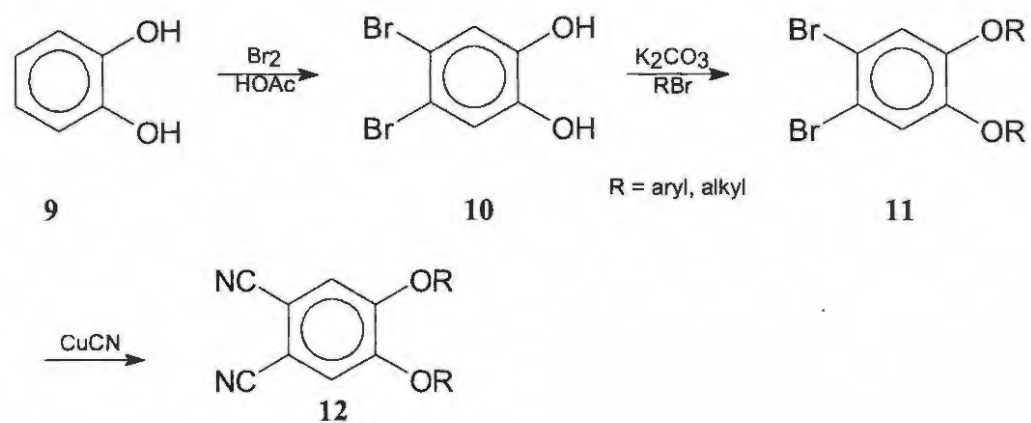
1.3.1 Phthalonitrile derivitization

Any substituted *o*-dibromo benzene may be converted by reaction with copper cyanide to the corresponding phthalonitrile.¹⁶ There are several methods available for the synthesis of substituted phthalonitriles and consequently substituted diiminoisoindolines. If a mono-substituted phthalonitrile is required, an etherification reaction of 3- or 4-nitrophthalonitrile¹⁷ (depending on the required product) with a phenolic compound is useful.

Disubstituted phthalonitriles may be obtained by various methods, most of them lead to diethereal compounds substituted by either aliphatic or aromatic chains. Scheme 5 shows a general procedure for synthesizing substituted

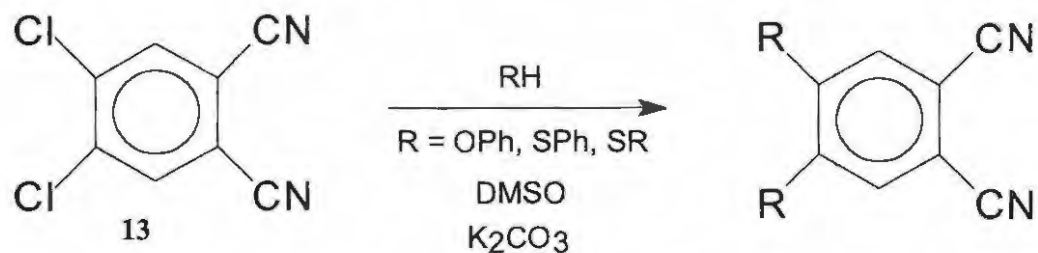
- Chapter 1 -

phthalonitriles. Starting from catechol **9** a standard bromination leads to the *o*-dibrominated catechol **10**. A reaction of **10** in basic medium with an alkyl halide leads to the diether **11**. Final reaction with copper cyanide produces the phthalonitrile **12**.^{18,19}



Scheme 5. Synthesis of disubstituted phthalonitriles.

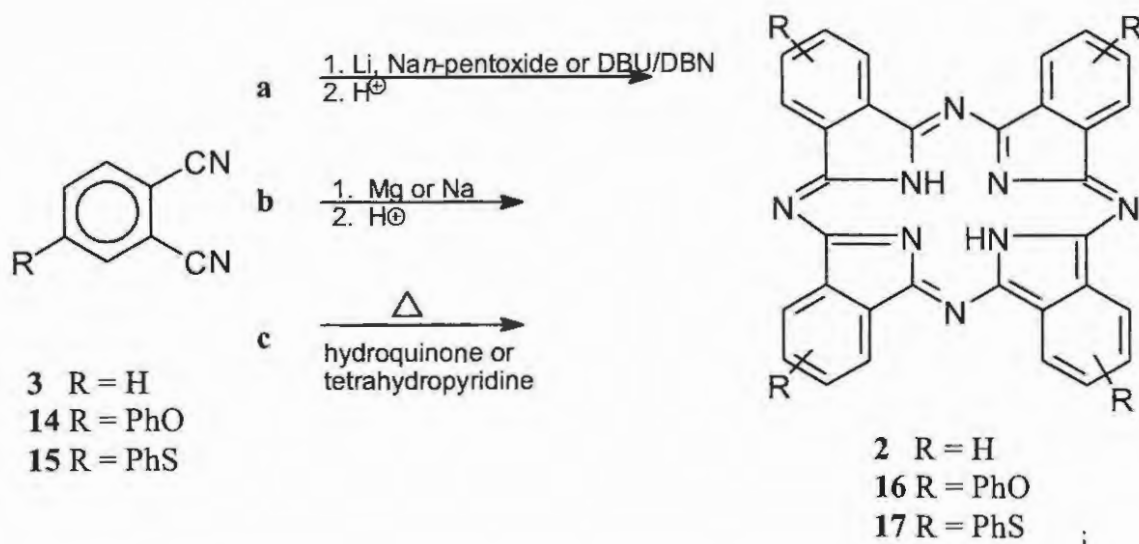
Disubstituted phthalonitriles may also be obtained by reaction of 4,5-dichlorophthalonitrile **13** with phenols, thiols or thiophenols (Scheme 6).



Scheme 6. Synthesis of a disubstituted phthalonitrile.

- Chapter 1 -

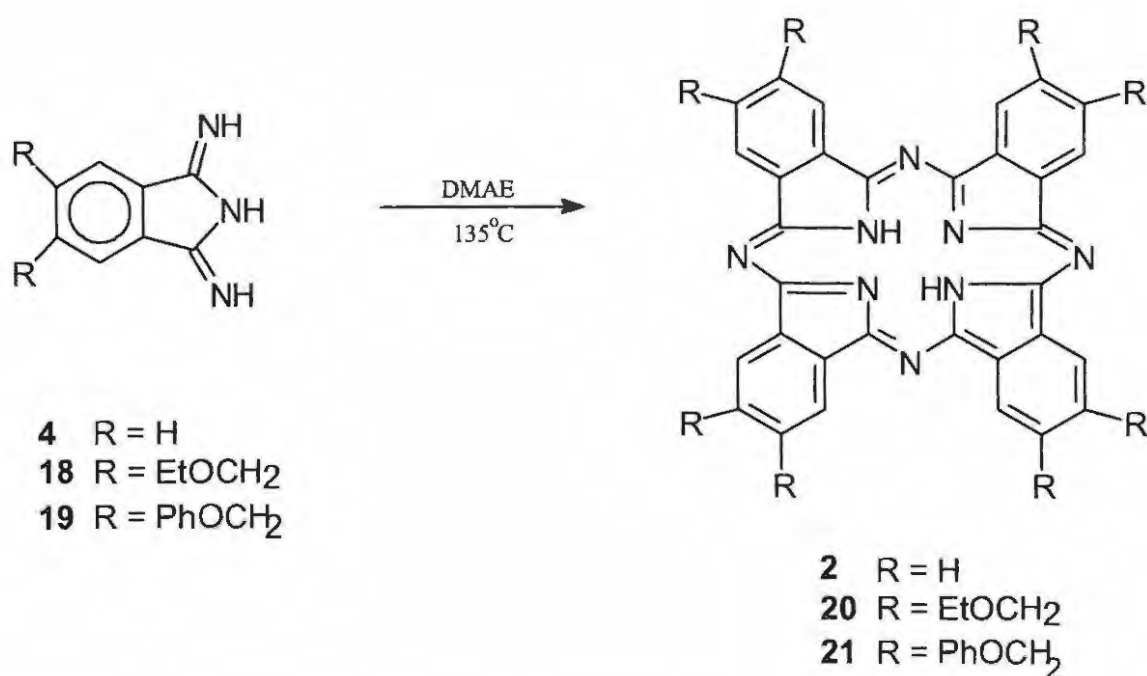
Most substituted phthalonitriles may be directly converted into a substituted phthalocyanine. For example, 4-phenoxyphthalonitrile **14** and 4-thiophenoxyphthalonitrile **15** gives 2,9,16,23-tetraphenoxyphthalocyanine **16** and 2,9,16,23-tetrathiophenoxyphthalocyanine **17** (Scheme 7), in 39% and 25% yield, respectively (route c),²⁰ as mixtures of isomers. More recently Wöhrle reported that substitution of the alkoxide bases for stronger bases such as 1,8-diazabicyclo[5.4.0]undec-7-ene (DBU) or 1,5-diazabicyclo[4.3.0]non-5-ene (DBN) gave **16** and **17** in yields of 77% and 96%, respectively (route a).²¹ Scheme 7 illustrates three methods of phthalocyanine synthesis from phthalonitrile. Route a is by the use of organic bases that are neutralized by acids in workup, in route b, inorganic bases have also been used with subsequent acid workup and in route c, the use of high boiling solvents also yield phthalocyanines but the yields are low.



Scheme 7. Phthalonitriles in phthalocyanine synthesis, where Ph = phenyl.

- Chapter 1 -

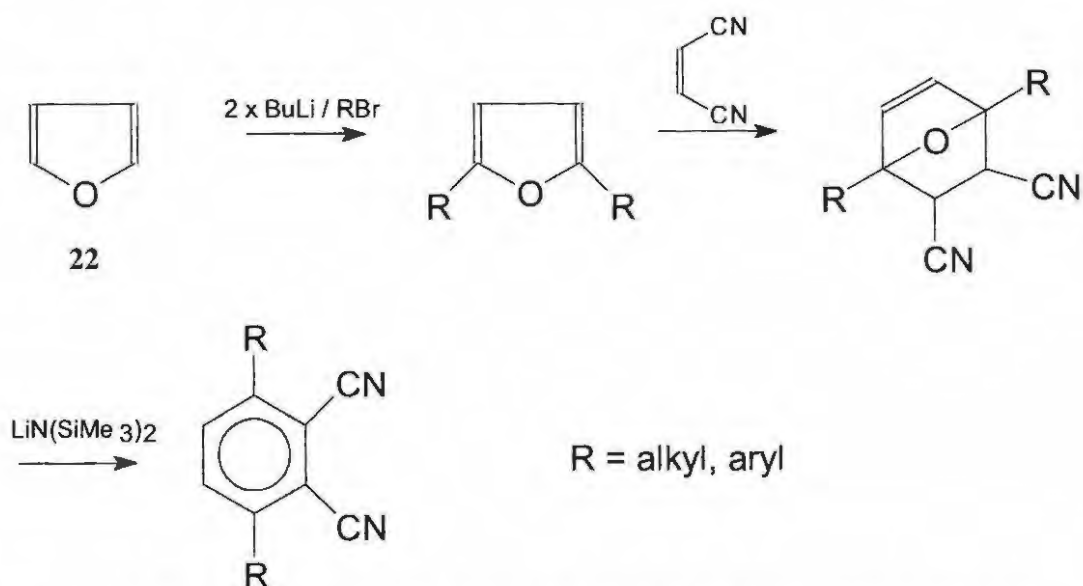
Diiminoisoindoline **4** may also be employed in the synthesis of phthalocyanine **2**, the reaction takes place in 85% yield by simply refluxing **4** in 2-N,N-dimethylaminoethanol²² (DMAE) as is shown in Scheme 8. Octasubstituted phthalocyanines, for example, have been prepared from 5,6-bis(ethoxymethyl)-1,3-diiminoisoindoline **18** or 5,6-bis(phenoxyethyl)-1,3-diiminoisoindoline **19** to give 2,3,9,10,16,17,23,24-octa(ethoxymethyl)-phthalocyanine **20** and 2,3,9,10,16,17,23,24-octa(phenoxyethyl)phthalocyanine **21** both in 80% yield²³ (Scheme 8).



Scheme 8. Diiminoisoindolines in phthalocyanine synthesis, where Et = ethyl and Ph = phenyl.

- Chapter 1 -

The phthalonitriles and diiminoisoindolines are the most important reagents for this work although some other starting materials such as substituted anhydrides and, to a lesser extent, *o*-diacids may also be used to produce phthalocyanines. In order to obtain non-peripherally substituted phthalocyanines Bryant et al.²⁴ have used furan **22** or thiophene,²⁵ which after 2,5-substitution may be converted into a substituted phthalonitrile as outlined in Scheme 9 for furan, wherein the substitution is done by basic reaction with an alkyl halide and then converted into a dinitrile by condensation with fumaronitrile. The final step leading to the disubstituted phthalonitrile is effected by trimethylsilyl reaction:



Scheme 9. Non-peripherally substituted phthalonitrile synthesis from furan.

As indicated, R may be a variety of groups and this procedure is thus very useful for obtaining a wide variety of substituted phthalonitriles. One of the aims of this study is to synthesise isomerically pure, peripherally substituted phthalocyanines that may aid in increasing the organic solvent solubility of the

- Chapter 1 -

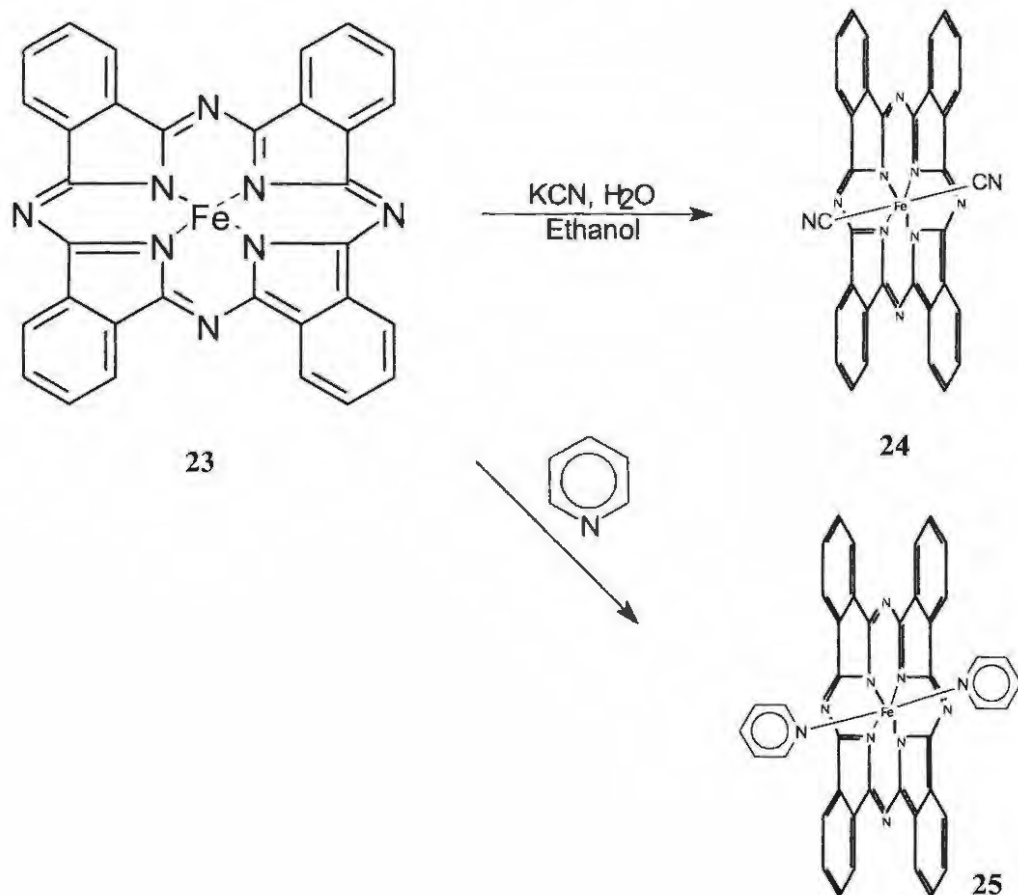
phthalocyanine macrocycle and additionally increase the red light absorbing properties of the macrocycle.

1.4 Axial modification of phthalocyanines

Depending upon the coordination behaviour of the central metal in the phthalocyanine core, many different axial substituents may be attached, or, in most cases coordinated to these metallated molecules. It is important to distinguish coordination behaviour in zinc phthalocyanine with pyridine molecules to the covalent nature of many axially substituted germanium phthalocyanines with alcohols.

1.4.1 Coordinative axially substituted phthalocyanines

Many phthalocyanine central metals form coordinative bonds with a variety of compounds as reviewed by Lever.¹ This is illustrated with the stable cyano **24** and pyridino **25** compounds formed with iron phthalocyanine²⁶ **23** in Scheme 10. This method of axial substitution does not pertain to the silicon phthalocyanines, which are the subject of this thesis and will not be discussed further.



Scheme 10. Coordinative bonding in iron phthalocyanine with pyridine and cyanide.

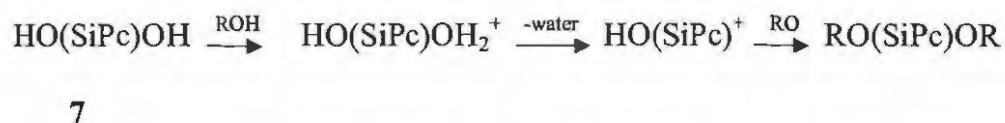
1.4.2 Axially substituted silicon phthalocyanines

The possibility of axial substitution of silicon phthalocyanines was recognized early on and various phenols, some silanols and acetic acid were attached axially to dichloro silicon phthalocyanine or dihydroxy silicon phthalocyanine in a covalent manner.^{9,27,28}

- Chapter 1 -

Immediately apparent when considering silicon phthalocyanines is the fact that they can only be octahedral, which is not common for silicon but has been documented in the $\text{Si}(\text{acac})_3^+$ series of compounds as well, the silicon atom being positive in both sets of octahedral compounds.

When considering the mechanism of axial substitution it is important to note that the acidity of the ligand is important and this then points to a probable delocalization of the positive charge of the silicon into the macrocyclic ring by the use of its $3d_{xz}$ and $3d_{yz}$ orbitals.²⁹ Taking this into consideration Krueger and Kenney⁹ proposed the following mechanism (Scheme 11) for axial ligand substitution in $\text{SiPc}(\text{OH})_2$ complexes:



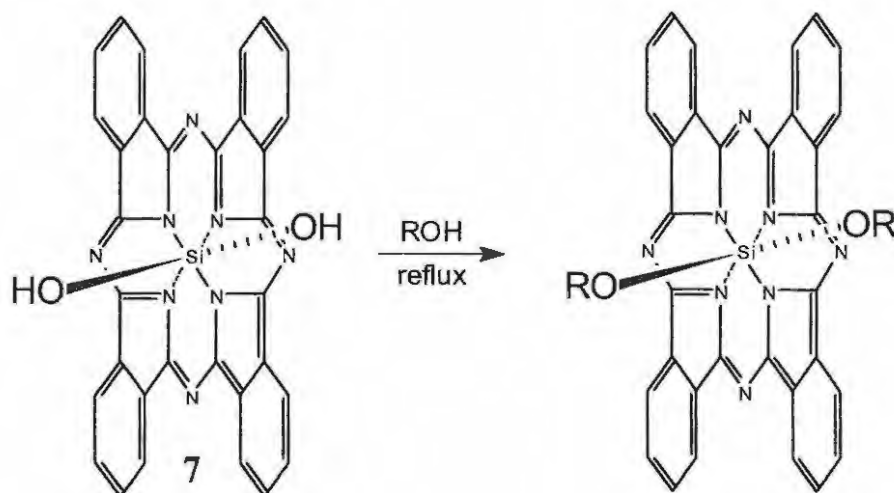
Scheme 11. Axial ligand substitution in dihydroxy silicon phthalocyanine.

1.4.3 Alcohols and phenols as ligands

Most alcohols satisfactorily react with dihydroxyl silicon phthalocyanine **7** or dichloro silicon phthalocyanine **5** without the need for an additional solvent. Ethanol, however, requires the use of NaBH_4 as co-reactant and long chain alcohols, such as octadecanol required the use of tetrahydronaphthalene as a solvent.⁹

- Chapter 1 -

The general reaction scheme for the production of these silyl ethers is shown below (Scheme 12):



Scheme 12. Axial ligand substitution of dihydroxy silicon phthalocyanine 7.

1.4.4 Silanols as ligands

Silanols have probably been the success story of silicon phthalocyanine usage in photodynamic therapy (PDT) as recently Le et al.³⁰ reported a very effective PDT agent commonly referred to as Pc-4 (**26**) shown in Fig. 2.

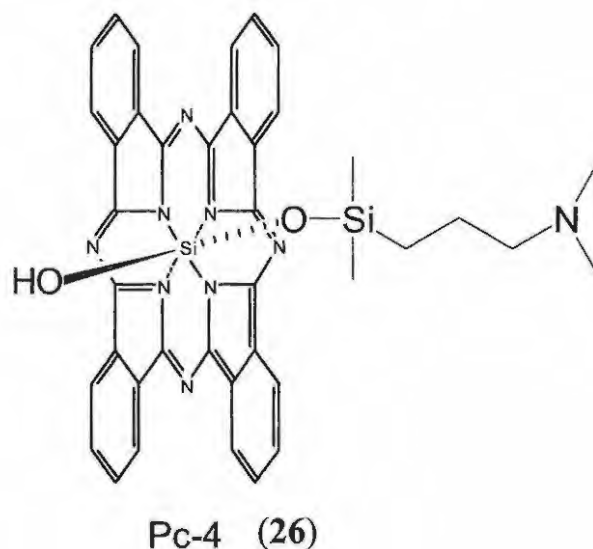


Fig. 2. The structure of Pc-4.

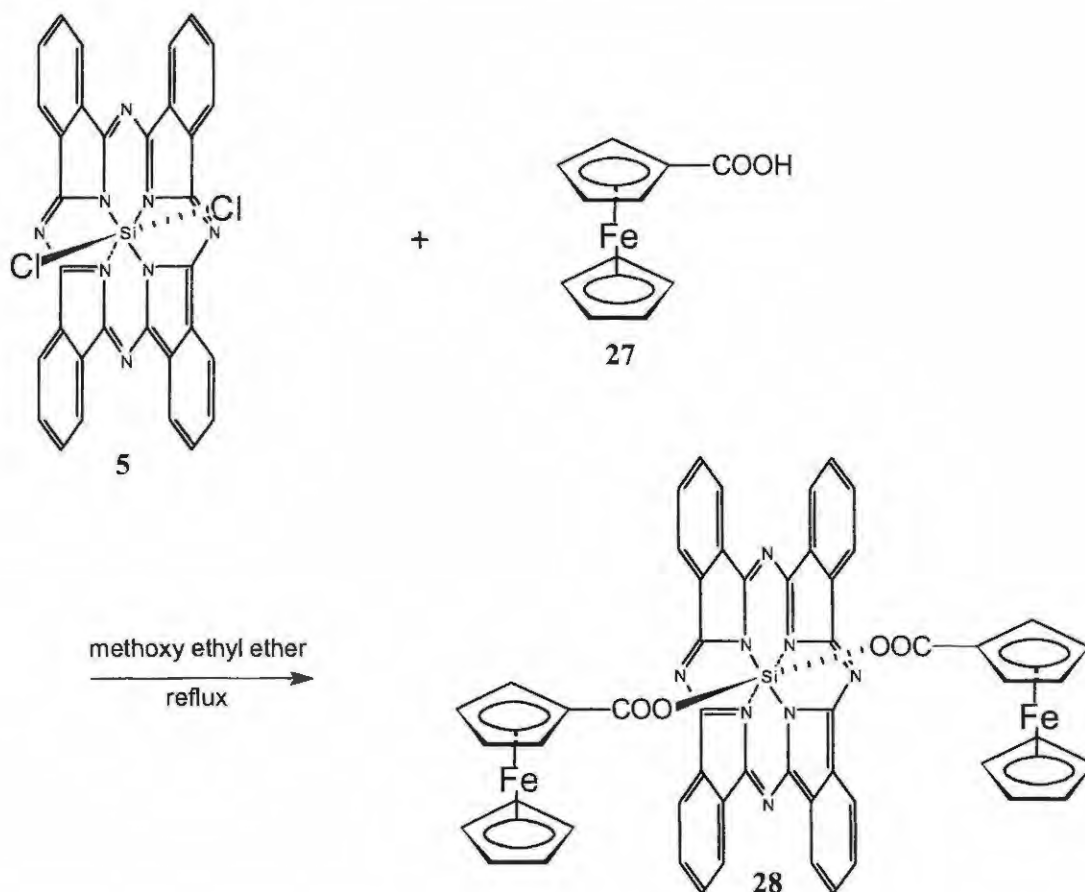
Axial silyl ether substituted SiPcs **26** may be obtained by reaction of dihydroxy silicon phthalocyanine **7** with chlorosilanes or silanols. Alternatively silanols may be reacted with dichloro silicon phthalocyanine **5** to deliver axial silyl ethers. Generally the only drawback of the silanols and chlorosilanes is the difficulty in removing them from the reaction mixture in comparison to alcohols or acids.

1.4.5 Organic acids as ligands

Generally solid acids need a solvent but liquid acids will most likely form a silyl ester with dichloro silicon phthalocyanine. Rafaeloff et al.²⁷ reacted glacial acetic acid with dichloro silicon phthalocyanine **5** for 5 hrs under reflux and produced the corresponding silyl ester. In the work of Silver et al.³¹ two

- Chapter 1 -

ferrocene (Fc) units were attached axially to dichloro silicon phthalocyanine **5** by reflux in methoxy ethyl ether (Scheme 13), giving complex **28**.

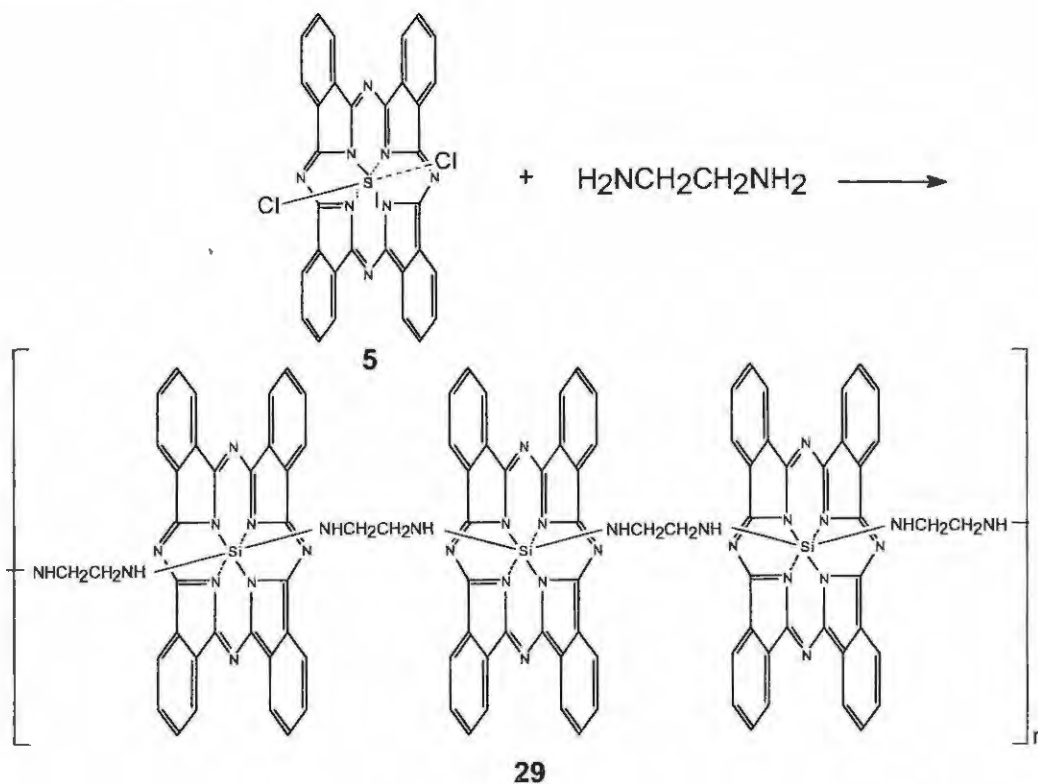


Scheme 13. Axial ligation of ferrocene carboxylic acid to silicon phthalocyanine.

Axial ligands increase organic solvent solubility and may play an important part in the localization of silicon phthalocyanines *in vivo*, therefore it is an aim of this study to synthesise a range of axially substituted phthalocyanines in order to establish a structure-activity relationship.

1.4.6 Miscellaneous ligands

The use of bidentate ligands may lead to oligomeric or polymeric molecules with alternating silicon phthalocyanine and ligand molecules. Chen and co-workers³² used ethylenediamine as a bifunctional ligand and upon reaction with dichloro silicon phthalocyanine **5** produced an oligomeric silicon phthalocyanine **29** as shown in Scheme 14.



Scheme 14. An oligomeric silicon phthalocyanine.

- Chapter 1 -

It is claimed that polymers containing a high concentration of phthalocyanine rings are excellent nonlinear optical absorbers³³ and thus Mandal et al.³⁴ made polyhydroxy silicon phthalocyanines **30** – **35** to be used as crosslinkers in a polyurethane film. The series of polyhydroxy phthalocyanines that they made is shown in Fig. 3.

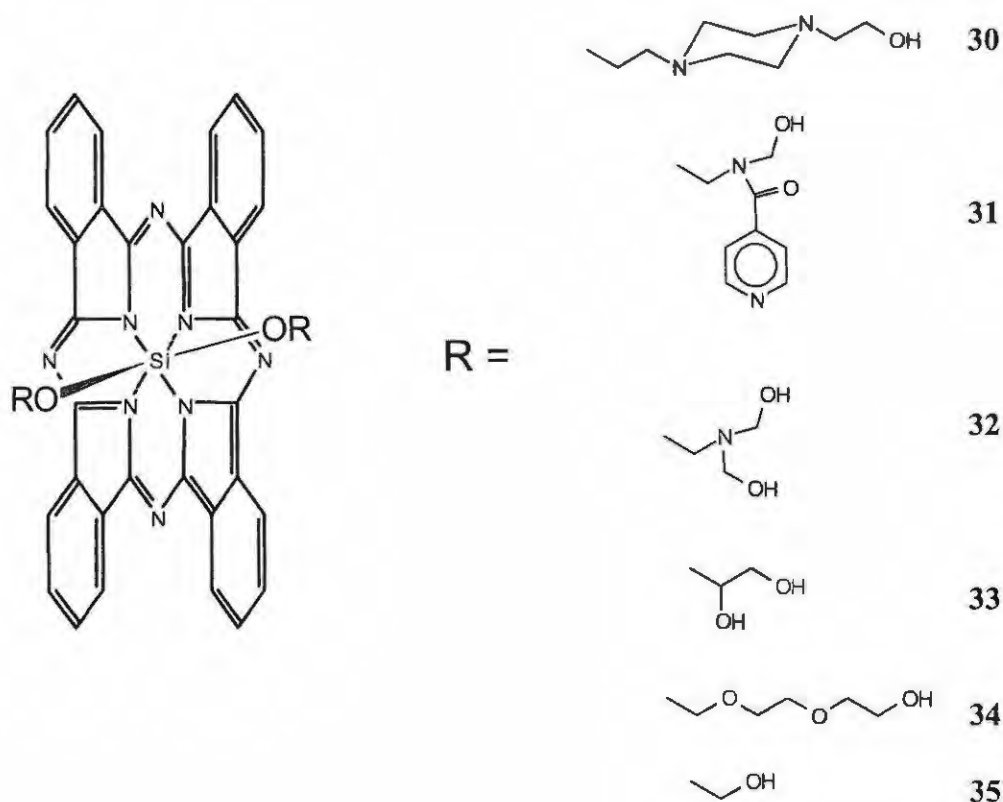
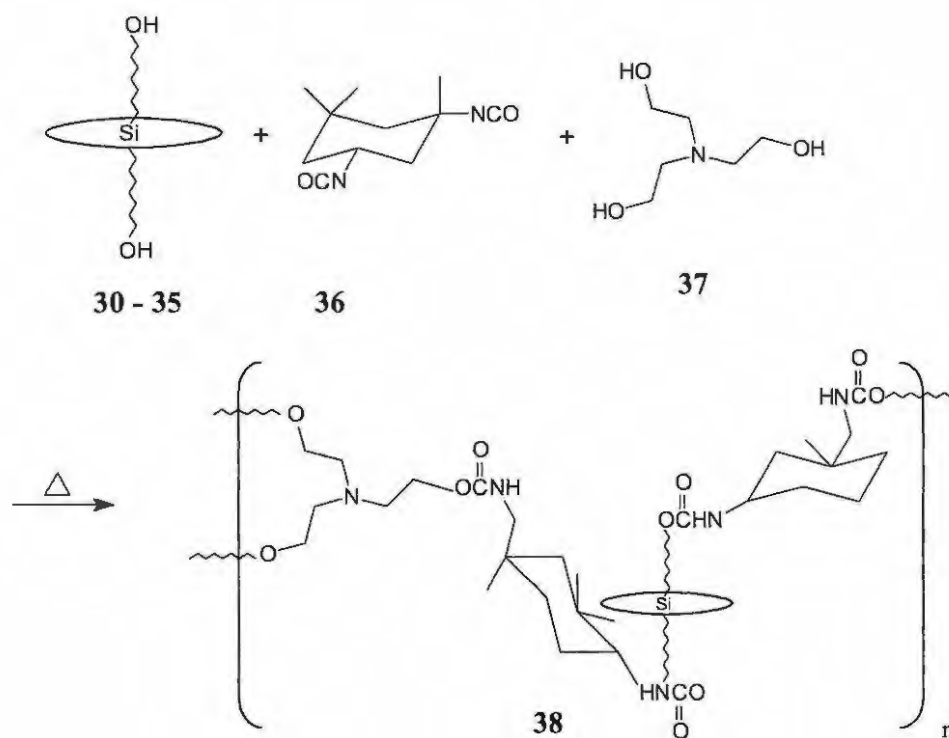


Fig. 3. A series of polyhydroxy silicon phthalocyanines used for polymer crosslinking.

These compounds were then processed into crosslinked polyurethane films as shown in Scheme 15:

- Chapter 1 -



Scheme 15. A crosslinked polymer containing silicon phthalocyanine units.

It has been mentioned that when dihydroxy silicon phthalocyanine **7** is heated at 400°C a polymeric silicon phthalocyanine forms. Similarly a trimer **39** of a silicon phthalocyanine with two axial aluminium phthalocyanines was the subject of a paper by Owen et al.³⁵ wherein the product was formed upon reflux reaction in 1-chloronaphthalene. The trimer **39** is shown in Fig. 4.

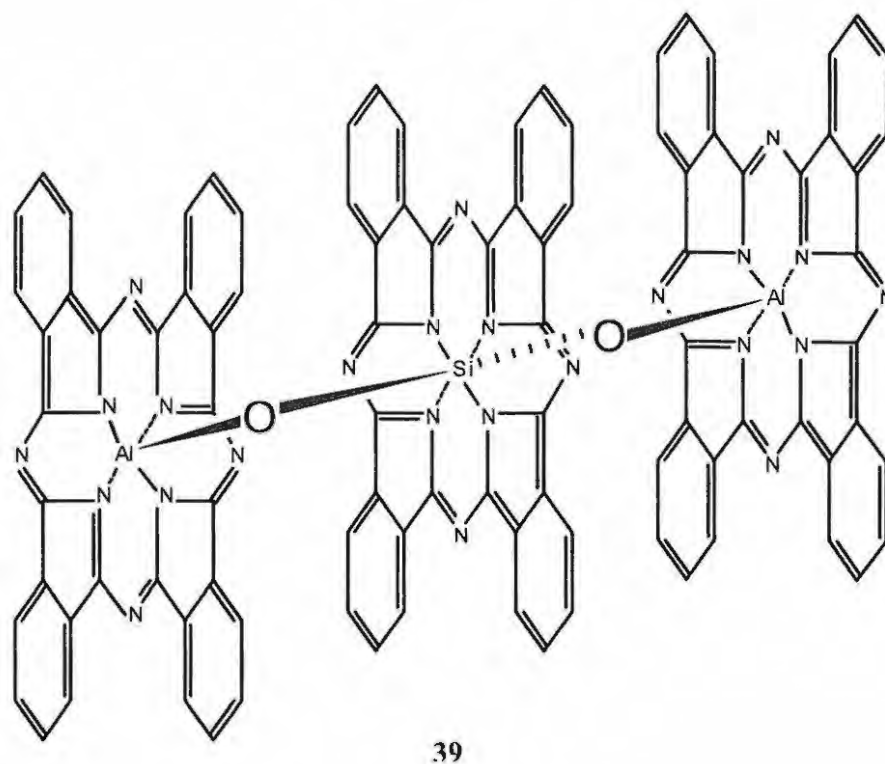
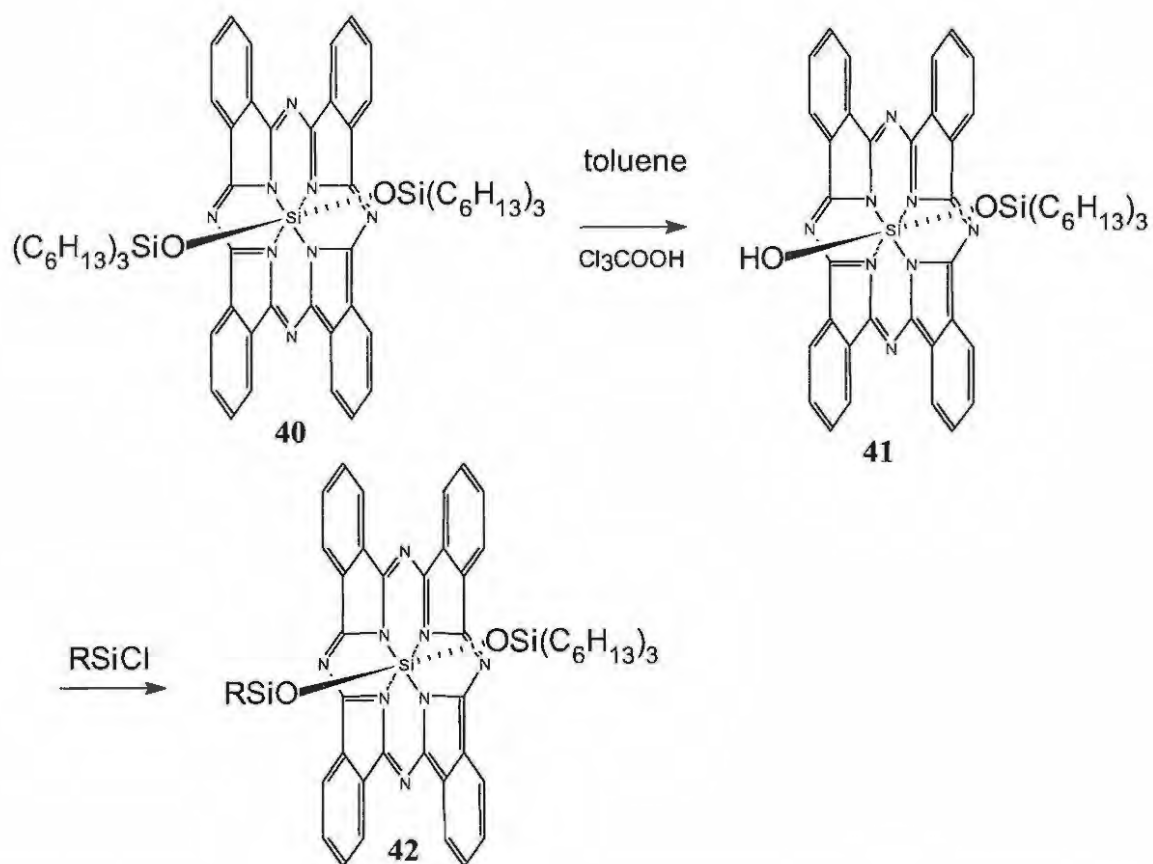


Fig. 4. A phthalocyanine trimer with silicon phthalocyanine in the centre.

Mention was made earlier of a silicon phthalocyanine made with two different axial ligands that suffer from instability in solution. An improved method of making a stable silicon phthalocyanine molecule with two different axial ligands was reported by Sounik et al.³⁶ wherein hydroxy (tri-n-hexylsiloxy) silicon phthalocyanine **41** was synthesised from bis(tri-n-hexylsiloxy) silicon phthalocyanine **40** by cleaving one of the hexylsiloxy groups using a two-fold excess of trichloroacetic acid in toluene as shown in Scheme 16.

Thereafter, they reacted a chlorosilane with the cleaved silicon phthalocyanine **41** to yield a stable product due to the fact that silyl ether bonds were formed.



Scheme 16. Synthesis of a silicon phthalocyanine with two different axial ligands using trifluoroacetic acid.

Since the currently approved PDT drug, hematoporphyrin derivatives (HPD) contains a mixture of oligomers which seem to be the active component in PDT action, a further aim of this study was to synthesise oligomers of the silicon phthalocyanine molecules wherein the oligomerisation was perpetuated on the silicon metal.

- Chapter 1 -

1.5 Microwave synthesis

As microwave synthesis has been used within this project, a discussion is warranted on the methods generally available. This field of organic synthetic chemistry has shown considerable development in the last 13 years since the publication of Gedye and co-workers.³⁷ Microwave synthesis is generally limited but very useful in some types of reactions such as when rapid reactions are required as in the synthesis of radio pharmaceuticals,³⁸ high temperature reactions for the preparation of various inorganic chemicals³⁹ and as in the case for this thesis, solvent free synthesis.^{40,41,42}

An important factor in microwave reactions is how well the reagents absorb microwave irradiation and when this is not satisfactory use may be made of solid supports such as montmorillonite,⁴³ alumina,⁴⁴ potassium fluoride on alumina^{45,46} or silica.^{47,48} These solid supports strongly absorb hyperfrequency beams and additionally, in many cases they act as catalysts.^{49,50,51}

1.5.1 Microwave synthesis of phthalocyanines

The first synthesis of phthalocyanine molecules utilizing microwaves was done by Shabaani⁵² wherein cobalt and iron phthalocyanines were made by microwaving the metal salts with phthalic anhydride and urea. This procedure was an improvement on all previous non-microwave syntheses of these molecules in terms of reaction yield and purity. Dichloro silicon octaalkoxy phthalocyanines have also been produced by use of microwave irradiation in

- Chapter 1 -

yields up to 95% but with the use of solvents.⁵³ In this thesis the effect of microwave synthesis on the yields and product purities of axial ligand substitution was studied.

1.6 Photodynamic therapy (PDT)

Apart from radical surgery, the two major techniques used for the treatment of cancer are radiotherapy and chemotherapy. Whilst combating tumour growth with some success, both methods can also induce disabling and life threatening side effects mainly because they destroy indiscriminately both normal and tumour tissue.⁵⁴ PDT has developed as an alternative for the treatment of cancer. In PDT, a photodynamically active drug, which is a photosensitiser, is administered to the body. It is totally inactive in the dark. Only when it is irradiated with light of the correct wavelength is it activated and then destroys living cells. This provides a unique way of introducing selective action in cancer therapy. The key to lack of side effects during photodynamic cancer therapy therefore does not hinge on the drug at all but rather on the capability of irradiation of cancerous growths without allowing light to fall on non-cancerous growths.

PDT employs the combination of light and a photosensitiser to selectively destroy tumour tissue. The first scientific observation of this phenomenon is found in the work of Raab⁵⁵ who found that paramecia were rapidly killed by visible light in the presence of oxygen and low concentrations of dyes. This

- Chapter 1 -

mechanism was further exploited after Auler and Banzer⁵⁶ established the affinity of various porphyrins, including hematoporphyrin **43**, preferentially to malignant as compared to adjacent healthy tissues.

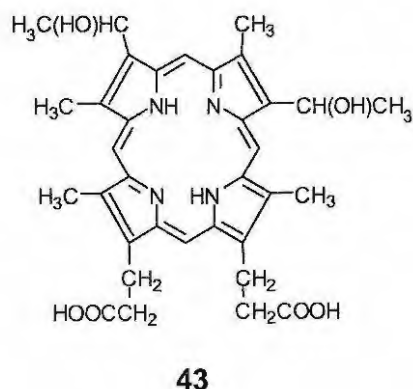
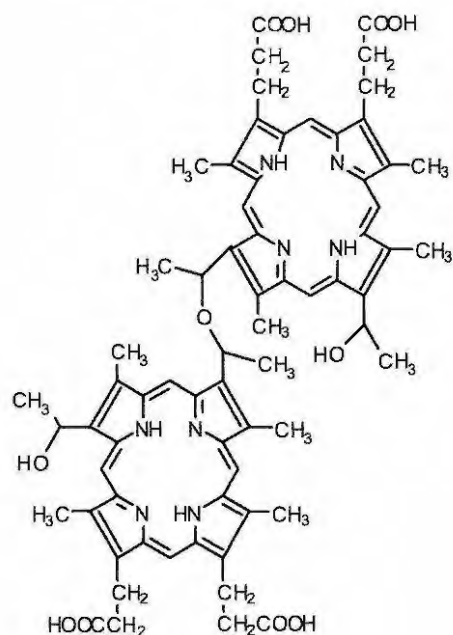


Fig. 5. Structure of hematoporphyrin **43**.

Treating hematoporphyrin **43** with a 19:1 mixture of acetic acid and sulphuric acid further optimised the tumour localizing ability, the resulting acetylated product was dissolved in dilute alkali to improve its solubility in water.⁵⁶ The new product was then named hematoporphyrin derivative (HPD), which is actually a mixture of products and is currently used widely for the treatment of a variety of malignancies.⁵⁷ The purified form of HPD is commercialised under the name of Photofrin II, this then being a mixture of dimers and oligomers in which the active component in the photodynamic action is believed to be the dihematoporphyrin ether **44**.⁵⁸



44

Fig. 6. Structure of dihematoporphyrin ether 44.

1.6.1 Localization of drugs

Photodynamic therapy depends on selective cell injury; thus the drugs should be retained selectively in tumour tissue and then, if this is not totally possible, additional selectivity can be attained by spatial localization of the illumination to the target tissue. Prior to localization at tumour tissue, the photosensitiser is transported by the blood and interacts with serum proteins. The serum proteins, albumin and low-density lipoprotein (LDL) have been identified as important natural drug carriers.⁵⁹ Various studies have shown that the more hydrophilic photosensitisers bind to albumin and are localized in the vascular

- Chapter 1 -

stroma. By contrast, the more hydrophobic photosensitisers are bound progressively more to the lipoprotein.⁶⁰

Recent studies also suggest that the pre-binding of high density lipoprotein (HDL) and low density lipoprotein (LDL) to photosensitisers (porphyrins, benzoporphyrins and phthalocyanines) leads to a significant increase in tumour localization.⁶¹ Recognition of the importance of the delivery mode in the overall therapeutic effectiveness has thus led to the study of liposomes,⁶⁰ cyclodextrin, pre-binding to proteins⁶² and conjugation to monoclonal antibodies⁶³ as delivery systems in PDT. The advantage of using delivery systems is an increase in solubility and an enhancement of tumour selectivity. Various researchers have suggested that the localization and retention of photosensitizers in malignant tissue is due to:

- a) Tumour cells having a higher vascular permeability due to the expression of a protein by the tumour to increase tumour growth.⁶⁴
- b) Poor lymphatic drainage of tumours due to the underdevelopment of the lymphatic system.⁶⁵
- c) The interstitial space difference between tumours and normal cells.
- d) A deficiency of the ferrochelatase enzyme in cancerous tissue which is responsible for the formation of heme and which is subsequently broken down by heme oxygenase.⁵⁸

- Chapter 1 -

- e) The relatively high collagen concentrations in tumour tissues facilitating the binding of porphyrins to the stroma and vessel walls of tumour tissue.⁶⁶
- f) Higher acidity of malignant tissue.

1.7 Phthalocyanines in photodynamic therapy

In the search for an ideal photodynamic drug the most important factors to be considered are: that the drug should possess a very low systemic toxicity, show a preferential affinity for malignant tumours, have a high photodynamic efficiency and have a maximum absorption in the red part of the visible spectrum. HPD complies with all the above except that its main absorption is around 400 nm, for therapy the dye is activated by red light ($\lambda = 630$ nm). In contrast the extended conjugated aromatic phthalocyanines possess an intense, more or less Gaussian Q-band at 650-700 nm ($\epsilon > 10^5 \text{ m}^{-1} \text{ cm}^{-1}$)⁶⁷ and are essentially transparent between $\lambda = 400$ -630 nm. These compounds, therefore, allow deeper light penetration of tissue and are substantially less efficient in inducing skin photosensitivity, which is a major problem with HPD.⁶⁸

The phthalocyanine macrocycle can coordinate with almost every metal on the periodic table and can be substituted at the periphery with a variety of substituents. Of all the possible phthalocyanines, the sulphonated zinc and sulphonated aluminium phthalocyanines, especially the di-sulphonated aluminium phthalocyanines **45** wherein the sulphonated benzene rings are

- Chapter 1 -

located on adjacent pyrrole moieties (indicated in Fig. 7 as rings A and B), seem to be the most potent photosensitisers of this class.⁶⁹

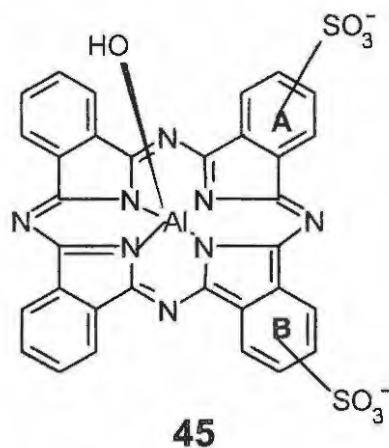


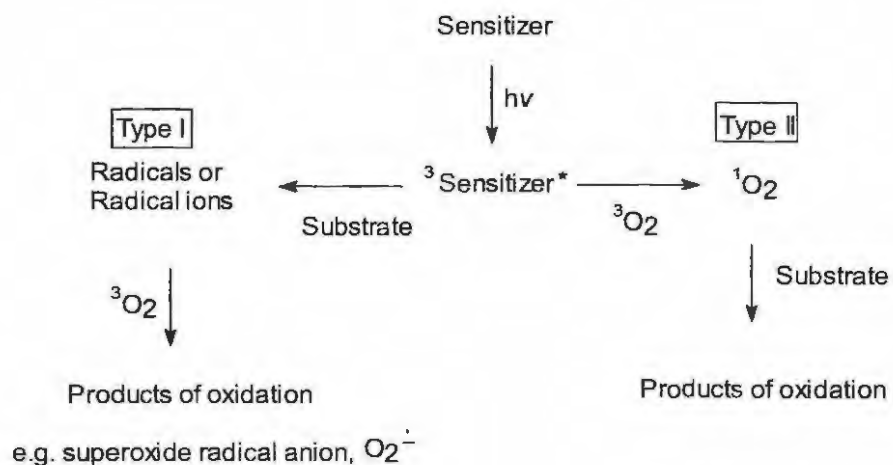
Fig. 7. Disulphonated aluminium phthalocyanine 45.

This thesis will be concerned with the synthesis of various axially substituted silicon octaphenoxy phthalocyanines for the primary purpose of developing drugs for PDT.

1.7.1 Photochemistry involved in photodynamic therapy

The cytotoxic agent in PDT is produced by one of two different processes, which, in photochemistry are referred to as a Type I or a Type II process. These processes are mediated by the excited triplet state of the photosensitiser, shown in Scheme 16.

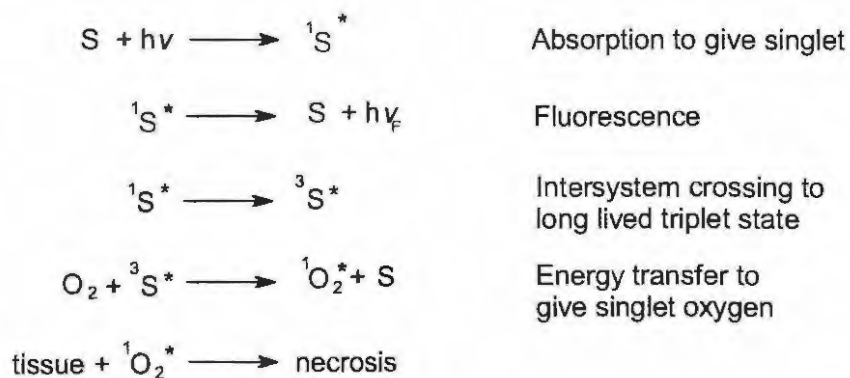
- Chapter 1 -



Scheme 17. Photochemical processes in PDT.

A Type I mechanism results in hydrogen atom or electron transfer reactions between the sensitizer and some substrate or the solvent to yield either radicals or radical ions.⁷⁰ Radicals and radical ions formed can then react with oxygen to yield superoxide radical anion (Scheme 17). The Type II process is detailed in Scheme 18, from which it can be seen that energy is transferred from a sensitizer, (such as a metallated phthalocyanine) denoted by the symbol S, to ground-state oxygen which results in singlet state oxygen.

- Chapter 1 -



Scheme 18. Type II mechanism wherein S represents a metallated phthalocyanine.

Both singlet oxygen and superoxide are cytotoxic species, causing oxidative destruction of tissue and they constitute the basis for photodynamic cancer therapy.⁷¹ Which mechanism (Type I or Type II) is operative has not yet been firmly established, however, the generation of singlet oxygen via the Type II pathway in solution is picked up by observation of its weak luminescence at $\lambda = 1270$ nm using a near infrared photodetector. Such luminescence has been seen widely in *in vitro* studies giving rise to the widespread belief that singlet oxygen is invariably the mediator (active substance) in PDT.⁶⁵

- Chapter 1 -

1.8 Photochemical processes

1.8.1 Singlet oxygen generation

In the presence of oxygen it is widely believed that sensitizers produce singlet oxygen, which then is the resultant cytotoxic species that causes cell destruction (via a Type II mechanism).^{72,73} Currently there are several methods of determining the quantum yield of singlet oxygen photogeneration in organic media as well as aqueous media. In general, singlet oxygen may be determined either by direct determination, which requires the use of a power meter or a chemical actinometer such as Reinecke's salt⁷⁴ for quantification. The actinometer works by considering the fraction of the incident light absorbed by the sensitizer (A) as shown:

$$1 - \frac{I}{I_0} = 1 - 10^{-\epsilon[A]l} \quad \dots \text{Eq. 1}$$

with ϵ the extinction coefficient of the actinometer and l the cell pathlength. The number of molecules formed n_b in time t is then determined by analysis. The intensity of the incident light beam (I_0') may then be determined according to the following equation where the quantum yield (Φ_B) of, for example, Reinecke's salt (in Reinecke's salt actinometry) is known:

$$I_0' = \frac{n_b}{(\Phi_B \times t \times (1 - 10^{-\epsilon[A]l})} \text{ quanta / sec} \quad \dots \text{Eq. 2}$$

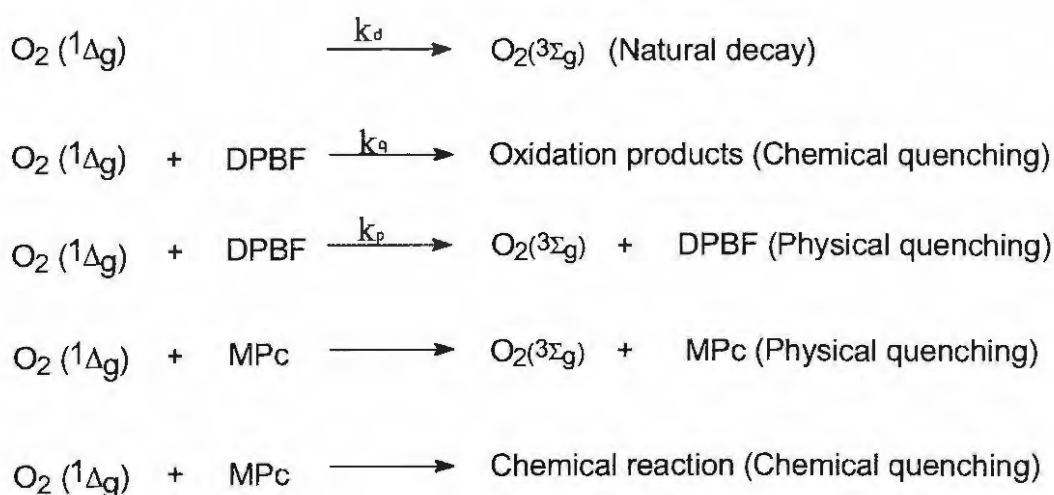
Singlet oxygen quantum yield determinations may also be done using a relative method⁷⁵ where a sensitizer is used that has a well-established singlet oxygen quantum yield. Singlet oxygen luminescence, which may be measured at 1270 nm,⁷⁶ is also used for determinations of singlet oxygen in organic solvents but this luminescence is very weak in aqueous solutions.

For metallated phthalocyanines (MPc) in solutions of dimethylformamide (DMF) and dimethylsulphoxide (DMSO) the singlet oxygen quencher 1,3-diphenylisobenzofuran (DPBF) may be used to determine singlet oxygen quantum yield by looking at its decomposition at 417 nm. In aqueous media a bleaching reaction of water-soluble *p*-nitroso-*N,N'*-dimethylaniline (NDA) with singlet oxygen in the presence of imidazole or histidine is a popular method.⁷⁷ The degree of photobleaching of this yellow dye ($\lambda_{\text{max}} = 440 \text{ nm}$) is directly proportional to the overall production of singlet oxygen. In this process imidazole (histidine) does the actual bleaching upon formation of a transient trans-annular peroxide species with singlet oxygen.⁷⁸ However, this method does have drawbacks, since the actual bleaching is a secondary process and imidazole or histidine may quench triplet excited states of sensitizers.

For PDT the triplet excited state of the sensitizer is responsible for the generation of the reactive singlet oxygen species, therefore the efficiency of the other processes that deactivate this state including its non-radiative decay and

- Chapter 1 -

phosphorescence must be minimal or controlled to give good PDT results. Knowing the overall efficiency of the different photochemical steps thus becomes important. The efficiency is expressed as quantum yield, which has been defined as the number of molecules of the process of interest formed for each photon of light absorbed. The decay of DPBF may thus be represented by the following mechanism (Scheme 19).



Scheme 19. Processes involved in DPBF photodegradation.⁷⁹

At low concentrations of MPc the physical quenching of singlet oxygen by MPc may be ignored. DPBF acts exclusively as a chemical quencher in DMSO and in other organic solvents, hence physical quenching of singlet oxygen by DPBF is not important. Chemical quenching of singlet oxygen with MPc is negligible compared to the rate of the reaction with DPBF, thus only the first two steps are important in the decay of $\text{O}_2(1\Delta_g)$. The rate of disappearance of DPBF in the presence of $\text{O}_2(1\Delta_g)$ is thus given by Eq. 3:⁷⁹

- Chapter 1 -

$$\frac{-[\text{DPBF}]}{dt} = k_q [\text{DPBF}] [\text{O}_2(^1\Delta_g)] \quad \dots \text{Eq. 3}$$

Applying the steady state approximation for $\text{O}_2 (^1\Delta_g)$ and rearranging gives:

$$[\text{O}_2(^1\Delta_g)] = \frac{\Phi_\Delta I_{\text{abs}}}{k_q [\text{DPBF}] + k_d} \quad \dots \text{Eq. 4}$$

Where I_{abs} is the amount of light absorbed by a photon of the sensitizer, and Φ_Δ is the singlet oxygen quantum yield. Substitution of Eq. 4 into Eq. 3 gives:

$$\frac{-[\text{DPBF}]}{dt} = \frac{k_q \Phi_\Delta I_{\text{abs}} [\text{DPBF}]}{k_d + k_q [\text{DPBF}]} \quad \dots \text{Eq. 5}$$

The quantum yield for DPBF disappearance is defined as:

$$\Phi_{\text{DPBF}} = \frac{-[\text{DPBF}]}{dt} \times \frac{1}{I_{\text{abs}}} \quad \dots \text{Eq. 6}$$

I_{abs} thus cancels out with substitution of Eq. 5 into Eq. 6 to give:

$$\Phi_{\text{DPBF}} = \frac{k_q \Phi_\Delta [\text{DPBF}]}{k_d + k_q [\text{DPBF}]} \quad \dots \text{Eq. 7}$$

- Chapter 1 -

If [DPBF] is low then $k_d \gg k_q[\text{DPBF}]$ and thus Eq. 7 simplifies to:

$$\Phi_{\text{DPBF}} = \frac{k_q \Phi_{\Delta} [\text{DPBF}]}{k_d} \quad \dots \text{Eq. 8}$$

At low DPBF concentrations, the following (Eq. 9) applies to MPc's

$$\Phi^{\text{MPc}} = \Phi_{\Delta}^{\text{MPc}} \frac{k_q}{k_d} [\text{DPBF}]^{\text{MPc}} \quad \dots \text{Eq. 9}$$

With the relative method, the reference material is also taken into consideration, thus for zinc phthalocyanine (ZnPc) as reference material, Eq. 10 applies:

$$\Phi^{\text{ZnPc}} = \Phi_{\Delta}^{\text{ZnPc}} \frac{k_q}{k_d} [\text{DPBF}]^{\text{ZnPc}} \quad \dots \text{Eq. 10}$$

Dividing Eq. 9 by Eq. 10, the following is obtained:

$$\Phi_{\Delta}^{\text{MPc}} = \Phi_{\Delta}^{\text{ZnPc}} \frac{\Phi^{\text{MPc}} [\text{DPBF}]^{\text{ZnPc}}}{\Phi^{\text{ZnPc}} [\text{DPBF}]^{\text{MPc}}} \quad \dots \text{Eq. 11}$$

In practice Φ^{MPc} and Φ^{ZnPc} are determined by the following general equation:

$$\Phi = \frac{(C_0 - C_t)V}{I_{\text{abs}} t} \quad \dots \text{Eq. 12}$$

where V is the sample volume, t is the photolysis time, C_0 and C_t are the DPBF concentrations at time 0 and time t. The absorbed light I_{abs} is determined by:

$$I_{\text{abs}} = \frac{\alpha S I}{N_a} \quad \dots \text{Eq. 13}$$

- Chapter 1 -

where S is the irradiated cell area, I the light intensity of the lamp, N_a is Avagadro's constant and α is the fraction of the light that is absorbed. Where S, I and V are constant for both the sample and the standard, the quantum yield of singlet oxygen may then be determined by substitution of Eq. 13 into Eq. 12 and Eq. 12 into Eq. 11 to give Eq. 14:

$$\Phi_{\Delta}^{MPc} = \Phi_{\Delta}^{ZnPc} \frac{(C_o - C_t)^{MPc} (\alpha t)^{ZnPc} [DPBF]^{ZnPc}}{(C_o - C_t)^{ZnPc} (\alpha t)^{MPc} [DPBF]^{MPc}} \dots \text{Eq. 14}$$

Singlet oxygen quantum yields of four axially substituted silicon phthalocyanines have been reported by He et al.³⁰ and these values ranged from 0.2 to 0.5.

1.8.2 Photobleaching

Upon irradiation most photosensitisers are degraded in a process involving singlet oxygen that is produced by the photosensitisers in solution although there is some speculation that free radicals may also play a role.^{80,81} Photobleaching of the sensitisers may thus be an advantage or a disadvantage in the treatment of solid tumours. The sensitiser will be ineffective if the photobleaching occurs too quickly⁸² and alternatively if the rate of photobleaching is more controlled the sensitiser concentration may be reduced in the body and thus reduce the damage to healthy tissue.⁸³ It should also be borne in mind, however, that photobleaching rates are different in various

- Chapter 1 -

media. Thus photobleaching behaviour in solutions, cells and tissues is different.⁸⁴

The quantum yield of photobleaching may be determined by an equation (Eq. 15) similar to Eq. 12.

$$\Phi_{\text{Photobleaching}} = \frac{(C_0 - C_t)v}{I_{\text{abs}} t} \quad \dots \text{Eq. 15}$$

where the symbols are as described above.

An intended aim of this thesis was to study the ability of the various axially substituted silicon phthalocyanines to generate singlet oxygen in solution as well as to study the photodegradation behaviour of these compounds.

1.9 Photophysical processes

If a photon passes close enough to a molecule there is an interaction between the electric fields of these entities. This interaction may result in no permanent change in the molecule or the molecule may absorb the photon and a 'reaction' thus occurs. This 'reaction' may then take on the form of a high enough energy absorption to enable an electron to move into a higher energy orbital. The excited states initially produced by photon absorption are almost always in their singlet states. An important process in PDT is the singlet to triplet transition (S \rightarrow T). This transition is highly forbidden and occurs only due to spin-orbit coupling.⁸⁵

- Chapter 1 -

An excited molecule dissipates excess energy with various pathways and these are shown in Fig. 8.

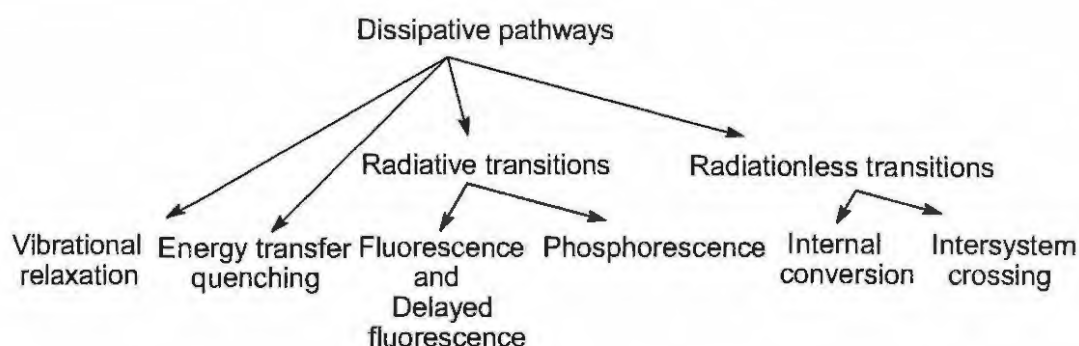


Fig. 8. Dissipation of electronic energy in an excited molecule.

1.9.1 Fluorescence lifetimes

Obtaining the radiative lifetimes (fluorescence lifetime as well as the triplet lifetime) is of importance to photodynamic therapy for comparative purposes. If a first order radiative process is experimentally observed, it may be assumed that no other decay process exists but that which is being studied. The populated electronically excited species will thus decay radiatively to the ground state. The process may thus be formulated by Eq. 16 and Eq. 17 below:

$$\frac{d[M^*]}{dt} = -A_{u1}[M^*] \quad \dots \text{Eq. 16}$$

$$\therefore [M^*] = M_0^* e^{-A_{u1}t} \quad \dots \text{Eq. 17}$$

where $[M^*]$ is the excited state concentration and M_0^* is the initial excited state concentration, A_{u1} is the Einstein coefficient, which is the number of times per

- Chapter 1 -

second that an excited state emits a photon. The radiative lifetime is defined as (Eq. 18):

$$\tau_0 = \frac{1}{A_{U1}} \quad \dots \text{Eq. 18}$$

which is the time taken to diminish the population to 1/e of its initial concentration. This first order exponential decay may be recorded by a pulsed laser able to pulse at picosecond (ps) intervals.⁸⁶ The lifetime is important because it determines the time available for the fluorophore to interact with or diffuse in its environment. Einstein showed that the probability of spontaneous emission is proportional to the corresponding absorption probability and the frequency of the transition to the third power. This derivation established a relationship between the strength of absorption and the spontaneous emission lifetime (i.e., the natural radiative lifetime). Knowledge of the natural radiative lifetime provides an indication of the expected lifetime in the absence of any non-radiative decay pathways.⁸⁷ The Einstein coefficients for absorption and emission were derived initially for atoms in vacuum. Strickler and Berg⁸⁸ proposed a method for calculating the natural or radiative lifetimes (τ_0) of molecules having broad absorption and emission bands. The Strickler-Berg derived equation uses parameters derived from spectral data as shown below:

$$1/\tau_0 = 2.880 \times 10^{-9} n^2 \langle \nu_f^{-3} \rangle_{AV}^{-1} \int \epsilon(\nu) d \ln \nu \quad \dots \text{Eq. 19}$$

$$\text{where } \langle \nu_f^{-3} \rangle_{AV} = \frac{\int \nu^{-3} F(\nu) d\nu}{\int F(\nu) d\nu}$$

- Chapter 1 -

In this equation, ν is the wavenumber (cm^{-1}), $F(\nu)$ is the fluorescence intensity in units of relative numbers of quanta, $\epsilon(\nu)$ is the molar absorption coefficient at a particular wavenumber, and n is the refractive index of the solvent. The fluorescence quantum yield (Φ_F) is described by the ratio of the observed fluorescence lifetime (τ_F) and the calculated natural radiative lifetime (τ_0), as shown below. In practice one usually knows Φ_F and wants to gain knowledge about the actual fluorescence lifetime:

$$\Phi_F = \frac{\tau_F}{\tau_0} \quad \dots \text{Eq. 20}$$

Given an absorption spectrum and an emission spectrum, Eq. 20 can be used to calculate the natural radiative lifetime. In conjunction with the experimentally measured quantum yield of fluorescence and the natural radiative lifetime derived from the Strickler-Berg equation, the expected fluorescence lifetime can be calculated. The equation however is only valid for molecules that do not interact with the solvent and that do not undergo geometric changes from the ground state to the excited state.⁸⁹ The most important application that has arisen from the fluorescence of phthalocyanines and porphyrins is the imaging of tumour tissue, as tumours are slightly more selective to these macrocycles. Fluorescence lifetimes for phthalocyanine compounds typically range from 1 to 7 ns.⁹⁰

1.9.2 Fluorescence quantum yields

In general, quantum yields may be described as the number of emitted photons relative to the number of absorbed photons. Practically the fluorescence quantum yields may be determined by a relative method using a reference material. Compounds that have known fluorescence quantum yields in specific solvents such as ZnPc in DMSO ($\Phi_F = 0.18$)⁹¹ may be used for unknown determinations. These measurements involve the absorption spectra as well as the emission spectra of a sample wherein the optical density is less than 0.1 due to fluorescence quenching at higher concentrations. The fluorescence quantum yields may thus be determined using Eq. 21, which is derived in the same manner as the singlet oxygen quantum yields above (Eq. 14):

$$\Phi_F = \Phi_{Fstd} \frac{A_s \times ABS_{st} \times \eta_s}{A_{st} \times ABS_s \times \eta_{st}}$$

... Eq. 21

Where A_s and A_{st} are the respective areas of the sample and standard under the emission bands (determined by simply adding up the relative emission of the Q-band and its vibrational bands). ABS_s and ABS_{st} are the absorptions at the excitation wavelengths of the sample and standard, respectively. Different excitation wavelengths may be used for excitation. η_s and η_{std} are the refractive indexes of the solvents used for the sample and standard respectively. Φ_F and Φ_{Fstd} are the fluorescence quantum yields of the sample and standard, respectively.

1.9.3 Triplet lifetimes and quantum yields

Deactivation of the triplet state, 3M , to the ground state, S_0 , may be described as in Eq. 22:

$$-\frac{d[{}^3M]}{dt} = k_1[{}^3M] + k_2[{}^3M][S_0] + 2k_3[{}^3M]^2 \dots \text{Eq. 22}$$

Where k_1 is the measured first order rate constant and is the sum of the radiative and non-radiative decay processes of the triplet state. The second term is due to quenching of the excited triplet state by ground state molecules, i.e., self quenching and the final term is due to quenching of the triplet state by another triplet state. The last two terms may be eliminated by using low sensitizer concentrations and using low laser power. The rate constant k_1 may thus be obtained from $\ln [{}^3M]_t - \ln [{}^3M]_0 = k_1 t$ (where $[{}^3M]_t$ and $[{}^3M]_0$ are the triplet concentrations at time zero and t respectively) and plotting $\ln [{}^3M]_t - \ln [{}^3M]_0$ vs t . The change in triplet concentration with time is directly proportional to the transmittance and thus the voltage measured on the oscilloscope. The change in absorbance (ΔA) may thus be calculated from the Beer-Lambert law:

$$\Delta A = \epsilon c l = \ln \frac{I_0}{I} = \ln \frac{V_\infty}{V_\infty - \Delta V} \dots \text{Eq. 23}$$

Where V_∞ is the 0-100% voltage and ΔV is the change in voltage observed. Linear plots of $\ln(A)$ versus time reveal the gradient k_1 and thus the triplet

- Chapter 1 -

lifetime by definition is determined by $\tau_t = 1 \times (k_1)^{-1}$. Triplet extinction coefficients, ϵ_t , were determined by the singlet depletion method.⁹² The triplet maximum absorption at ~ 490 nm as well as the singlet maximum absorption at ~ 690 nm were then related by $(\Delta A)_{490} = \epsilon_t[{}^3\text{Pc}]l$ and $(\Delta A)_{690} = \epsilon_s[{}^3\text{Pc}]l$ where $[{}^3\text{Pc}]$ is the concentration of triplet phthalocyanine molecules and ϵ_s is the singlet state extinction coefficient. Therefore, ϵ_t is given by Eq. 24

$$\epsilon_t = \frac{(\Delta A)_{490} \epsilon_s}{(\Delta A)_{690}} \quad \dots \text{Eq. 24}$$

Using values of ϵ_t from Eq. 24 the triplet quantum yields may then be determined by Eq. 25⁹³:

$$\Phi_x = \Phi_{st} \frac{(\Delta A)_x \epsilon_{st}}{(\Delta A)_{st} \epsilon_x} \quad \dots \text{Eq. 25}$$

where Φ_x and Φ_{st} are the triplet quantum yields of sample and standard, ΔA_x and ΔA_{st} are the respective absorbance changes at the triplet maxima of the sample and standard, ϵ_x and ϵ_{st} are the triplet extinction coefficients of the sample and standard, respectively. With photophysical studies done for this study it was aimed to gain a better understanding of the effects of molecular structure on the fluorescence as well as the triplet properties of the silicon octaphenoxy phthalocyanines. Furthermore with isomerically pure compounds that are not aggregated it is possible to attempt theoretical correlation of the experimentally determined results with the theoretical Strickler-Berg equation.

1.10 Electrochemistry of phthalocyanines

Cyclic voltammetry was used as the electrochemical technique in this study. Cyclic voltammograms provide information on the reversibility, kinetics, formal reduction potentials as well as formal oxidation potentials of a system. Generally when a redox potential is observed while applying a potential scan an oxidation in the system will result in an anodic peak current (i_{pa}) and a reduction in the system will give a cathodic peak current (i_{pc}). The peak potentials (anodic peak potential (E_{pa}), cathodic peak potential (E_{pc})) are then also obtained from the voltammogram. Eq. 26 then defines the half wave potential ($E_{1/2}$):

$$E_{1/2} = \frac{1}{2}(E_{pa} + E_{pc}) \quad \dots \text{Eq. 26}$$

The difference in the redox potentials (ΔE) allows the determination of the number of electrons involved as in Eq. 27:

$$\Delta E = E_{pa} - E_{pc} = \frac{RT}{nF} \quad \dots \text{Eq. 27}$$

Where R is the gas constant ($8.314 \text{ J.K}^{-1} \text{ mol}^{-1}$), T the temperature in Kelvin, n the number of electrons and F is Faraday's constant. At 298 K $RT/nF = 0.059 \text{ V/n}$ and thus in a reversible one electron process $\Delta E = 0.059 \text{ V}$. A reversible system is one wherein the starting reagent is regenerated after oxidation or reduction and during both processes a rapid exchange of electrons between the working electrode and the molecule has taken place. Mathematically for

- Chapter 1 -

reversible reactions $\frac{i_{pa}}{i_{pc}} = 1$ and the current is defined by the Ilkovic equation

(Eq. 28):

$$i_p = 2.69 \times 10^5 n^{3/2} A D^{1/2} C \nu^{1/2} \quad \dots \text{Eq. 28}$$

Where i_p is the peak current, n the mol equivalents, A the electrode area, D the diffusion coefficient, C the analyte concentration and ν the scan rate.

Cyclic voltammograms that show a single oxidation or reduction wave indicate an irreversible system. Slow electron exchange or chemical reactions at the electrode surface are common reasons for irreversibility. Quasi-reversibility may be seen when the return peak current is smaller than its couple or when a larger peak potential separation is observed than is the case for reversible systems. A very large peak current separation (> 200 mV) indicates irreversibility. The current may be controlled by mass transport of reactant and product or by competing charge transfer reactions.⁹⁴ Since some electrochemical properties of selected phthalocyanines were probed, it is necessary to include in this literature a survey of examples of cyclic voltammograms of selected compounds to illustrate the basic cyclic voltammetric behaviour of the phthalocyanines. The electrochemistry of metallophthalocyanine species is very rich with many redox processes. Incorporation of different metals into the core of the phthalocyanine ring and variations in the substituents on the periphery of the ring result in complexes that have varied properties.⁹⁵ Redox processes occurring in MPc complexes may be centred at the phthalocyanine ring or at the central metal and are

- Chapter 1 -

affected by several factors⁹⁶, including i) the nature of the substituents on the phthalocyanine ring, ii) the nature and oxidation state of the central metal, and iii) the nature of the axial ligands and solvents. Changes in the oxidation states often result in reversible and dramatic colour changes because of ring based redox processes in MPc complexes.⁹⁵ Pc is a dianion represented as Pc(-2). It is possible to observe two successive one-electron oxidations of the phthalocyanine ring by removal of electrons from the a_{1u} orbital and four successive one-electron reductions into the e_g orbital (Fig. 9). If metal orbitals lie at energies within the highest occupied molecular orbital (HOMO)-lowest unoccupied molecular orbital (LUMO) gap of the ring, oxidation or reduction, or both, may occur at the central metal.⁹⁵

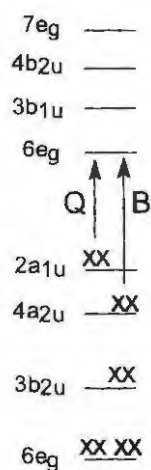


Fig. 9. The origin of the so-called Q and B bands in the UV-Visible spectrum of phthalocyanines

Typical ring based redox processes are shown by the cyclic voltammogram of zinc(II)tetraneopentoxophthalocyanine⁹⁷ [ZnTnPc(-2)] in 1,2 dichlorobenzene containing 0.2 M tetrabutylammonium perchlorate (TBAP) vs Ag/Ag⁺. Two oxidation couples at 1.23 V and 0.55 V and two reduction couples at -0.98 V

- Chapter 1 -

and -1.24 V were observed. The oxidation couples correspond to two one electron removals from the phthalocyanine ligand and thus the formation of the π -cation radical species $[\text{ZnTnPc}(1-)]^+ / [\text{ZnTnPc}(0)]^{2+}$ and $[\text{ZnTnPc}(2-)] / [\text{ZnTnPc}(1-)]^+$. The two reduction couples are summarised in Table 1.

Table 1 Reduction couples of zinc(II)tetraneopentoxophthalocyanine

$E_{1/2} / \text{V vs Ag/Ag}^+$	Assignment
-0.98	$[\text{ZnTnPc}(2-)] \rightarrow [\text{ZnTnPc}(3-)]^{1-}$
-1.24	$[\text{ZnTnPc}(3-)]^{1-} \rightarrow [\text{ZnTnPc}(4-)]^{2-}$

In cyclic voltammetry the reduction or oxidation of the metal centre of metallated phthalocyanines can also be observed, for example, the oxidation of cobalt in cobalt(II)tetrasulfonated phthalocyanine **46** occurs at lower potentials than the oxidation of the ligand⁹⁸, the cyclic voltammogram shown in .. 10 shows the $\text{Co}^{\text{II}} / \text{Co}^{\text{III}}$ couple indicated by **A** and the $\text{Co}^{\text{II}} / \text{Co}^{\text{I}}$ couple indicated by **B**.

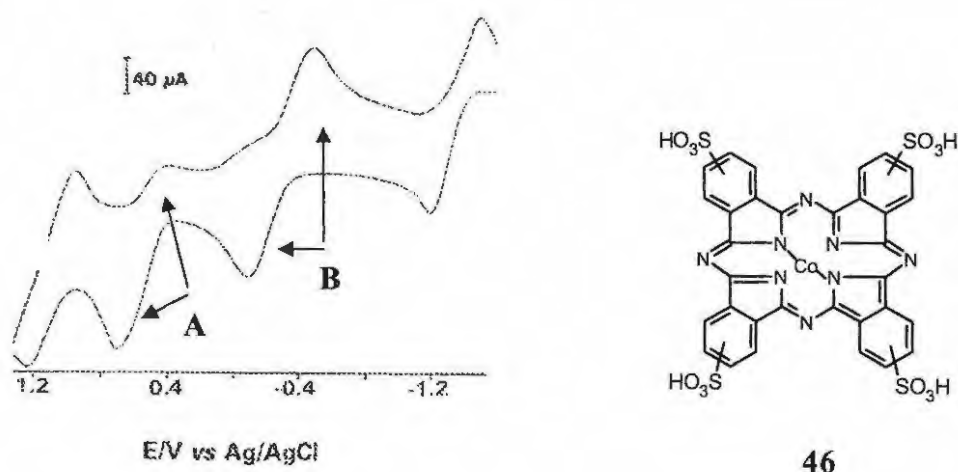


Fig. 10. Cyclic voltammogram of cobalt tetrasulfonated phthalocyanine (**46**) in DMF.⁹⁹

- Chapter 1 -

No metal-based processes occur in SiPc complexes. It is typically found that the cyclic voltammograms of silicon naphthalocyanines and phthalocyanines exhibit two reductions and two oxidations as in the cyclic voltammogram of bis(tri-*n*-hexylsiloxy) (2,3-naphthalocyaninato) silicon [SiNc(OR)₂]¹⁰⁰ which shows two reversible one electron transfers. The average values of the reduction and oxidation potentials of the naphthalocyanine and its phthalocyanine analog obtained at several scan rates are given in Table 2 versus the saturated calomel electrode (SCE). Noticeable is that while it is easier to oxidize the naphthalocyanine than its phthalocyanine analog, potentials for the reduction processes are nearly the same.

Table 2. E_{1/2} values for SiPc(OR)₂ and SiNc(OR)₂ in CH₂Cl₂.

	SiPc(OR) ₂ , V vs. SCE	SiNc(OR) ₂ , V vs. SCE
2 nd ox.		+1.24
1 st ox.	+1.00	+0.58
1 st red.	-0.90	-1.01
2 nd red.	-1.48	-1.55

The study of the electrochemical behaviour of silicon octaphenoxy phthalocyanines is an intended aim of this study. The cyclic voltammograms may provide valuable clues as to the mechanism of the redox behaviour during photochemical experimentation.

1.11 Characterisation of phthalocyanines

1.11.1 $^1\text{H-NMR}$ spectroscopy of phthalocyanines

The 2,9,16,23-tetrasubstituted phthalocyanines generally exhibit broad absorptions in the aromatic and other spectral regions in $^1\text{H-NMR}$ spectroscopy due to the presence of four isomers.¹⁰¹ Similarly 1,8,15,22-tetrasubstituted phthalocyanines or analogs can exist as a distribution of four isomers.¹⁰² Phthalocyanines however may give well-defined $^1\text{H-NMR}$ spectra if they are symmetrical or if they are sterically hindered and do not form isomers. This was demonstrated by the work of Leznoff et al.¹⁰³ who found that by condensing 3-*p-n*-butylbenzyloxyphthalonitrile in lithium octoxide the resultant 1,8,15,22-tetra(*p-n*-butylbenzyl-oxy)phthalocyanine existed as a single isomer.¹⁰³ The presence of the bulky butylbenzyloxy groups thus sterically inhibits the formation of isomers.

1.11.2 UV-visible spectroscopy of phthalocyanines

The UV-Visible spectra of phthalocyanines are characterised by two distinct bands referred to as the Q-band and the Soret (or B) band (Fig. 11). The Q-band is in the visible region of the spectrum and is usually found at wavelengths above 600 nm while the Soret band is found at ~ 350 nm.¹⁰⁴ The electronic transitions responsible for the absorptions are the lower energy $2a_{1u}$ to $6e_g$ for the Q-band and the $4a_{2u}$ to $6e_g$ transition for the B-band as shown in Fig. 9 for a metallated phthalocyanine.^{105,106,107} The arrows indicate that a



- Chapter 1 -

single electron that increases in energy will be responsible for the indicated Q or B bands as seen in Fig. 9.

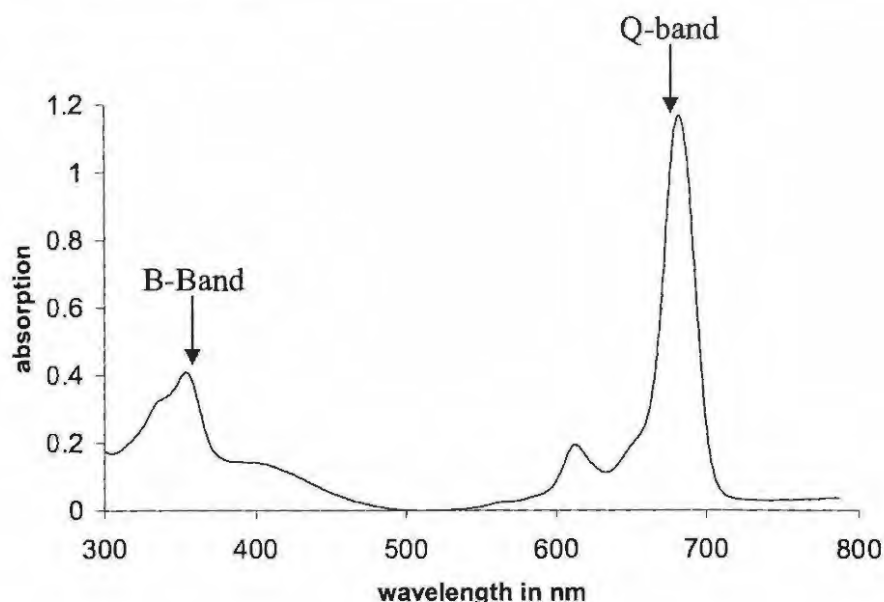


Fig. 11. A typical UV-visible spectrum for metallated phthalocyanines showing the Q-band and the B-band (or Soret Band).

Tetra- and octa-substituted phthalocyanines have a tendency to induce an upward Q-band shift, that is, a shift towards longer wavelengths of Q-band maximas. Of particular interest is the effect of alkoxy¹⁰⁸ and the amino¹⁰⁹ groups. For example, tetraamino vanadyl naphthalocyanine ((NH₂)₄VONc) shows the Q-band maximum at 870 nm in quinoline. Absorption coefficients of the Q band of metallated naphthalocyanines are generally found larger than those of metallated phthalocyanines with similar substituents. Together with the longer wavelength shift of the Q-band, the Soret band region also spreads towards longer wavelengths on going from phthalocyanines to naphthalocyanines.

1.11.3 IR spectroscopy

The infrared spectra of various tetra-*tert*-butylated phthalocyanines are shown in Fig. 12. The spectra of the phthalocyanines are somewhat complex. Except for the bands assignable to the *tert*-butylated phthalocyanines, the characteristic bands common to metallated phthalocyanines are observed at 670-700, 750-790 (C-H out of plane bending), 840-850, 940-945, 1090-1120 (C-H in-plane bending), 1140-1147, 1200-1210, 1240-1290, 1305-1320, 1400-1430, 1490-1540 and 1600-1625 (benzene ring vibrations).¹¹⁰ The bands at 670-700, 750-790, 1240-1300 and 1400-1430 are well-defined doublets and those at 1090-1120 quite intense.

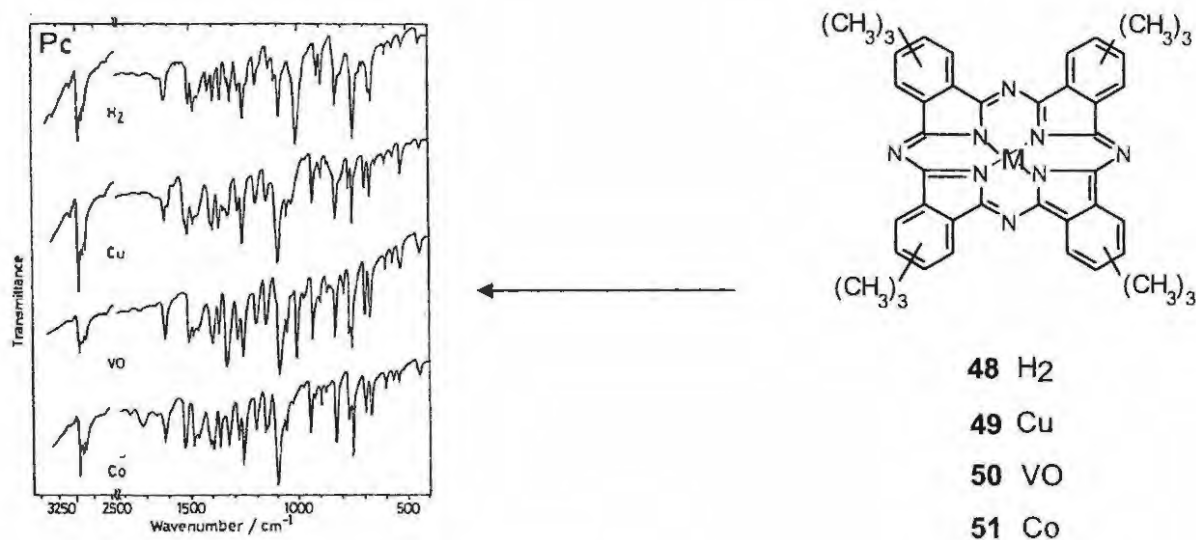


Fig. 12. Infrared spectra of phthalocyanines.¹¹⁰

Silicon phthalocyanines have characteristic bands in the infrared spectra due to the Si-O interactions. A Si-O stretch is prevalent at $\sim 1040 \text{ cm}^{-1}$ and this is assigned to the Si-O-Si stretching vibration.²⁷ A weak band at 864 cm^{-1} is attributed to the Si-O bond.

- Chapter 1 -

1.12 Summary of aims

This introduction chapter thus highlighted the intentions of this thesis, which were firstly to synthesise isomerically pure, peripherally substituted phthalocyanines that may aid in increasing the organic solvent solubility of the phthalocyanine macrocycle and additionally increase the red light absorbing properties of the macrocycle. Variations in the molecule was done by changing the axial ligands in order to further increase organic solvent solubility and hopefully have a molecule that plays an important part in the localization of silicon phthalocyanines *in vivo*. Since the currently approved PDT drug, hematoporphyrin derivatives (HPD) contain a mixture of oligomers which seem to be the active component in PDT action, oligomers of the silicon phthalocyanine molecules wherein the oligomerisation was perpetuated on the silicon metal was deemed a valuable study. The ability of the various axially substituted silicon phthalocyanines to generate singlet oxygen in solution is an important aspect of this work as well as the photodegradation behaviour of these compounds upon prolonged exposure to light. With photophysical studies done for this study it was aimed to gain a better understanding of the effects of molecular structure on the fluorescence as well as the triplet properties of the silicon octaphenoxy phthalocyanines. Furthermore, with isomerically pure compounds that are not aggregated it is possible to attempt theoretical correlation of the experimentally determined results with the Strickler-Berg equation.⁸⁸ The study of the electrochemical behaviour of selected silicon octaphenoxy phthalocyanines in the form of cyclic voltammograms may provide valuable clues as to the mechanism of the redox behaviour during photochemical experimentation.

-Chapter 2-

Results and Discussion

2.1 Introduction

The synthetic work undertaken in this study led to the production of 24 different axially substituted silicon phthalocyanines. The syntheses were done by conventional methods as well as the novel microwave synthesis of axial substitution. Oligomeric silicon phthalocyanines were also produced, although in low yields. These compounds' photochemical (singlet oxygen quantum yield, photodegradation and phototransformation rates and quantum yields) and photophysical (fluorescence quantum yields and fluorescence lifetimes as well as triplet quantum yields and triplet lifetimes) properties were then studied with a good correlation being found between the experimental and theoretical (Strickler-Berg equation) fluorescence lifetime values. Two processes were observed during the photodegradation process (phototransformation of the axial ligands occurred together with photodegradation). Some aspects of the mechanism of phototransformation of axial ligands have been studied in this work, but this is still not completely understood and thus a few processes that may result in central silicon atom hydroxylation will be discussed. The final section describes the electrochemistry of selected molecules using different electrode surfaces to probe the nature of these molecules.

-Chapter 2-

2.2 Synthesis

In the synthetic work undertaken many aspects were first considered before embarking on the synthesis of the silicon phthalocyanine compounds. Firstly, solubility was of great importance for the oligomers to be synthesised as well as for their application in PDT. To a lesser extent increased solubility was expected to increase product yields of the axial modification of silicon phthalocyanines. The insolubility of the symmetrical phthalocyanine structure is well known and although central metals do increase solubility in many cases the corresponding dichloro silicon phthalocyanine is not soluble enough for purposes of this thesis, thus the initial phthalonitrile was modified to contain two phenoxy groups on their 4,5 positions.

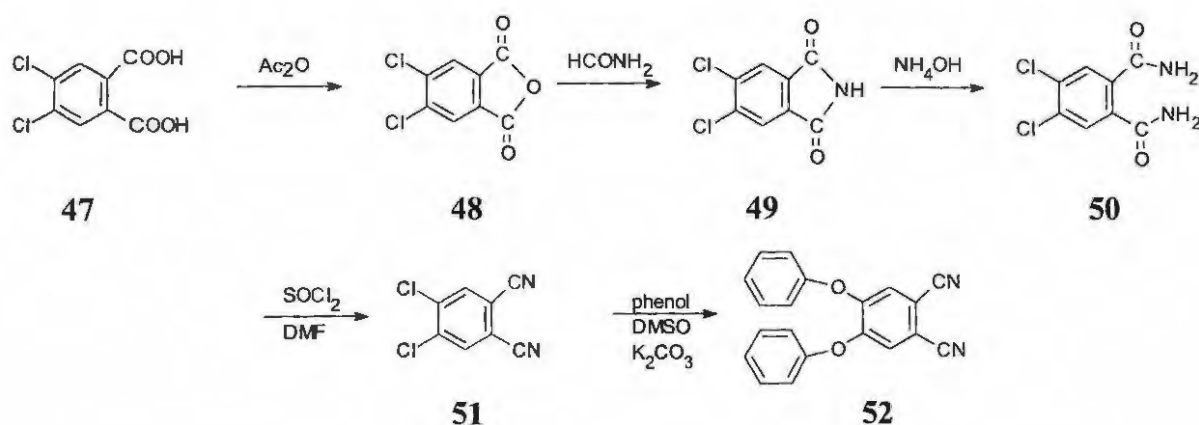
This would then lead to an octaphenoxy silicon phthalocyanine which in fact, as the dichloro derivative, was conveniently soluble in chloroform, DMF and DMSO. The purity of the eventual silicon phthalocyanines was of importance and in this regard it was thought that the diiminoisoindoline derivatives would lead to a greater purity of eventual product.

-Chapter 2-

The phenoxy groups were also expected to effect a red-shift of the Q-band of the eventual phthalocyanines due to the slight electron donating effect of these groups.

2.2.1 Synthesis of 4,5-diphenoxyphthalonitrile

Due to the availability of 4,5-dichlorophthalic acid **47** in our laboratory, the following reaction pathway (Scheme 20) was followed toward the synthesis of 4,5-diphenoxyphthalonitrile **52**.¹¹¹



Scheme 20. The synthesis of 4,5-diphenoxyphthalonitrile **52**, Ac = acetyl.

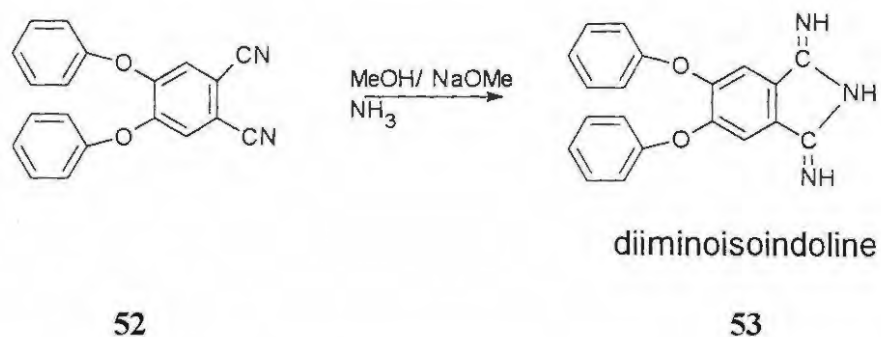
The first step of the synthesis is the trickiest one due to the build-up of acetic acid, which is formed as a by-product during this step. The acetic acid causes

-Chapter 2-

equilibrium with the acetic anhydride to be present in the system and thus lowers the product yields. This may be overcome by allowing the acetic acid to distill off while the reaction is in progress and practically this is done by lowering the temperature of the reaction mixture to below the boiling point of acetic anhydride. Distillation leads to higher reaction yields and the ensuing reactions are straightforward. Furthermore, dry solvents and reagents increase reaction yields, especially in the thionyl chloride step.

The final step leading to the 4,5-diphenoxypthalonitrile **52** requires the reaction temperature to be set to $\sim 90^{\circ}\text{C}$ and should definitely not be above 100°C . Although this compound may be used to synthesize a silicon phthalocyanine, the reaction products are invariably quite impure and yields are below 60%. A more reactive starting material for the SiPc is thus desirable and in this study it was formed by converting **52** into the diiminoisoindoline **53** as outlined below.

-Chapter 2-



Scheme 21. The synthesis of diphenoxy diiminoisoindoline **53**.

As is shown in Scheme 21, the phthalonitrile **52** is converted to the diiminoisoindoline **53** by bubbling ammonia through a methanol solution of the phthalonitrile with a catalytic amount of sodium methoxide. This then completes the synthesis of a phthalocyanine precursor containing two phenoxy groups. As mentioned before this was done in order to increase the red absorbing properties of the eventual phthalocyanine as phenoxy groups are more electron donating than hydrogen atoms and this is desirable for molecules to be used as sensitizers in photodynamic therapy.

-Chapter 2-

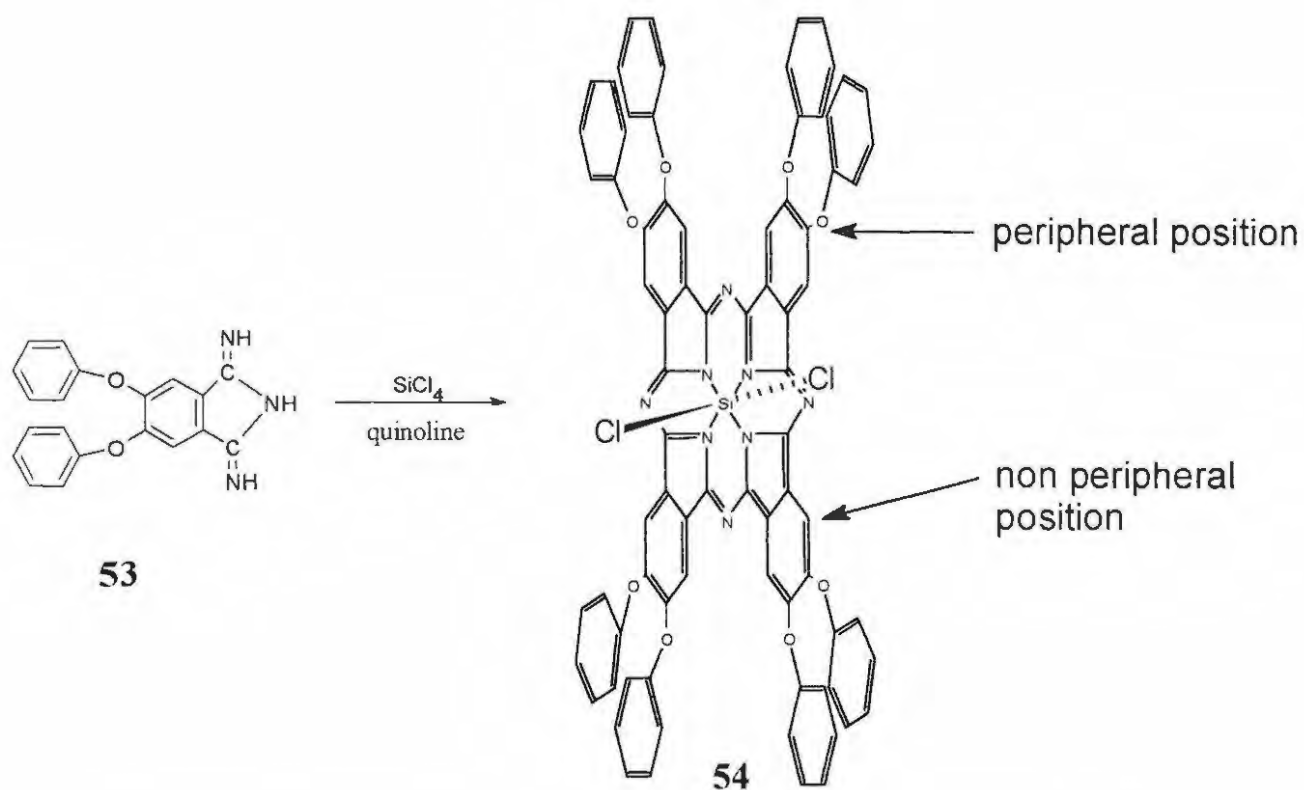
2.2.2 Synthesis of octaphenoxy silicon phthalocyanine^a

In addition to the red-shift, phenoxy groups were also expected to increase the solubility of the phthalocyanine molecule and additionally give it some lipophilic character which may be beneficial in biological applications. The diiminoisoindoline **53** was then reacted with silicon tetrachloride (SiCl_4) in dry quinoline resulting in a 67% yield of the dichloro silicon octaphenoxyphthalocyanine **54** accordingly shown in Scheme 22.

This reaction did work very well in terms of product yield (67%) and the reaction was repeated for comparison using diphenoxy phthalonitrile **52** with SiCl_4 in quinoline. With the diphenoxy phthalonitrile **52**, a messier reaction ensued with some sublimation taking place, which was notably absent in the reaction using diphenoxy diiminoisoindoline **53**. The reaction products, using **52** as reactant, were not easily purified in comparison to the use of **53**.

^a Published as M. David Maree and T. Nyokong, *J. Porphyrins. Phthalocyanines*, **5**, 555-563 (2001).

-Chapter 2-



Scheme 22. Synthesis of dichloro silicon octaphenoxyphthalocyanine **54**.

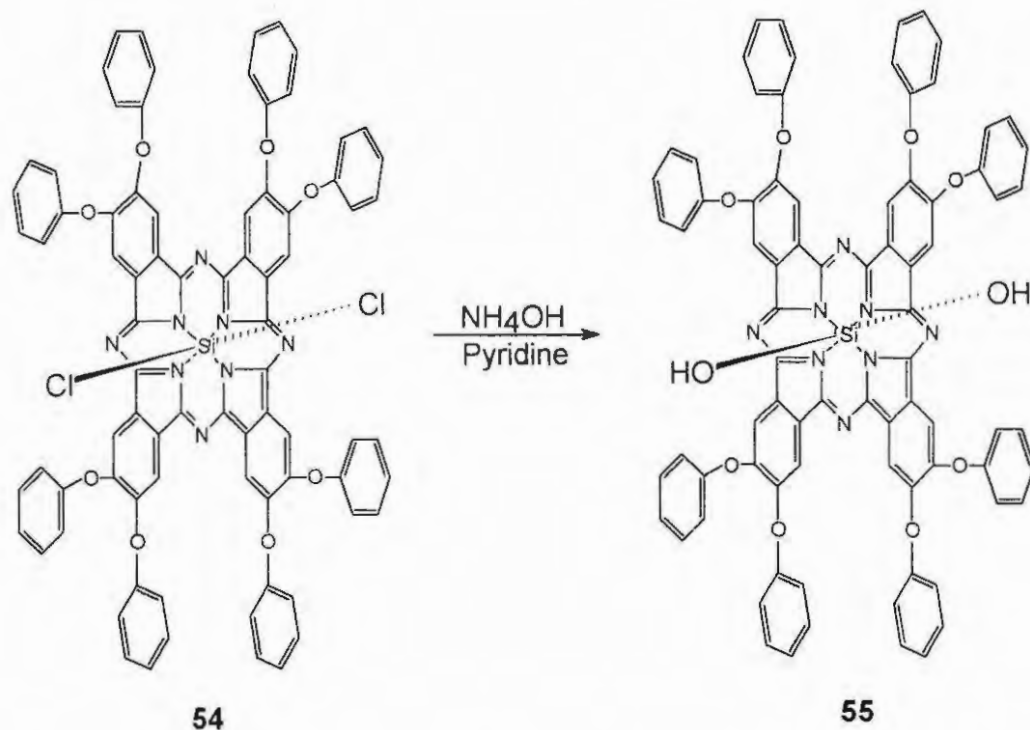
Unlike the unsubstituted dichloro silicon phthalocyanine **5**,¹¹² compound **54** is purified by Soxhlet extraction with methanol, yielding a very pure complex, which is soluble in many organic solvents, including, chloroform, DMF and DMSO.

-Chapter 2-

In fact, compound **54** is soluble enough in chloroform to allow structure determination by use of $^1\text{H-NMR}$ spectroscopy. The axial hydrolysis reaction of compound **54** may be performed by one of several methods including reaction in ethanol with sodium methoxide or sodium ethoxide as base.¹¹³ The method of choice, however, is a reflux reaction in a 50:50 solution of pyridine and 25% ammonium hydroxide, Scheme 23.¹¹⁴ The reaction takes approximately 5h and gives a complete axially hydrolysed silicon phthalocyanine **55**. This reaction is a typical hydrolysis reaction wherein hydroxyl groups replace the chlorine atoms. The reaction time is rather long and this is due to the chloride atoms leaving ability being diminished by the nature of the phthalocyanine ring.

This compound was necessary for comparison purposes, as it is known that in unsubstituted dichloro silicon phthalocyanine **5**, air hydrolysis takes place over time¹¹⁵ and it proved to be important in this work during the photochemical reactions as the octaphenoxy dihydroxy silicon phthalocyanine **55** was produced during photolysis.

-Chapter 2-



Scheme 23. Synthesis of the dihydroxy silicon phthalocyanine **55**.

Compound **55** was found to be much more insoluble in all organic solvents compared to compound **54**. The same property was observed in the unsubstituted silicon phthalocyanine compound **5**.¹¹⁴ Although compound **55** could be used in the synthesis which follow, it was found more convenient to use the dichloro compound **54**, this had to do with the increased solubility and thus less reaction time and additionally more complete reactions. The decreased solubility of compound **55** is probably due to the increased hydrogen bonding on the axial positions as illustrated below (Fig. 13).

-Chapter 2-

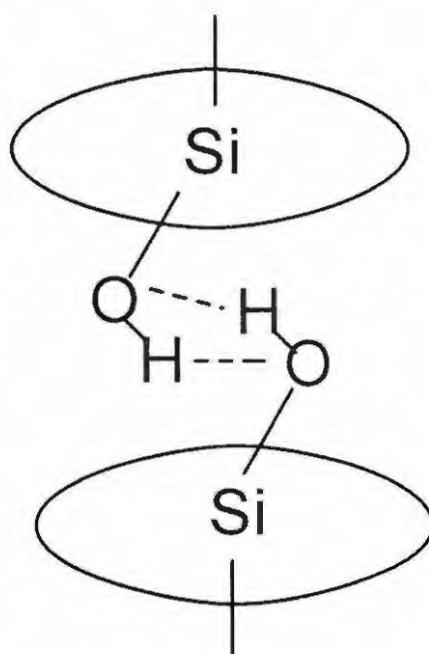



Fig. 13. Hydrogen bonding in compound **55**  = Pc ring.

Due to the insolubility of **55** its $^1\text{H-NMR}$ spectrum is not available, but it could be partially characterised by IR and its formation from **54** is witnessed by the appearance of bands at 3393 cm^{-1} and also at 831 cm^{-1} , which are attributed to the hydroxyl function. The IR spectrum is shown below (Fig. 14) and the two compounds (**54** and **55**) have remarkably similar spectra with the obvious exception of the hydroxyl peak appearance at 831 cm^{-1} and at 3353 cm^{-1} for compound **55**.

-Chapter 2-

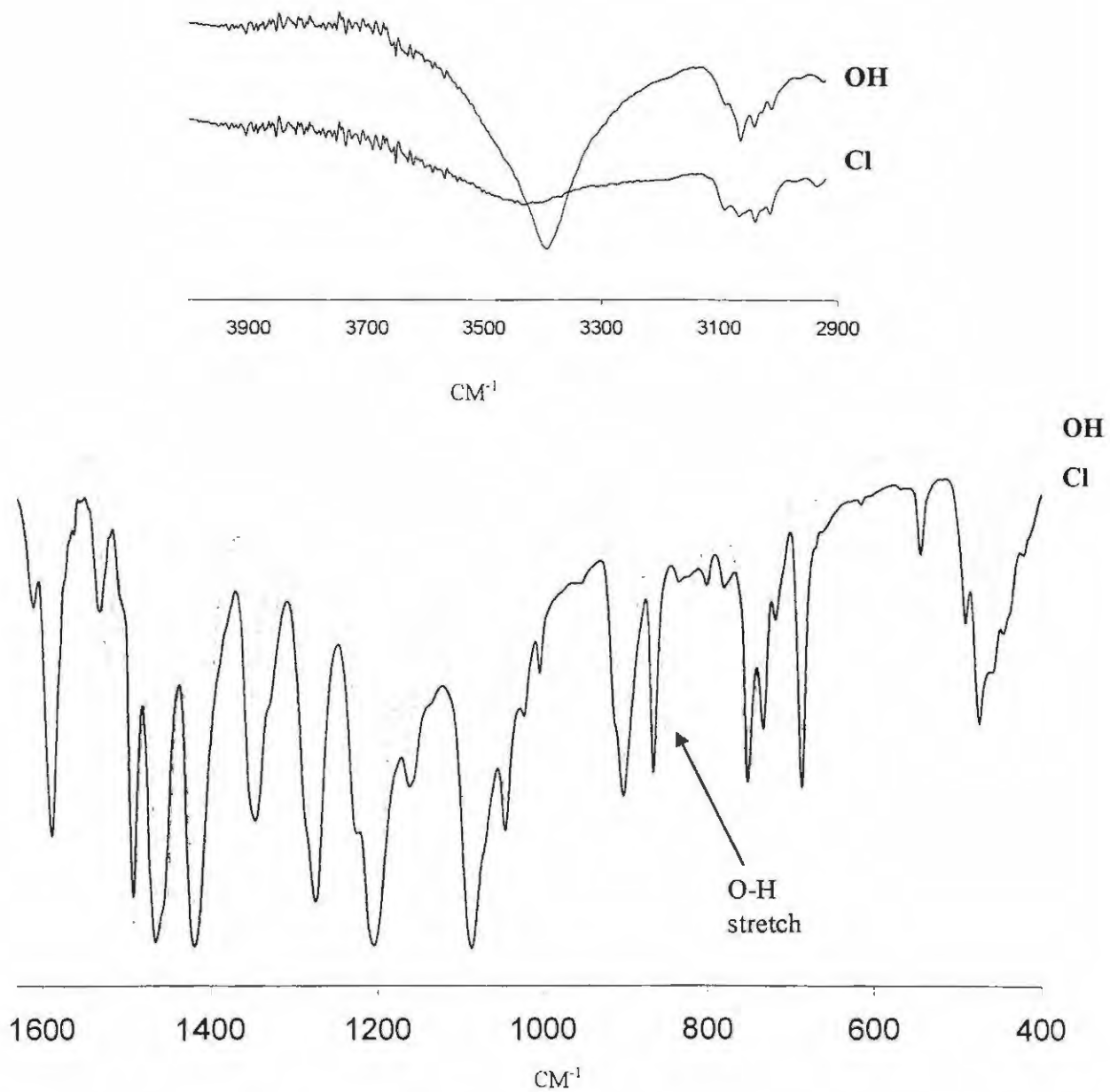


Fig. 14. The IR spectra of compounds 54 and 55 overlain.

-Chapter 2-

The UV-visible spectra of compounds **54** (Fig. 15) and **55** are, however, practically identical and thus this could not be used as part of the characterization process of compound **55**. Since compound **55** was insoluble, **54** was used for the axial substitution reactions of the phthalocyanines to be discussed below.

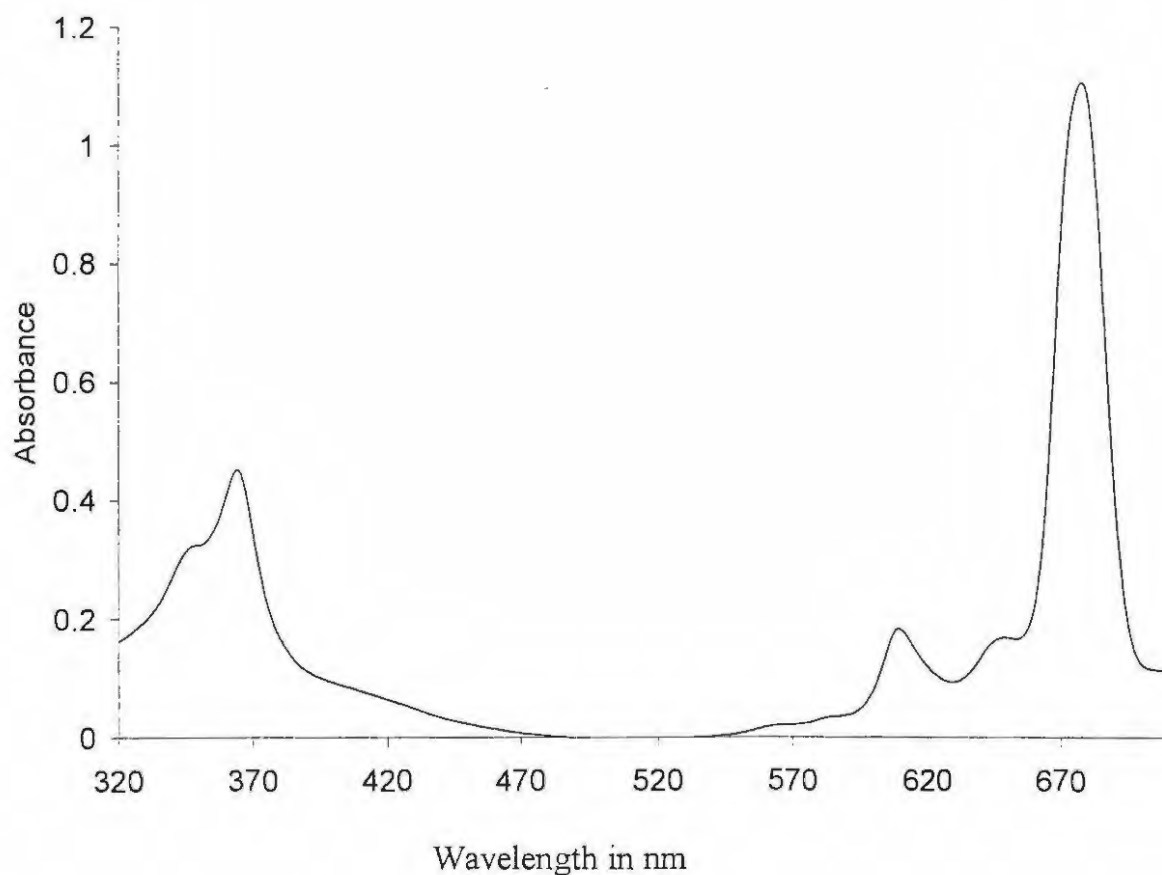
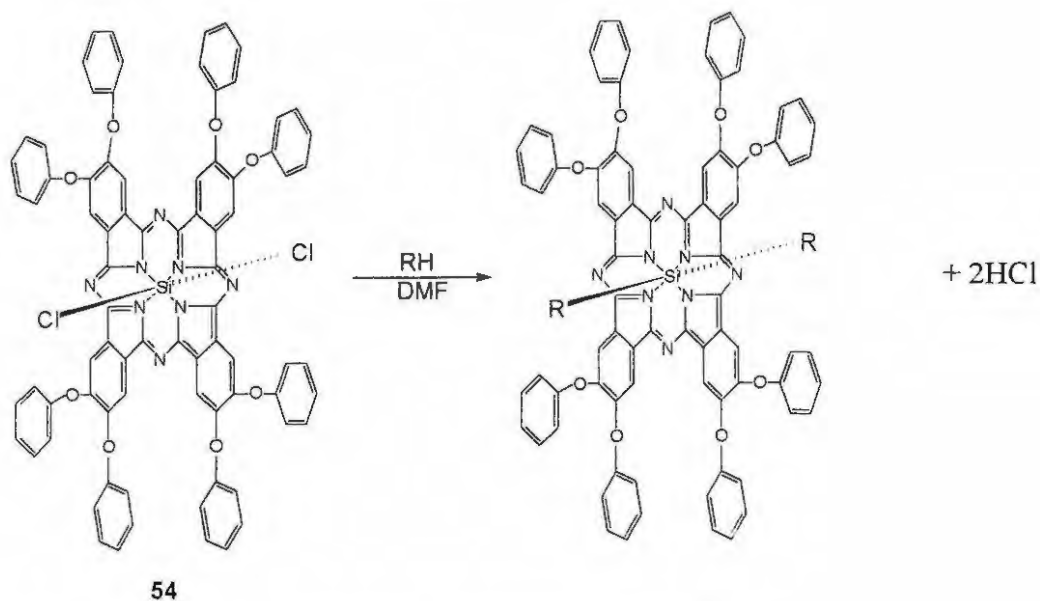


Fig. 15. The UV-visible spectrum of compound **54**.

-Chapter 2-

2.2.3 Synthesis of axially-substituted phthalocyanines

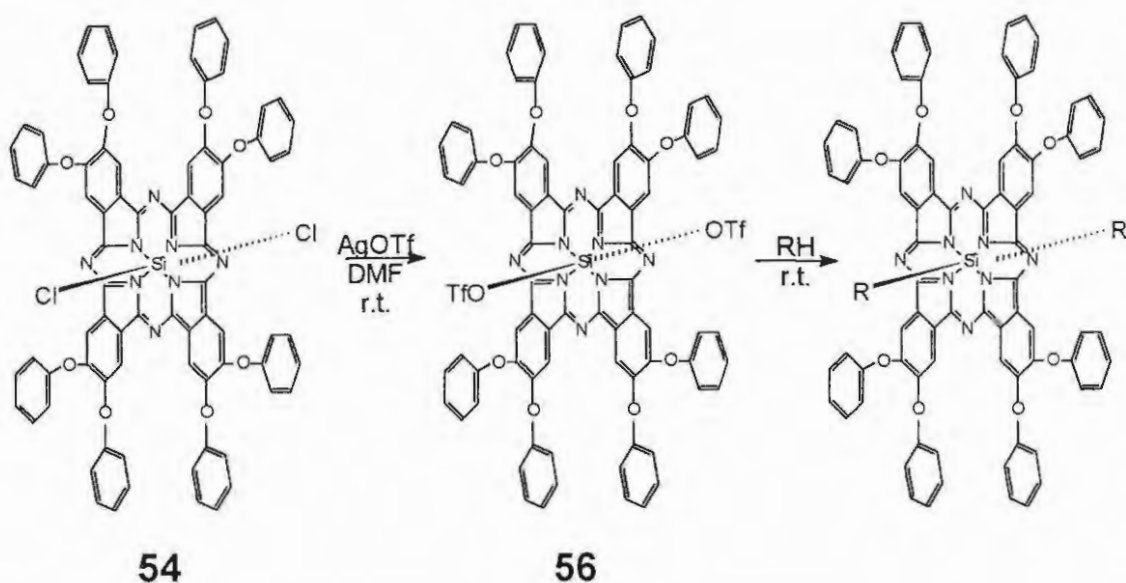
The synthesis of the 18 compounds formed by axial ligand substitution of Cl in dichloro silicon octaphenoxypthalocyanine **54** makes up the bulk of the synthetic work of this thesis and the range of compounds made caters for a variety of electronic environments. The choice of reagents was limited to those that possess acidic protons, which are naphthols, phenols, alcohols, acids, sulphonic acids and silanols. These reagents are a particularly attractive choice because most of them are easily separated from the reaction products by solvent extraction. The exceptions, however, are the two silanols and succinic anhydride that have to be separated by means of preparative thin layer chromatography (TLC). The general reaction scheme is shown below, Scheme 24.



Scheme 24. Axial substitution of phthalocyanine **54**.

-Chapter 2-

During the course of this work, four methods of axial ligand substitution were evaluated. Firstly, the established method of axial substitution using tetrahydronaphthalene as solvent was found to work well but the separation of the products was not easily done, since tetrahydronaphthalene is a high boiling solvent and is also not water-soluble. Another way to attach axial ligands to the silicon phthalocyanine structure is to mimic a method used for hydroxy aluminum phthalocyanine with silver triflate as a coupling agent.¹¹⁶ In this reaction, which is done at room temperature, the silver triflate oxygen acts as a nucleophile to replace the abstracted chlorine atoms as is shown in Scheme 25.



Scheme 25. Silver triflate activated axial ligand substitution, Tf = triflate, r.t. = room temperature.

-Chapter 2-

It was, however, found that the coupling does not proceed as completely as in the case reported for aluminum phthalocyanine, yields below 50% were obtained in the case of $(Cl_2)SiOPPc$. It has been documented that the dihydroxyl silicon phthalocyanines are not able to form sodium salts upon reaction with sodium as their aluminum counterparts do.¹¹⁷ This is thus an indication that the hydroxy protons may not be acidic enough to form stable complexes with the sodium triflate and thus lower yields of axially substituted products result. The method that was initially found to work the best was a reflux reaction in DMF of **54** and the axial ligand of interest. This resulted in yields in excess of 95% for all but three of these green axially substituted compounds. These reactions needed approximately 30 minutes to complete. The DMF reactions probably work the best due to enhanced solubility of the phthalocyanine reagents in this solvent. In addition to this, is the possibility of a more complete recovery of materials due to the water-solubility of the DMF resulting in easy product separation (all products are hydrophilic) from the solvent.

The fourth method using microwave irradiation was found to reduce reaction times without the use of a solvent and will be discussed in more detail in section 2.2.4. The axially substituted SiPc compounds **57** to **73** are shown in Fig. 16. Herein the axial ligands are indicated on the central figure as being the X component.

-Chapter 2-

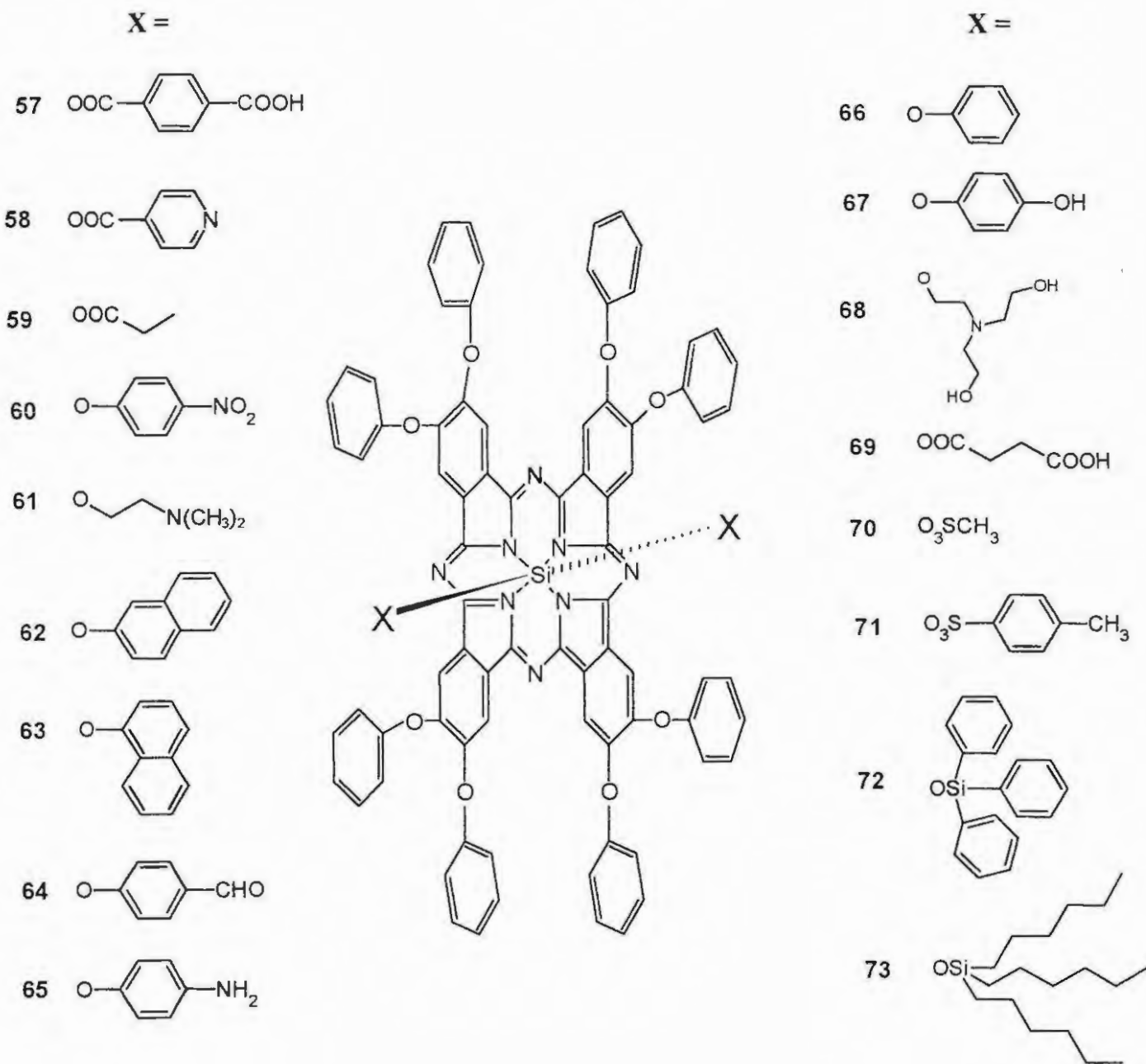


Fig. 16. Axially substituted octaphenoxy silicon phthalocyanines made in this study.

-Chapter 2-

Reaction times of the DMF solutions exceeding 1 hr were not desirable since a blue compound formed instead of the green compound expected for **60** in a test reaction of p-nitrophenol (as an axial ligand) with dichloro silicon octaphenoxyphthalocyanine **54**. This blue compound had a wavelength ~ 20 nm lower than that of the desired product and no further attempt was made to characterize it. The reactants were thus added to refluxing DMF and allowed to react for approximately 30 mins. (reaction completion was initially determined by TLC). The products of these condensation reactions were worked up in three different ways after quenching with water.

1) Excess ligands present following the synthesis of compounds **57**, **58**, **60**, **62**, **63**, **64**, **65**, **66**, and **67** were removed by dissolving the precipitate (containing both the unreacted acidic axial ligand compounds and the phthalocyanine) in chloroform and extracting with a 10% NaOH solution. The last step removed the base-soluble reagents completely as could be witnessed by clear colour changes in the aqueous layers. Compound **65** was additionally washed with a 1M HCl solution. The chloroform layer was then evaporated off to yield compounds **57**, **58**, **60**, **62**, **63**, **64**, **65**, **66**, and **67** all in quantitative yields (excess of 95%).

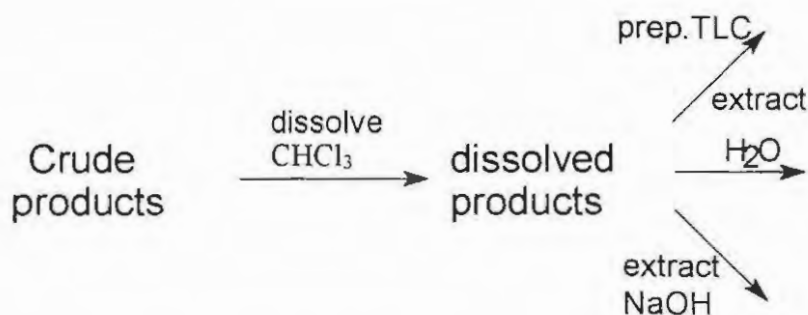
-Chapter 2-

2) Excess ligands from the synthesis of **61**, **68**, **70** and **71** were removed by dissolving the respective precipitates in chloroform and washing with water (removing all the water-soluble acidic reagents), the chloroform was again evaporated off to give **61**, **68**, **70** and **71** in quantitative yields (greater than 95%).

3) Compounds **69**, **72** and **73** were isolated from their respective precipitates by TLC using chloroform as an eluent to give the following yields for **69** (82%), **72** (57%) and **73** (60%). Compound **69** actually showed three products after the reaction and these were the phthalocyanine (green), the anhydride (colourless) and also the succinic acid (colourless). These three products separate well chromatographically.

The three methods of workup are summarised below, Scheme 26

-Chapter 2-



Scheme 26. Summary of the workup procedures followed, prep. = preparative.

The yields of compounds **69**, **72** and **73** are lower due to the necessary chromatographic step and especially compounds **72** and **73** had only 60% yields which may be attributed to the decreased acidity of the silanol hydroxyl groups. The axial ligands confer lipophilic and in some cases (compounds **57**, **61**, **65**, **69**) slight hydrophilic properties although none of the compounds synthesised are water-soluble. It is expected that the variety of axial ligands will cause the molecules to behave differently in *in vivo* as well as in *in vitro* studies with regards to cell uptake, and will contribute to determining a structure-activity relationship for these types of compounds in photodynamic cancer therapy.

Compounds **67** and **68** possess terminal hydroxyl functions and these functions have been proven to be beneficial in cellular attachment and uptake.¹¹⁸ Compound **58** possesses pyridine terminal groups and this could be beneficial to

-Chapter 2-

deoxyribonucleic acid (DNA) or ribonucleic acids (RNA) binding or even protein binding. The lipophilic terminal groups are expected to increase cellular attachment or uptake in comparison to the non-lipophilic substituents. This has been observed in other studies.¹¹⁹

2.2.4 Synthesis by microwave irradiation^b

Microwave irradiation was also used to effect the exchange of the axial chloro ligands in compound **54** for the ligands listed in Table 3. Some of the compounds utilized in this study are not good microwave absorbers and thus straight reaction with the phthalocyanine did not deliver any product. In these cases an alumina bath was used which is claimed to be a good hyperfrequency beam absorber¹²⁰. The chromatographic grade aluminium oxide has a resonant frequency in the correct range for the absorption of microwaves. Typically the experiments required a homogenous solid mixture of compound **54** and the acidic compound to be used as an axial ligand. This solid mixture was then irradiated in a microwave oven using the quantities and in the reaction times listed in Table 3.

^b published as M. David Maree and T. Nyokong, *J. Chem. Res.*, **4** (2001).

-Chapter 2-

Table 3 Reaction details for axial modifications using microwave irradiation.

Reagent Product nr.	Quantity (g)	Reaction time (mins.)	Alumina	Yield (%)
<i>p</i> -nitrophenol 60	0.4	3.5	yes	95
Dimethylaminoethanol 61	0.4	4	no	96
2-naphthol 62	0.4	3	yes	93
1-naphthol 63	0.4	3	yes	94
<i>p</i> -hydroxy benzaldehyde 67	0.4	3	yes	94
Triethanolamine 68	0.4	4	no	93
Succinic anhydride 69	0.4	4.5	yes	95

The yields were all in excess of 92%. The complexes formed were characterised by ¹H-NMR and elemental analysis. The ¹H-NMR peaks of the axial ligands showed considerable upfield shifts on coordination to the phthalocyanine macrocycle, as has been the case for all axially ligated compounds thus far. This method of axial substitution is a significant improvement on the previous methods used due to the fact that no solvent is required, reaction yields are satisfactory and reaction times are short. The microwave synthesis of these axially substituted compounds is dependant upon the melting of the acidic compound used. The shortening of the reaction times, however, also points to the catalytic effect of the microwave radiation in the reactions. Axially substituted phthalocyanines were

-Chapter 2-

also made by just melting the acidic compound on a heat source (not microwave) in the presence of **54**. The reaction times in this method are relatively long and reaction yields are low thus the increase in product yield and decrease in reaction time warrants the microwave assisted method of axially substituting silicon phthalocyanines.

Recently there has been a report on the microwave assisted synthesis of silicon phthalocyanines¹²¹ using a solvent claimed to improve reaction yields and this was investigated. Reaction of both the diphenoxy phthalonitrile **52** as well as the diphenoxy diiminoisoindoline **53** with SiCl_4 in quinoline was investigated under microwave irradiation conditions. Each of **52** or **53** was added to a sample vial with quinoline and silicon tetrachloride. The vials were then irradiated for 15 minutes and allowed to cool to room temperature. The workup was as for the conventional methods as discussed above. It was found that a moderate (~10%) increase in reaction yield was prevalent for the diiminoisoindoline reagent (total of 80% yield) and the dicyanobenzene reagent reacted to give the dichloro silicon phthalocyanine in 75% yield. The yields do not differ to such an extent as in the conventional methods above. Again the reduction in reaction times indicates a strong specific microwave effect upon the reaction pathway.

-Chapter 2-

2.2.5 Synthesis of oligomers^c

Compounds **74** to **78** (Fig. 17) were synthesised from bis(chloro) silicon octaphenoxyphthalocyanine **54** by refluxing a solution of the phthalocyanine in dry DMF under nitrogen. To this solution was added terephthalic acid in the amounts required for the different oligomers (see Chapter 3 for details) that was previously completely dissolved in dry DMF. The reaction was monitored by TLC and upon completion p-hydroxybenzaldehyde was added to the DMF solution and reflux was continued until the reaction was complete. The reaction mixture was allowed to cool and water was added to quench the solution. After filtration the precipitate was washed with a 10% NaOH solution until the phenol and acid were washed out completely. A final wash with water and drying at 60°C under vacuum delivered the impure product which was then further purified by preparative TLC using chloroform as an eluent to deliver products **74** to **78**.

^c published as M. David Maree and T. Nyokong, *J. Photochem. Photobiol. A: Chem.*, **142**, 39-46 (2001)

-Chapter 2-

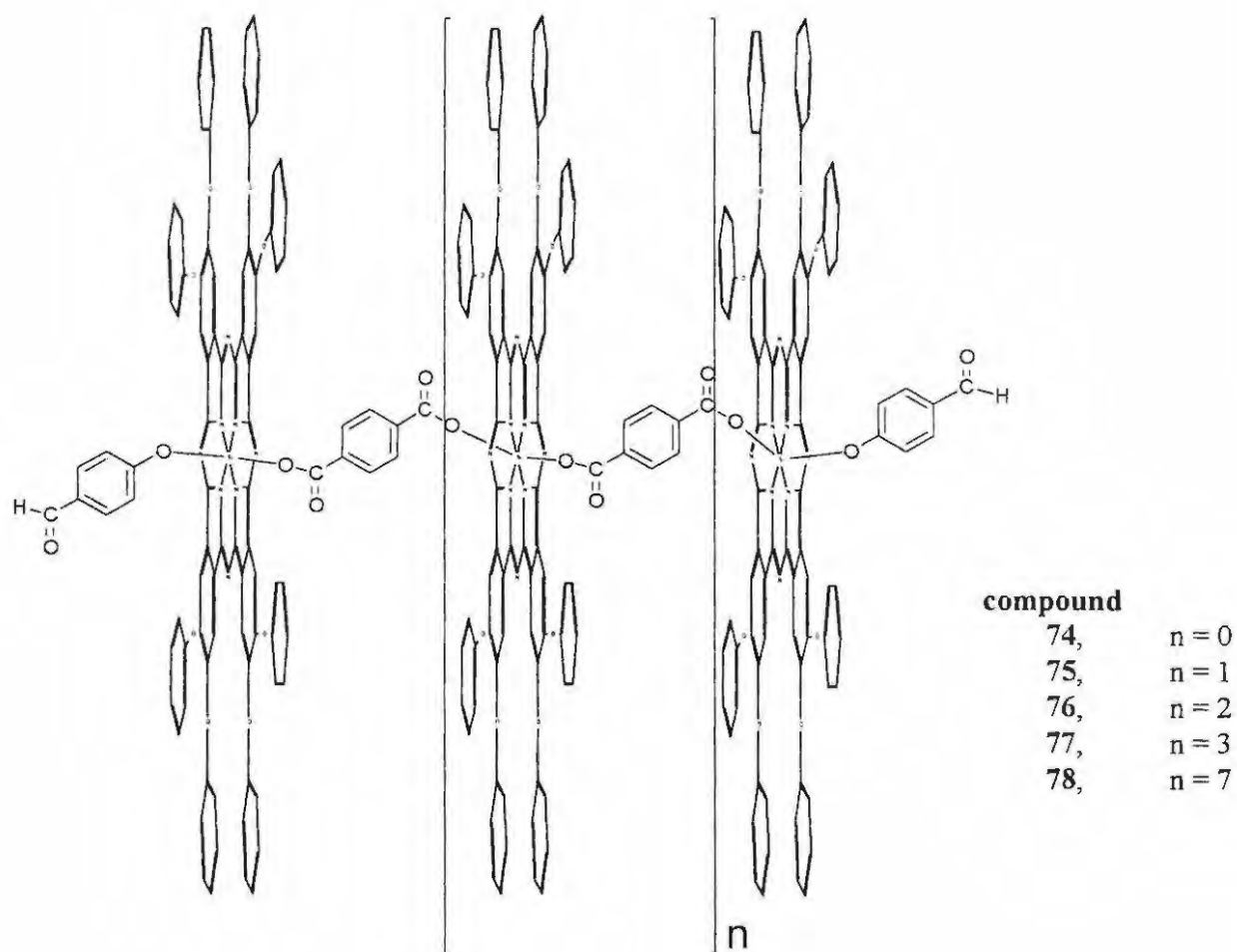


Fig. 17. Structures of the oligomers 74 to 78 synthesised.

-Chapter 2-

The synthetic procedures used are similar to polymerisation reactions using exact molar amounts of substance and thus it is vitally important to have all components dissolved before attempting reactions. The use of p-hydroxybenzaldehyde is a convenient way to terminate the oligomers to enable simple $^1\text{H-NMR}$ determination of the degree of oligomerisation due to the formyl proton having a very distinct shift of > 9.2 ppm which is well clear of the non-peripheral phthalocyanine proton shift at ~ 9 ppm.

The highest reaction yields were obtained by slow addition of the terephthalic acid to a solution of the dichloro silicon phthalocyanine **54**, thus minimizing monomer formation. This happens due to the statistical distribution of the acid units that do not favour reaction of two acid units with a single phthalocyanine unit. Due to the very low amounts of terephthalic acid used in the reactions a 10 ml solution was generally made with a tenfold excess of the required acid and then 1 ml of this solution was added to the reaction mixture. The rate of addition was approximately 0.2 ml per minute. The solubility generally decreased with an increase in the degree of oligomerisation. The yields of these reactions are low but acceptable in comparison to the axial ligation reactions of monomeric species due to the statistical nature of the reactions and the effect of reagent purity especially prominent in the formation of compound **78**.

-Chapter 2-

2.3 Spectroscopic characterization

2.3.1 ¹H-NMR spectroscopy

Table 4 shows the ¹H-NMR data for all the silicon octaphenoxyphthalocyanine compounds synthesised in this work.

Table 4 ¹H-NMR (number of protons in brackets) data for the (X)₂SiOPPc compounds.

Compound	¹ H-NMR data of Pc Ring	¹ H-NMR data of Pc ligand
54 Bis(chloro) silicon octaphenoxyphthalocyanine	9.21 (8, s), 7.50 (16, t), 7.30 (24, m)	-
55 Bis(hydroxy) silicon octaphenoxyphthalocyanine	low solubility	-
57 Bis(terephthaloyl) silicon octaphenoxyphthalocyanine	8.96 (8, s), 7.50 (16, t), 7.31 (24, m)	6.95 (4, d), 5.18 (4, d)
58 Bis(isonicotinoyl) silicon octaphenoxyphthalocyanin	8.98 (8, s), 7.51 (16, t), 7.33 (24, m)	7.61 (4, d), 4.97 (4, d)
59 Octaphenoxyphthalocyanina to bis(propionato) silicon	8.99 (8, s), 7.50 (16, t), 7.32 (24, m)	-0.8 (4, q), -1.1 (6, t)
60 Bis(<i>p</i> -nitrophenoxy) silicon octaphenoxyphthalocyanine	8.94 (8, s), 7.53 (16, t), 7.32 (24, m)	6.59 (4, d), 2.44 (4, d)
61 Bis(2-aminoethoxy) silicon octaphenoxyphthalocyanine	8.95 (8, s), 7.49 (16, t), 7.35 (24, m)	1.23 (2, s), -1.28 (4, t), - 2.47 (4, t)
62 Bis(2-naphthyl) silicon octaphenoxyphthalocyanine	9.00 (8, s), 7.51 (16, t), 7.29 (24, m)	7.05 (2, d), 6.93 (4, m), 6.43 (2, d), 6.21 (2, d), 2.79 (2, s),

-Chapter 2-

63 Bis(1-naphthyl) silicon octaphenoxyphthalocyanine	8.98 (8, s), 7.47 (16, t), 7.30 (24, m)	7.04 (4, t), 6.92 (4, m), 6.44 (2, d), 6.18 (2, d)
64 Bis(<i>p</i> -formyl phenoxy) silicon octaphenoxyphthalocyanine	8.96 (8, s), 7.50 (16, t), 7.32 (24, m)	9.14 (2, s), 6.26 (4, d) 2.54 (4, d)
65 Bis(<i>p</i> -amino phenoxy) silicon octaphenoxyphthalocyanine	9.02 (8, s), 7.51 (16, t), 7.32 (24, m)	5.04 (4, d), 3.22 (4, s), 2.26 (4, d)
66 Bis(phenoxy) silicon octaphenoxyphthalocyanine	8.98 (8, s), 7.49 (16, t), 7.28(24, m)	5.76 (4, t), 5.65 (4, t), 2.41 (2, d)
67 Bis(<i>p</i> -hydroxy phenoxy) silicon octaphenoxyphthalocyanine	8.97 (8, s), 7.49 (16, t), 7.29 (24, m)	5.12 (4, d) 3.48 (2, s), 2.27 (4, d)
68 Bis(diethanolamino-2- ethoxy) silicon octaphenoxyphthalocyanine	9.04 (8, s), 7.53 (16, t), 7.30 (24, m)	0.95 (8, t), 0.5 (8, s), - 1.21 (4, t), -2.20 (4, t)
69 Bis(succinoyl) silicon octaphenoxyphthalocyanine	9.05 (8, s), 7.51 (16, t), 7.32 (24, m)	-0.91 (4, t), -2.10 (4, t)
70 Bis(methane sulfonoyl) silicon octaphenoxyphthalocyanine	8.98 (8, s), 7.57 (16, t), 7.34 (24, m)	0.28 (3, s)
71 Bis(<i>p</i> -toluene sulphonoyl) silicon octaphenoxyphthalocyanine	8.49 (8, s), 7.48 (40, m),	7.21 (8, m), 2.95 (6, s)
72 Bis(triphenylsiloxy) silicon octaphenoxyphthalocyanine	8.92 (8, s), 7.54 (16, t), 7.30 (24, m)	6.81 (6, d), 6.53 (12, t), 4.88 (12, t)

-Chapter 2-

73 Bis(tri-n-hexyl siloxo) silicon octaphenoxypthalocyanine	9.02 (8, s), 7.49 (16, t), 7.29 (24, m)	0.91 (12, t), 0.73 (18, d), 0.51 (12, t), -1.20 (12, t), -2.41 (12, d)
74 Oligomeric dimer	9.16 (2, s), 9.00 (16, s), 7.51 (32, t), 7.29 (48, m)	6.31 (4, d), 2.87 (4, d), 2.57 (4, d)
75 Oligomeric trimer	9.15 (2, s), 8.99 (16, s), 8.97 (8, s), 7.50 (48, m); 7.30 (72, m)	6.30 (4, d), 2.89 (8, m), 2.58 (4, d)
76 Oligomeric tetramer	9.15 (2, s), 9.00 (16, s), 8.98 (16, s), 7.50 (64, m), 7.30 (96, m)	6.29 (4, d), 2.87 (12, m), 2.60 (4, d)
77 Oligomeric pentamer	9.16 (2, s), 8.99 (16, s), 8.97 (16, s), 8.95 (8, s), 7.49 (80, m), 7.29 (120, m)	6.31 (4, d), 2.89 (16, m), 2.57 (4, d)
78 Oligomeric nonamer	9.15 (2, s), 9.00 (16, s), 8.98 (16, s), 8.96 (40, m); 7.50 (144, m); 7.30 (216, m)	6.30 (4, d), 2.89 (32, m), 2.57 (4, d)

The $^1\text{H-NMR}$ spectra of the silicon phthalocyanines are interesting in the sense that two extremes are observed on the same molecule. Due to the conjugated macrocycle, a ring current above and below the plane of the flat molecule is present.¹²² This ring current results in extreme deshielding of the protons on the periphery of the molecule and oppositely extreme shielding of any protons on the axial positions of the molecule. All the silicon octaphenoxo phthalocyanine

-Chapter 2-

complexes reported in this work show $^1\text{H-NMR}$ spectra that are well defined, thus in phthalocyanine terms, this indicates isomeric purity. The future of phthalocyanine drugs is to have isomerically pure compounds that are well characterised. The dihydroxyl compound **55** was not sufficiently soluble in chloroform for NMR analysis. As mentioned above the NMR shifts of phthalocyanine compounds are highly dependent upon the conjugated nature of the phthalocyanine ring. Deshielding of protons of the starting materials occurs on formation of the phthalocyanine ring.

For example, diphenoxy dicyanobenzene **52**, which is a precursor to the silicon octaphenoxypthalocyanine complexes, displayed a singlet integrating for 2 protons (the 3, 6 protons) at a chemical shift of 7.33 ppm. The protons responsible for this singlet shifted to 9.21 ppm in the dichloro octaphenoxypthalocyanine silicon complex **54** indicating that the protons are deshielded due to the anisotropic effect of the conjugated molecule. Fig. 18 shows the $^1\text{H-NMR}$ spectrum of compound **54** with the 3, 6 protons of the dicyanobenzene **52** superimposed.

-Chapter 2-

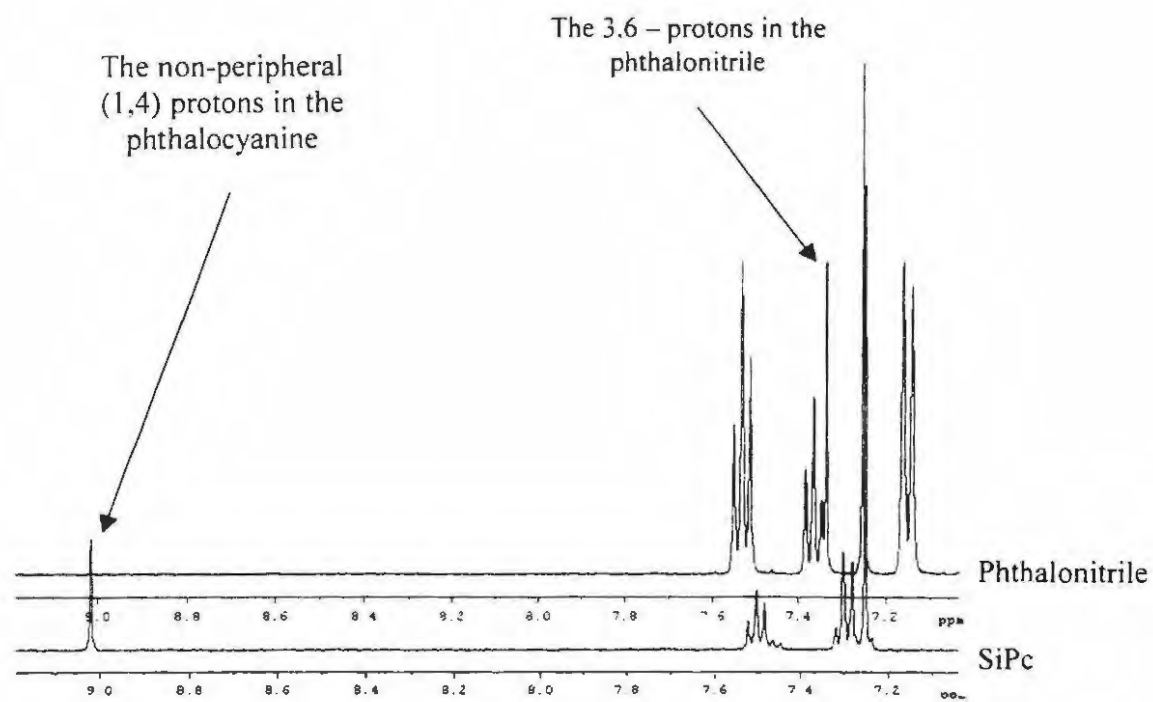
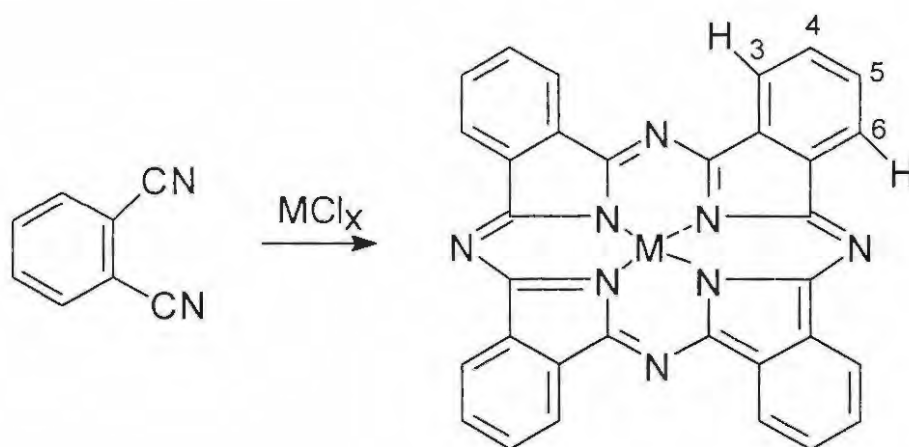


Fig. 18. The $^1\text{H-NMR}$ spectrum of compounds **52** and **54** in CDCl_3 overlain

-Chapter 2-

This NMR spectrum is thus the basic structure for almost all of the derivatives to be discussed and as such warrants explanation. The singlet at 9.21 ppm is due to the so-called non-peripheral protons (Scheme 27) on the phthalocyanine (also referred to as the 1,4 protons). Each phthalocyanine ring has 8 of these protons.



Scheme 27 The 8 non-peripheral (or 1,4) protons on the macrocycle

-Chapter 2-

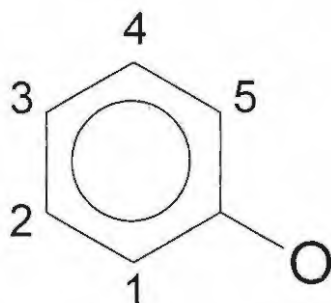


Fig. 19 $^1\text{H-NMR}$ assignments for the phenoxy group on the octasubstituted phthalocyanine

The triplet at 7.50 ppm comes from the protons on the phenoxy ring closest to the oxygen atoms (indicated as 2 and 4 in Fig. 19), and as such with two neighbouring protons has a triplet multiplicity. Remembering that there are two phenoxy groups on each phthalonitrile there are 16 of these protons in total on the phthalocyanine. At 7.30 ppm there is a triplet and a doublet superimposed upon each other, this multiplet is due to the remaining protons on the phenoxy ring (indicated at positions 1, 3 and 5 in Fig. 19) and there are 24 of them (these resonances are also marked as “phenoxy” in Fig. 20).

The axially modified silicon phthalocyanine compounds show well-defined resonance's due to the axial ligands, in addition to those of the peripheral phenoxy groups. The axial ligands retained their multiplicities following coordination to

-Chapter 2-

the silicon phthalocyanine complexes and integrate correctly. The opposite effect that was observed for the phthalocyanine non-peripheral protons, which are deshielded compared to the parent dicyanobenzene, was manifested in a shielding effect of the protons on the axial ligands. Based on the above it may be said that ^1H -NMR data unequivocally proves that bonding of the axial ligands takes place onto the phthalocyanine. The nature of the bond has been proven to be a strong covalent bond involving the central silicon atom in the phthalocyanine and the oxygen atoms in the axial ligands.¹²³

This shielding of the axial ligand protons was so intense for protons close to the phthalocyanine ring that aromatic axial ligand protons were observed as low as 2.44 ppm for compound **60** as compared to a usual aromatic resonance of at least 7 ppm. Fig. 20 shows the ^1H NMR spectrum for compound **60** with the resonances of the aromatic axial ligand protons enlarged. The upfield shift of the axial ligand protons is most likely due to the combined effects of the nitro group and the phthalocyanine ring.

-Chapter 2-

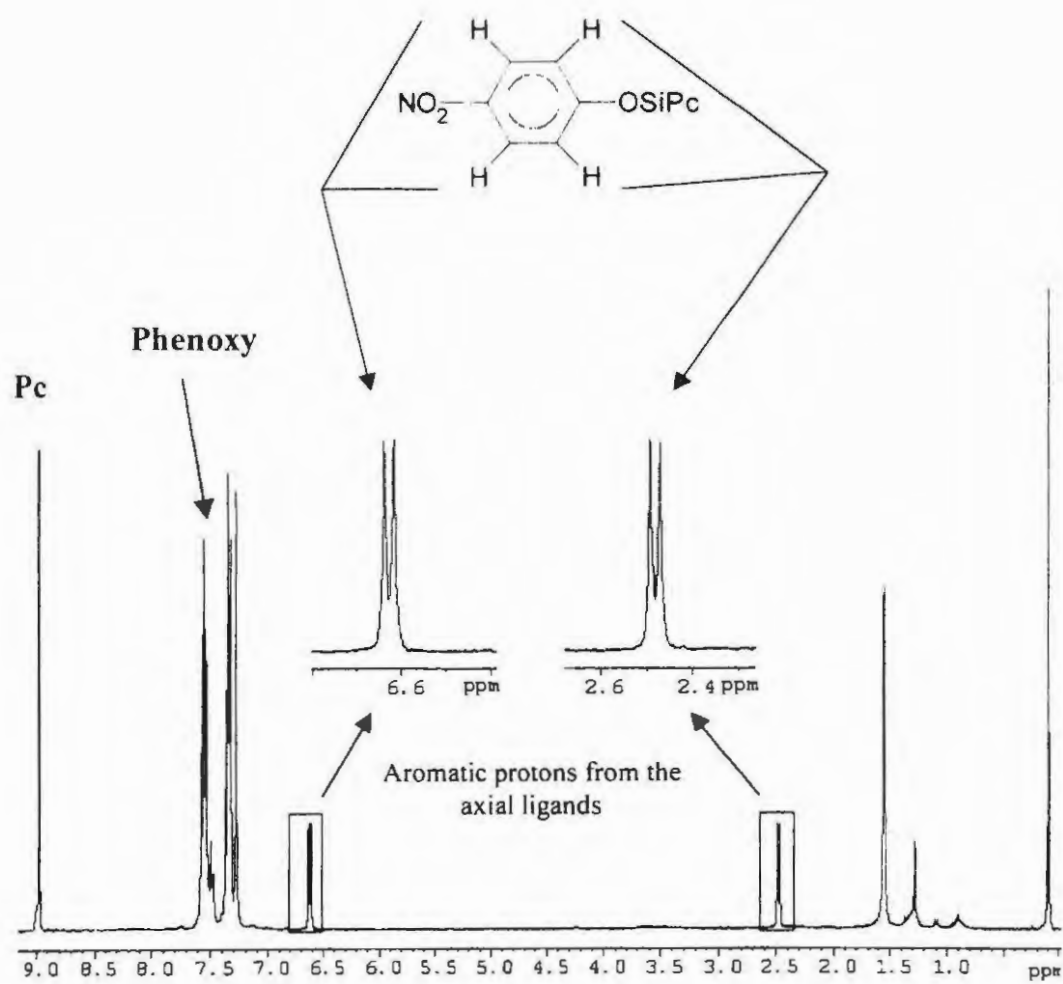


Fig. 20 ¹H-NMR spectrum of compound 60 in CDCl₃ with aromatic protons at 2.44 ppm

-Chapter 2-

Aliphatic protons are also affected in the same manner and depending on the proximity to the ring resonances are observed negative to TMS. Fig. 21 shows the ^1H -NMR spectrum of compound **61** in the aliphatic region where the coupled aliphatic protons of the axial ligands increase in ppm value, as they are further away from the phthalocyanine ring.

Fig. 22 summarizes the resonances of the axial ligands of compounds **57** to **73**

-Chapter 2-

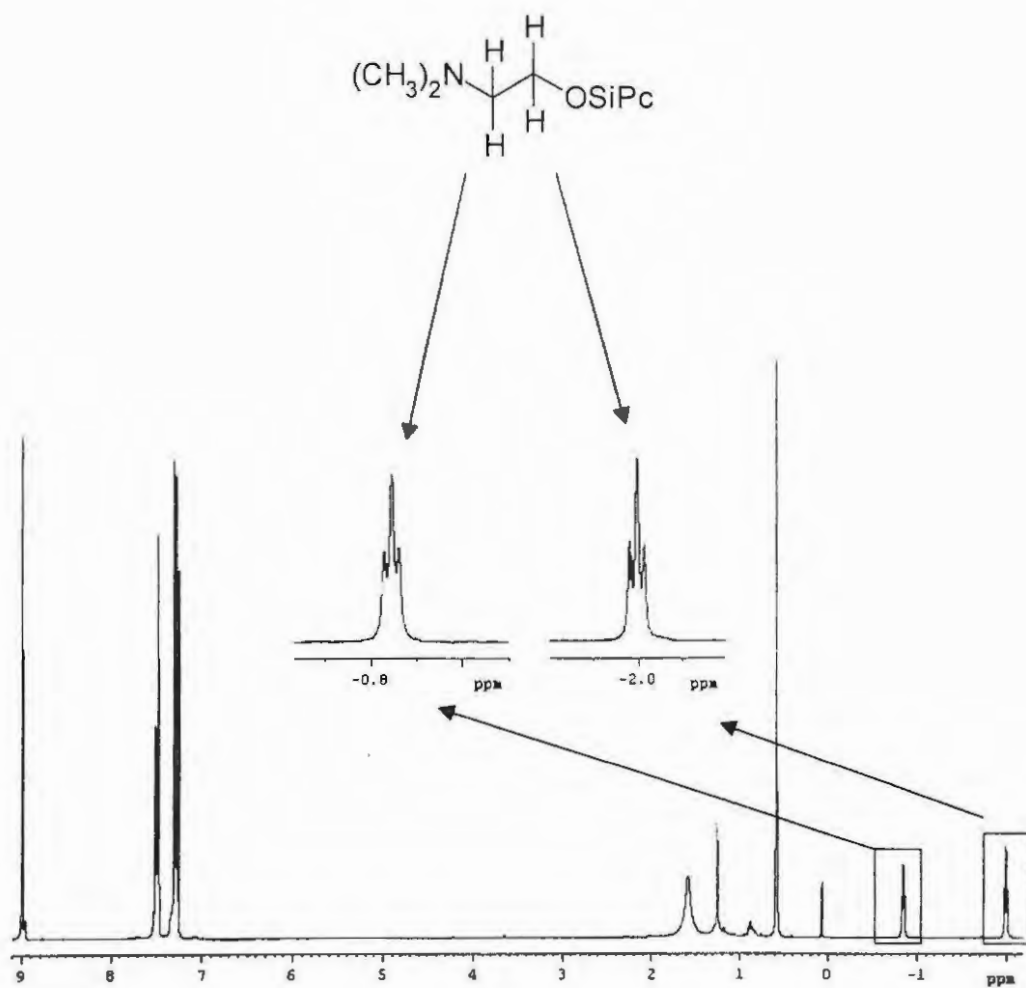


Fig. 21 Aliphatic negative resonances of compound **61** in CDCl_3

-Chapter 2-

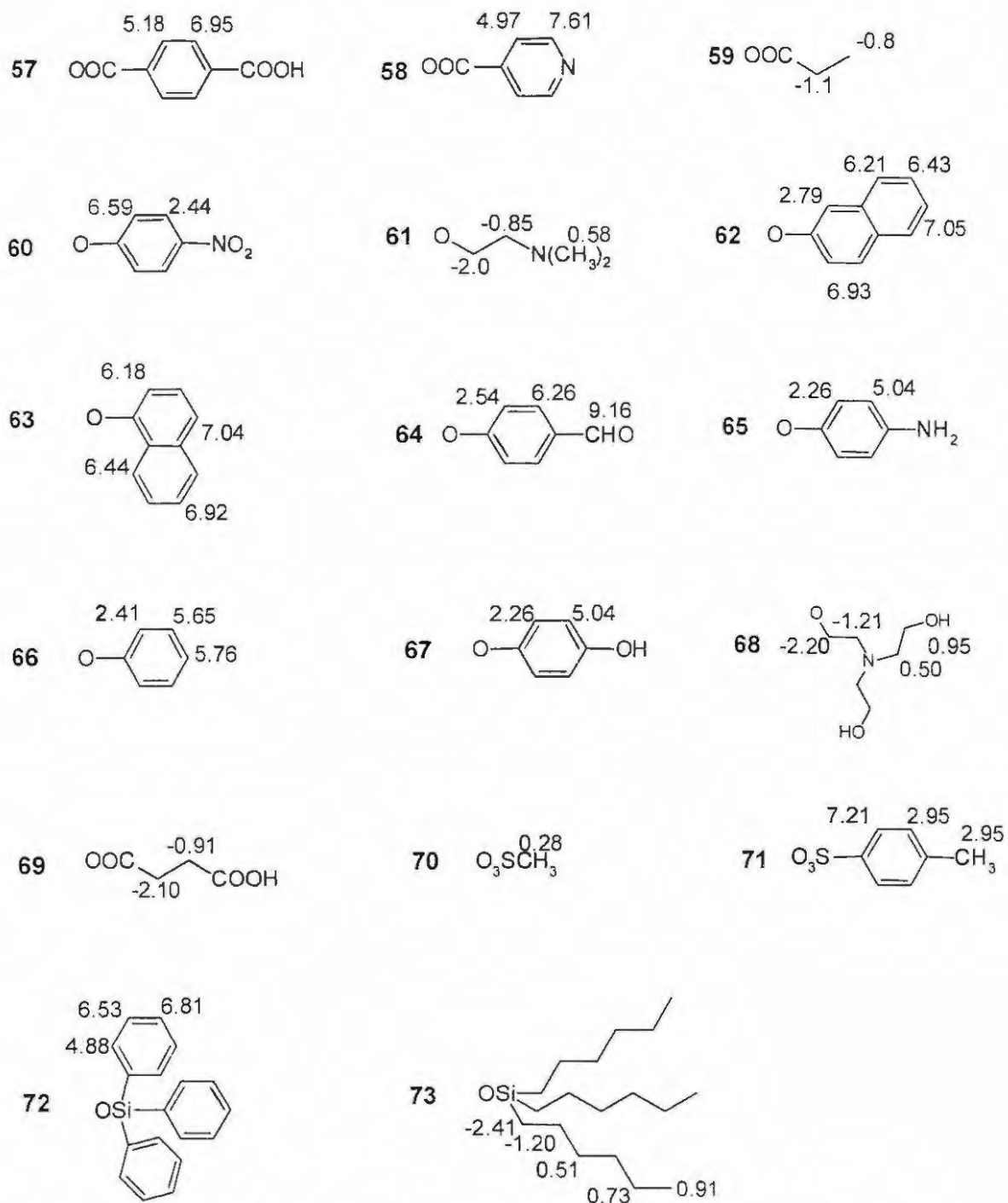


Fig. 22. Axial ligands of compounds 57 to 73 with their chemical shifts.

-Chapter 2-

The oligomers **74-78** synthesised in this study are essentially different molecules to the monomeric species discussed above and as such require a separate discussion on their $^1\text{H-NMR}$ spectra. The $^1\text{H-NMR}$ spectrum of the oligomers **74-78** was the principal method for the determination of their degree of oligomerisation. The compounds displayed similar $^1\text{H-NMR}$ behavior, as expected, with slight differences for the phthalocyanine ring protons. The $^1\text{H-NMR}$ spectrum of compound **75** is shown in Fig. 23 with the relevant structures that represent each resonance.

The deshielded protons responsible for the singlet near 9 ppm were due to the non-peripheral protons of the phthalocyanine ring and integrated for 8 protons for all phthalocyanine rings. The integrals of these peaks could actually allow confirmation of the number of rings in a complex in that compound **74** displayed a singlet of 16 protons (both phthalocyanine rings are in the same environment) and compound **75** (Fig. 23) displayed singlets at 8.99 ppm (16 protons) and 8.97 ppm (8 protons) indicating two phthalocyanine rings in the same environment and a third ring slightly more shielded. In general, the phenoxy ring protons nearest the ether bond were more deshielded than their neighboring aromatic protons and integrated as a triplet for **74** and multiplets for **75 - 78** at ~ 7.5 ppm. All compounds displayed a multiplet of phenoxy protons at 7.3 ppm. The $^1\text{H-NMR}$

-Chapter 2-

data for the axial ligands on each of the compounds displayed very similar shifts and all the linking aromatic terephthalate protons displayed multiplets at ~2.9 ppm which is indicative of the extreme high shielding of these aromatic protons by the phthalocyanine rings. The terminal aldehyde groups provided an easy method of determining the degree of oligomerisation by comparison of the area integral of their resonances at ~9.15 ppm (for the aldehyde protons) to the combined non-peripheral phthalocyanine ring resonances at ~9 ppm. Thus compound **75** had a calibrated area integral of 2 protons at 9.15 ppm and a combined area integral of 24 at 8.97 and 8.99 ppm. Each ring in the system has 8 protons thus there are 3 rings in compound **75** (Fig. 23).

-Chapter 2-

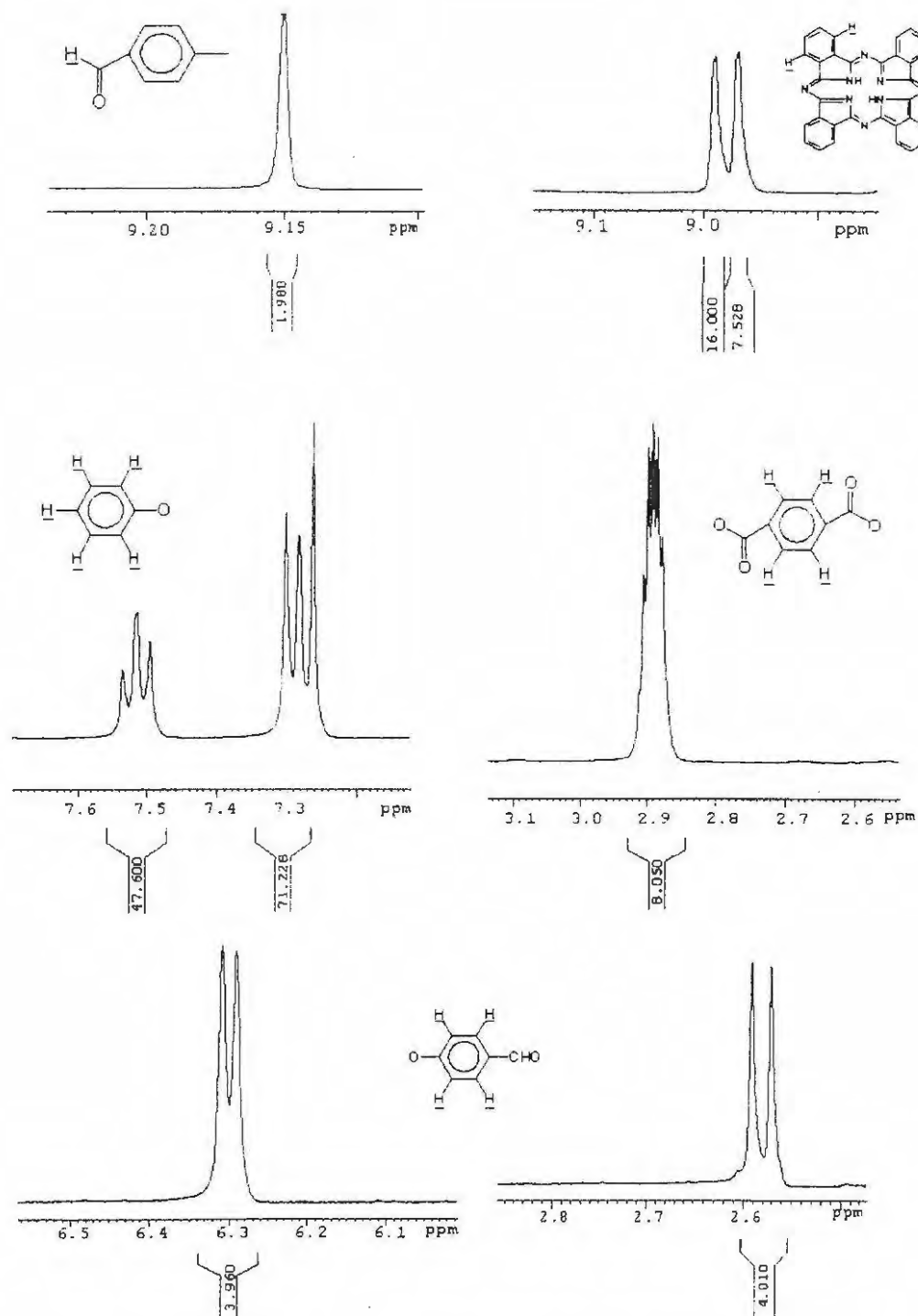


Fig. 23 Fragments of the $^1\text{H-NMR}$ spectrum of oligomer **75** in CDCl_3

-Chapter 2-

2.3.2 UV-visible spectra

The spectra of MPc complexes is characterised by an intense band in the visible region called the Q band, and a weaker band in the UV region called the Soret or B band (Fig. 24). The UV-Visible spectra of the phthalocyanine molecules synthesised in this study showed a variation of Q-band maxima mostly between 678 nm to 700 nm (Table 5), thus the compounds were red shift by approximately 10-25 nm as compared to axially substituted silicon phthalocyanines without peripheral substituents.^{124,125} The red shift is desirable for the possible use of these complexes as photosensitisers. The B band maxima of all the phthalocyanines are observed at almost identical wavelengths. The B band in MPc complexes is known to be less affected by peripheral substitution of the phthalocyanine ring than the Q band. The isomeric purity of the compounds is also evident in the general shape of the spectra, which are well defined in all regions as is seen for compounds **54**, **57** and **69** (Fig.24).

-Chapter 2-

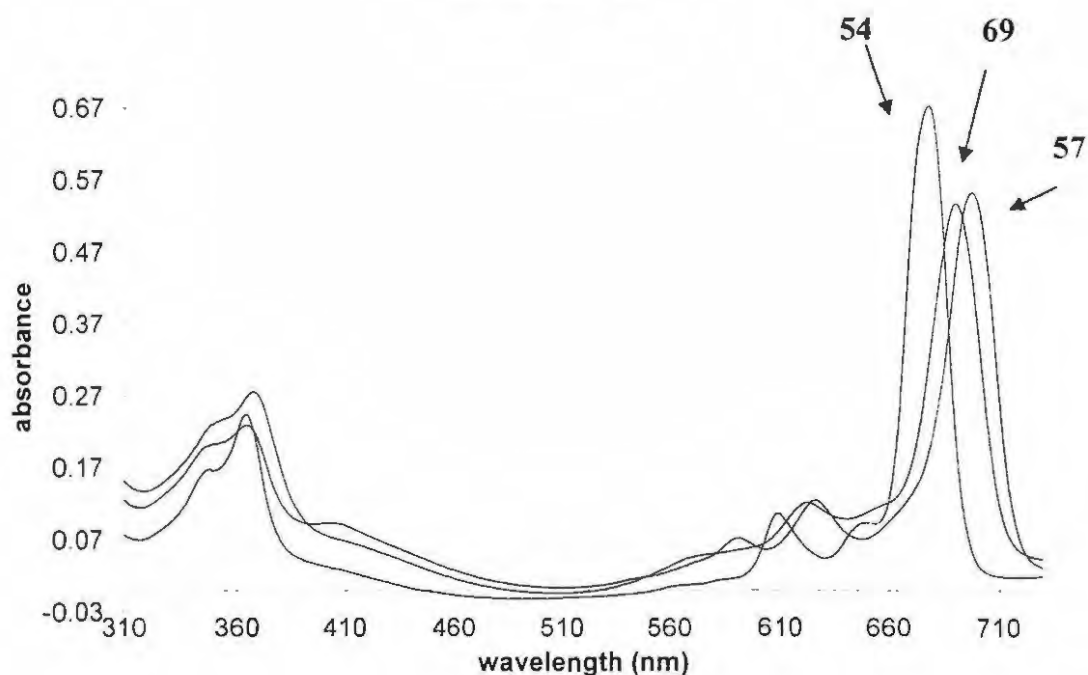


Fig. 24. UV-Visible spectra of compounds **54**, **57** and **69** in DMF.

The wavelength shifts also depend upon the electron donating or electron withdrawing abilities of the axial ligands. The relationship between axial substituent structure and Q-band absorption maxima point to a red-shift being preferred for a combination of electron withdrawing substituents and aromatic functions on the axial ligand. Photochemical processes are known to occur more readily when photosensitisers are in the monomeric state.^{126,127} The spectra of all the compounds were typical of monomeric species with a sharp Q band. Among the non-oligomeric compounds studied only the dichloro silicon phthalocyanine **54** and the dihydroxyl silicon phthalocyanine **55** showed some deviation with

-Chapter 2-

regards to Beer's law. This implies aggregation for **54** and **55** in solution at concentrations of up to $\sim 10^{-6}$ M. Compound **55**, was found to be less soluble than the rest of the compounds. This behaviour of compound **55** is typical of the peripherally unsubstituted dihydroxy silicon phthalocyanine, which is much less soluble in all solvents than its dichloro silicon phthalocyanine counterpart.¹¹⁵ The rest of the axially substituted monomeric compounds showed no deviation for Beer's law up to concentrations of $\sim 10^{-4}$ M. Among the oligomeric compounds a progressive increase in aggregation was observed with increase in ring number as is shown in Fig. 25. The oligomeric compounds have UV-vis spectra very similar to the monomers as seen for compound **76** in Fig. 26.

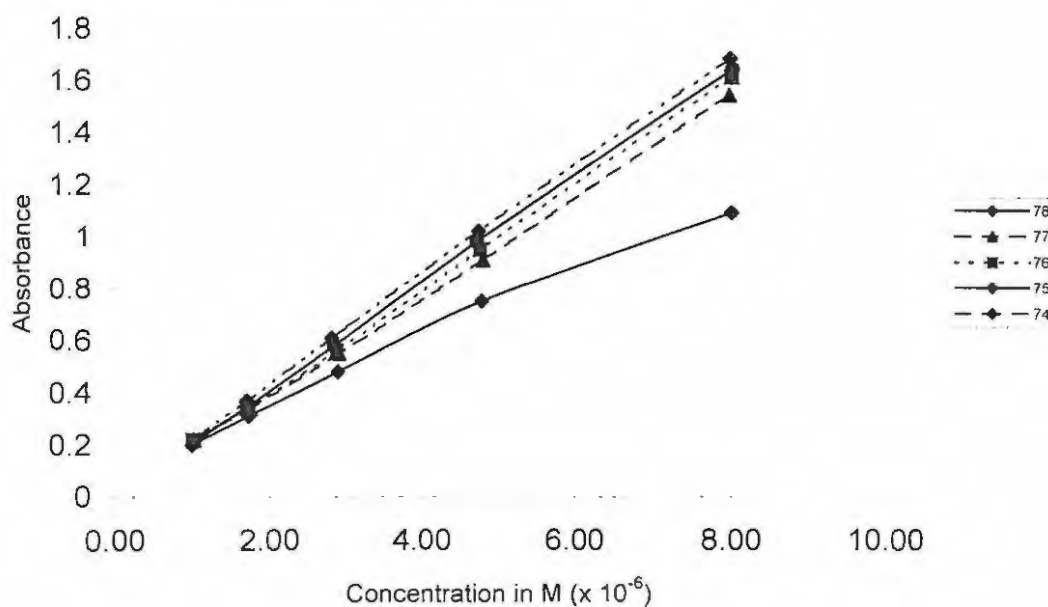


Fig. 25. Beer's law deviation for the oligomers **74** to **78** in DMF.

-Chapter 2-

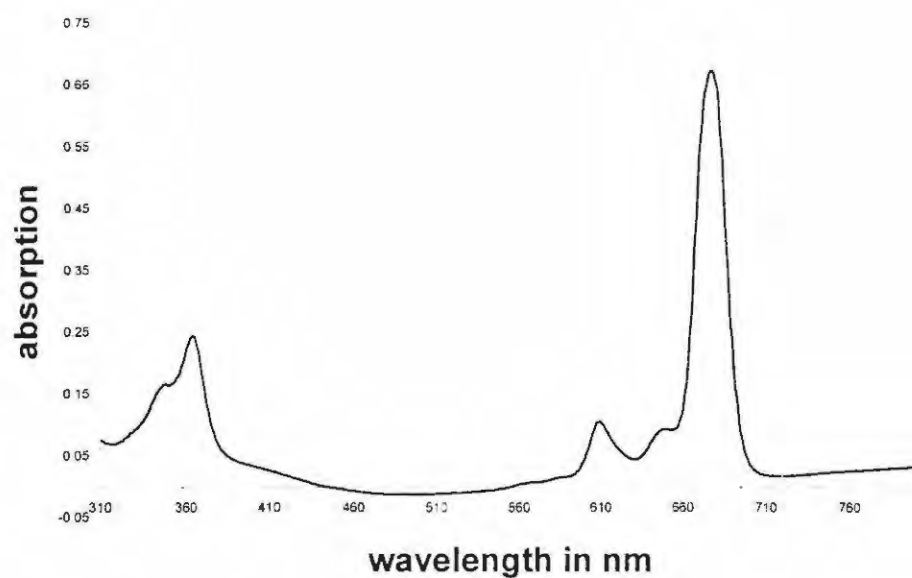


Fig. 26. UV-Vis spectrum of compound 76 in DMF.

The spectra obtained of the phthalocyanines had several general trends, A Q-band at 678 nm and above, two vibrational bands at ~650 nm and 610 nm, a B-band at ~ 360 nm with an additional band at ~340 nm. Table 5 shows the electronic absorption spectroscopic data of all the phthalocyanine complexes synthesised in this work.

-Chapter 2-

Table 5. The UV-Visible data of all the phthalocyanines synthesised in DMF.

Compound	UV/vis maxima nm (log ϵ)
54	678(5.31), 649(4.50), 609(4.52), 364(4.92), 344(4.76)
55	678(5.17), 642(4.25), 609(4.39), 364(4.72), 343(4.55)
57	695(5.32), 661(4.51), 626(4.53), 366(4.86), 346(4.76)
58	697(5.09), 662(4.35), 626(4.46), 364(4.71), 346(4.65)
59	690(5.07), 660(4.42), 621(4.42), 367(4.78), 347(4.70)
60	696(5.06), 665(4.38), 625(4.30), 365(4.68), 337(4.77)
61	683 (5.39), 650 (4.53), 614 (4.59), 362 (4.93), 341(4.78)
62	684 (5.11), 651 (4.47), 612 (4.47), 364 (4.83),340 (4.69)
63	684(5.12), 650 (4.43), 614 (4.89), 365 (4.80), 338 (4.70)
64	690 (5.11), 659 (4.41), 620 (4.45), 368 (4.80),348 (4.75)
65	688 (5.07), 657 (4.39) 618 (4.44), 366 (4.84), 347 (4.80)
66	688 (5.13), 658 (4.42),618 (4.41), 365 (4.78), 346 (4.76)
67	690 (5.14), 660 (4.45),622 (4.43), 366 (4.77), 348(4.77)
68	679 (5.17), 642 (4.26), 610 (4.37), 364 (4.74),343 (4.75)
69	686 (5.17), 655(4.40), 615(4.39), 365(4.77), 345(4.77)
70	682 (5.34), 651(4.55), 613(4.61), 364(4.78), 340 (4.71)

-Chapter 2-

71	714 (5.31), 678(4.66), 648 (4.48), 369(3.71), 342(4.78)
72	687 (5.21), 658(4.55), 617(4.58), 364(4.79), 3.44(4.75)
73	681 (5.24), 650(4.51), 611(4.58), 365(4.74), 339 (4.71)
74	684 (5.26), 650 (4.47), 613(4.55), 354(4.74)
75	682 (5.28), 650(4.49), 615(4.61), 353(4.71)
76	681 (5.26), 615(4.71), 354(4.69)
77	681 (5.28), 614(4.69), 354(4.77)
78	680 (5.25), 611(4.77), 352(4.81)

2.3.3 Infrared spectra

Infrared spectra observed for the phthalocyanine complexes are all very similar. Some general infrared bands were observed such as a band at $\sim 1200\text{ cm}^{-1}$ which is characteristic of a diphenyl ether functionality that comes from the 8 phenoxy groups that are attached to the phthalocyanine structure. The axial position also displayed a variety of absorptions as could be seen in Fig. 12 where the dihydroxyl **55** differs only from the dichloro **54** with O-H bands at 3393 cm^{-1} and 850 cm^{-1} . both bands have been reported to be characteristic of the Si-OH and the Si-O bonds respectively.¹²⁸ No bands characteristic of the Si-Cl bond in compound **54** could be observed.

-Chapter 2-

All compounds synthesised which contained the Si-O-C linkage, where the silicon is the central metal of the phthalocyanine, had a characteristic peak at $\sim 1015\text{ cm}^{-1}$. Similarly the two compounds **72** and **73** that contain the Si-O-Si linkage had an additional absorption at 1041 and 1053 cm^{-1} respectively, typical of the Si-O-Si vibration.²⁷ All silyl esters, that is compounds made from carboxylic acids, showed a distinctive carbonyl stretch at $\sim 1685\text{ cm}^{-1}$. Compound **64** showed an aldehyde band at 1707 cm^{-1} , which is expected of an aldehyde carbonyl stretch.

Compounds **67** and **68** both contained terminal hydroxyl functions and as such had OH stretches at 3620 and 3638 cm^{-1} respectively. Compound **60** had typical nitro stretches at 1515 and 1340 cm^{-1} with compound **65** displaying typical amine bands at 3325 , 1621 and 1254 cm^{-1} . Compounds **59**, **62**, **63**, and **66** showed enhanced C-H stretches due to the aromatic axial ligands at their respective aromatic and aliphatic places (~ 2950 and $\sim 1600\text{ cm}^{-1}$). The oligomers **74** to **78** all had characteristic carbonyl stretches at $\sim 1690\text{ cm}^{-1}$ that indicated the presence of the ester connecting groups.

Table 6. Distinguishing IR bands for all the compounds made.

Compound	Distinguishing bands (cm ⁻¹)	Functionality
55	3393	OH
	850	Si-OH
57	1687	Si- <u>OCO</u>
58	1686	Si- <u>OCO</u>
59	1691	Si- <u>OCO</u>
60	1515, 1340	NO ₂
61	1301	C-N
62	1600*	CH
63	1600*	CH
64	1707	CHO
65	3325, 1621, 1254	NH ₂
66	1601*	CH
67	3620	OH
68	3638	OH
69	1685	Si- <u>OCO</u>
70	-	-
71	1605*	CH

-Chapter 2-

72	1044	Si-OSi
73	1051	Si-OSi
74-78	~1690	Si-OCO

* Indicates the absorptions due to the C-H band were enhanced compared to the other phthalocyanines

2.4 Photochemistry^d

In this section some basic photochemistry was undertaken to determine the efficiency of some photochemical processes for the compounds prepared. Firstly, under Q-band excitation, the rate of macrocycle photobleaching was measured and quantified as a quantum yield by a method to be discussed. In the process of photobleaching, one quick process (involving the phototransformation of the axial ligands) and one slow process (macrocycle photobleaching) were observed and are discussed separately. The phototransformation quantum Φ_p yields were determined according to Eq. 12, introduced in section 1.8.1.

$$\Phi_p = \frac{(C_o - C_t)V}{I_{\text{abs}} \times t} \quad \dots \text{Eq. 12}$$

^d Published as M. David Maree, N. Kuznetsova and T. Nyokong, *J. Photochem. Photobiol. A: Chem.*, **140**, 117-125 (2001).

-Chapter 2-

Similarly, the photobleaching quantum yields ($\Phi_{\text{photobleaching}}$) were also determined as in Eq. 15, Section 1.8.1. The I_{abs} coefficient is determined according to Eq. 13 as described in Chapter 1.

$$I_{\text{abs}} = \frac{\alpha S I}{N_a} \quad \dots \text{Eq. 13}$$

An example of the way in which α is calculated is shown in Table 7.

Table 7. Calculation of the alpha coefficient for photochemical quantum yields.

λ	T_{filter}	T_{dye}	$1 - T_{\text{dye}}$	$T_{\text{filter}} \times (1 - T_{\text{dye}})$
680	0.128	19.5	80.5	$0.128 \times 0.805 = 0.10$
690	0.779	11.7	88.3	0.69
700	0.785	25.2	74.8	0.59
710	0.743	55.8	44.2	0.33
720	0.668	74.2	25.8	0.17
730	0.053	80.4	19.6	0.01
	$\Sigma = 3.156$			$\Sigma = 1.895$

$$\alpha = \frac{\Sigma T_{\text{filter}}(1 - T_{\text{dye}})}{\Sigma T_{\text{filter}}}$$

$$\text{Therefore } \alpha = \frac{1.895}{3.156} = 0.60$$

-Chapter 2-

This then allows the determination of I_{abs} according to Eq. 12 with I_{λ} (the intensity of light) being determined using a light power meter, as will be explained in Chapter 3.

2.4.1 Phototransformation involving axial substituents

Under Q-band excitation of complexes **57** - **78** in air, an initial relatively quick decrease in the Q-band occurs with an accompanying appearance of a new band at 678 nm was observed. This is indicative of the phototransformation of the axial substituents upon photolysis. This phototransformation followed first order kinetics and an example is shown for compound **58** in Fig. 27.

-Chapter 2-

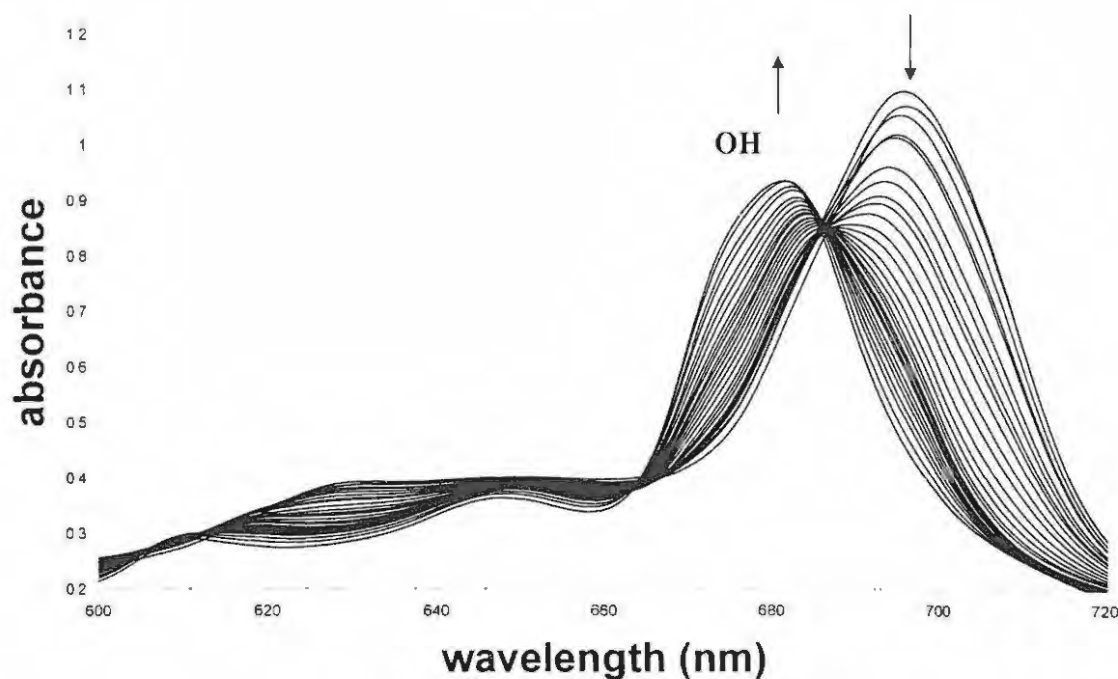


Fig. 27. Phototransformation of compound 58 to the dihydroxyl 55 in DMSO.

The presence of a diffuse isosbestic point indicates that photobleaching of the phthalocyanine macrocycle is occurring to a small extent during the phototransformation of the axial substituents. The overlapping of the absorption spectra of products formed for compounds 57 - 78 following the axial substituent phototransformation shows that the same product is formed. Complexes 54 and 55 have the same absorption maxima as the product of phototransformation of complexes 57 - 78. TLC (eluent, chloroform) indicates that 54 is also phototransformed into the dihydroxy derivative 55 as was witnessed by its different chromatographic behaviour to that of the dichloro derivative. Axial

-Chapter 2-

ligands in complexes **57** - **78** thus have a propensity to be substituted by hydroxyl groups to form compound **55**. The quantum yields for the phototransformation (Φ_P) of the axial substituents for **57** - **78** are summarized in Table 8 and were determined according to Eq. 12. Using TLC transformation times, the quantum yield for axial substituent phototransformation of complex **54** to complex **55** was estimated to be approximately equal to 1×10^{-5} . The oligomeric compounds **74** - **78** displayed very similar phototransformation quantum yields as was expected due to the geometric dependence of the phototransformation quantum yields (see mechanism below).

Table 8 The quantum yields of phototransformation (Φ_P) in DMSO

Compound	Φ_P
54	$\sim 1 \times 10^{-5}$
57	1.8×10^{-5}
58	7.0×10^{-5}
60	1.0×10^{-3}
61	1.7×10^{-3}
62	1.7×10^{-3}
63	1.7×10^{-3}
64	2.0×10^{-3}
65	3.3×10^{-3}
66	1.6×10^{-3}
67	4.0×10^{-3}
68	1.9×10^{-3}
69	1.4×10^{-3}
70	1.5×10^{-2}
71	0.8×10^{-2}

-Chapter 2-

72	3.0×10^{-5}
73	4.1×10^{-5}
74-78	$\sim 8 \times 10^{-5}$

It was found that the axial ligands have an influence as large as 3 orders of magnitude on the Φ_p varying from 8×10^{-5} for complexes 74-78 to 1.5×10^{-2} for complex 70. Thus, it is concluded that ligand substitution in silicon octaphenoxyphthalocyanine from any covalently bound axial group to the hydroxyl ligand occurs for all of the complexes under discussion. The following types of axial ligands were used in this study: aryloxy, siloxy, aminoalkoxy, esters of carboxylic acids and sulphonic acid ester residues. It was found that although members of each group have very similar values of Φ_p , groups differ in Φ_p by orders of magnitude from each other (with the exception of 64 in the aryloxy row).

No relationship between electronic structure and reactivity in phototransformation of axial substituents was observed. Therefore it may be concluded that geometry rather than electronic properties is responsible for the reactivity of silicon octaphenoxyphthalocyanine derivatives during the axial substituent phototransformation. To further look at the mechanism of this phototransformation the effects of oxygen concentration, a singlet oxygen

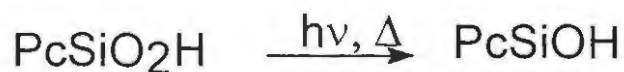
-Chapter 2-

inhibitor, a radical scavenger and deuterated solvent on the rate of phototransformation of axial substituents were studied with **60** as an example.

It was found that Φ_p in saturated oxygen (4.5×10^{-3}) in DMSO solutions were higher than air saturated (1.1×10^{-3}) solution, showing that O_2 is involved in the phototransformation process. The singlet oxygen quencher diazabicyclooctane (DABCO) and the radical scavenger (2,4-ditertbutyl phenol) do not inhibit the axial substituent phototransformation process. The most pronounced effect on phototransformation efficiency is the deuterium effect of the solvent. The value of Φ_p for compound **60** in deuterated DMSO in air decreases to 1.0×10^{-4} from 1.0×10^{-3} , indicating that hydrogen atom abstraction from the solvent is involved in the process. Obviously nucleophilic photosubstitution of axial ligands by the hydroxyl anion is not significant in DMSO.

Photochemical cleavage of Si-C bond has been observed.¹²⁹ There is possibility that photoinduced homolytic cleavage of Si-O bond may be supposed as a key step of phototransformation followed by a sequence for dark reactions of radicals with oxygen as follows (Scheme 28):

-Chapter 2-



Scheme 28. A possible mechanism of axial ligand phototransformation.

Although the main relationships observed for the phototransformation can be explained in the frames of this mechanism, this route under visible light may be improbable from the thermodynamic point of view. The energy of the filtered light used is too low to induce homolytic cleavage of the Si-O bond (bond energy about 110 kcal/mole¹³⁰).

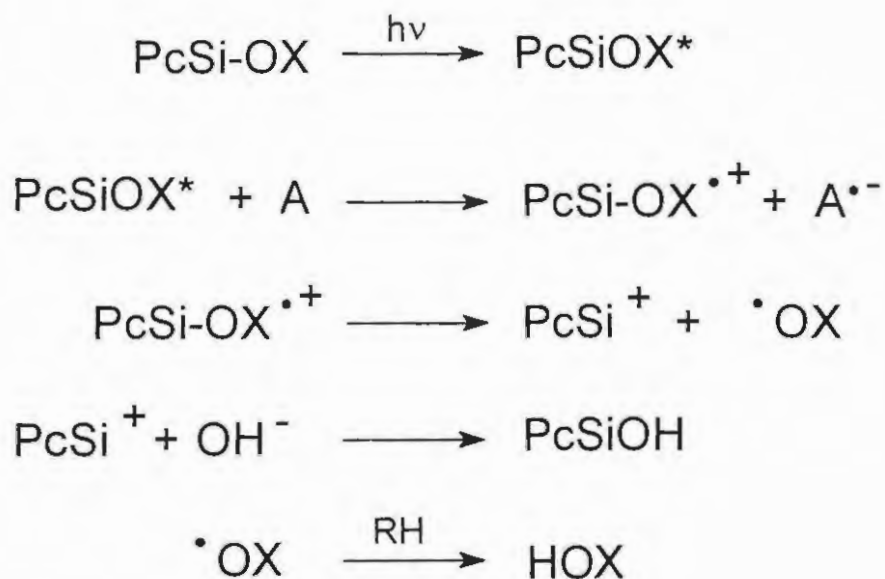
It is well known that in polar solvents like DMSO heterolysis is the preferred mode of cleavage.¹³¹ Solvation benefits the decrease in activation energy (E_a) of reaction. Thus, for example, the cluster model of hydrolysis of Si-O bridge

-Chapter 2-

predicts a low activation energy of the process, for the $(\text{HO})_3\text{Si-O-Si}(\text{OH})_3$ molecule $\Delta E_a = 17$ kcal/mole.¹³² Photoinduced heterolytic cleavage leads to radical ion formation and subsequent reactions of this species with oxygen and solvent may result in Si atom hydroxylation as well. However it is worth mentioning that the phthalocyanine chromophore results in $\pi\pi^*$ -excited states of the ring upon Q-band irradiation as a first step.

Other excited states, responsible for charge transfer between axial ligands and the central metal atom, are supposed to lie at higher energies, thus an intramolecular charge transfer mechanism is doubtful.¹³³ Intermolecular electron transfer between phthalocyanine $\pi\pi^*$ -excited state and electron acceptors, particularly oxygen, is known¹³⁴ and may be considered as a first step of photooxidation leading to hydroxylation of Si central metal. A cation radical is formed in this initial photochemical step and these have a propensity to fragment into a cation and radical.¹³⁵ In the frames of this mechanism the following scheme for photohydrolysis may be proposed (Scheme 28):

-Chapter 2-



Scheme 29. An alternative mechanism of phototransformation where A is an electron acceptor and RH is the solvent.

Some influence of axial substituent electronic properties on the rate of one-electron ring photooxidation is possible. The observed high deuterium isotope effect of the solvent indicates the important role of hydrogen atom abstraction in the proposed mechanism. This is shown by the interaction of the XO^\bullet radical with the solvent (shown in the last step of Scheme 28). In the absence of oxygen the radical cation may be produced in a bimolecular electron transfer reaction of the excited phthalocyanine with a ground state phthalocyanine.

-Chapter 2-

The finding that 2,4-ditertbutyl phenol does not inhibit the process indicates an absence of long radical chains. So far the main peculiarities of phototransformation may be explained by the mechanism above, which is initiated by intermolecular electron transfer. Based upon the above discussion, this mechanism seems to be the most reasonable.

2.4.2 Photobleaching studies

Photobleaching (the degradation of the phthalocyanine macrocycle) of complex **55** was observed as the second photochemical process following the axial substituent phototransformation discussed above for all the axially substituted compounds. Irradiation of compound **55** in the Q-band region resulted in its photobleaching with a quantum yield $\sim 5 \times 10^{-6}$. A typical degradation is shown in Fig. 28.

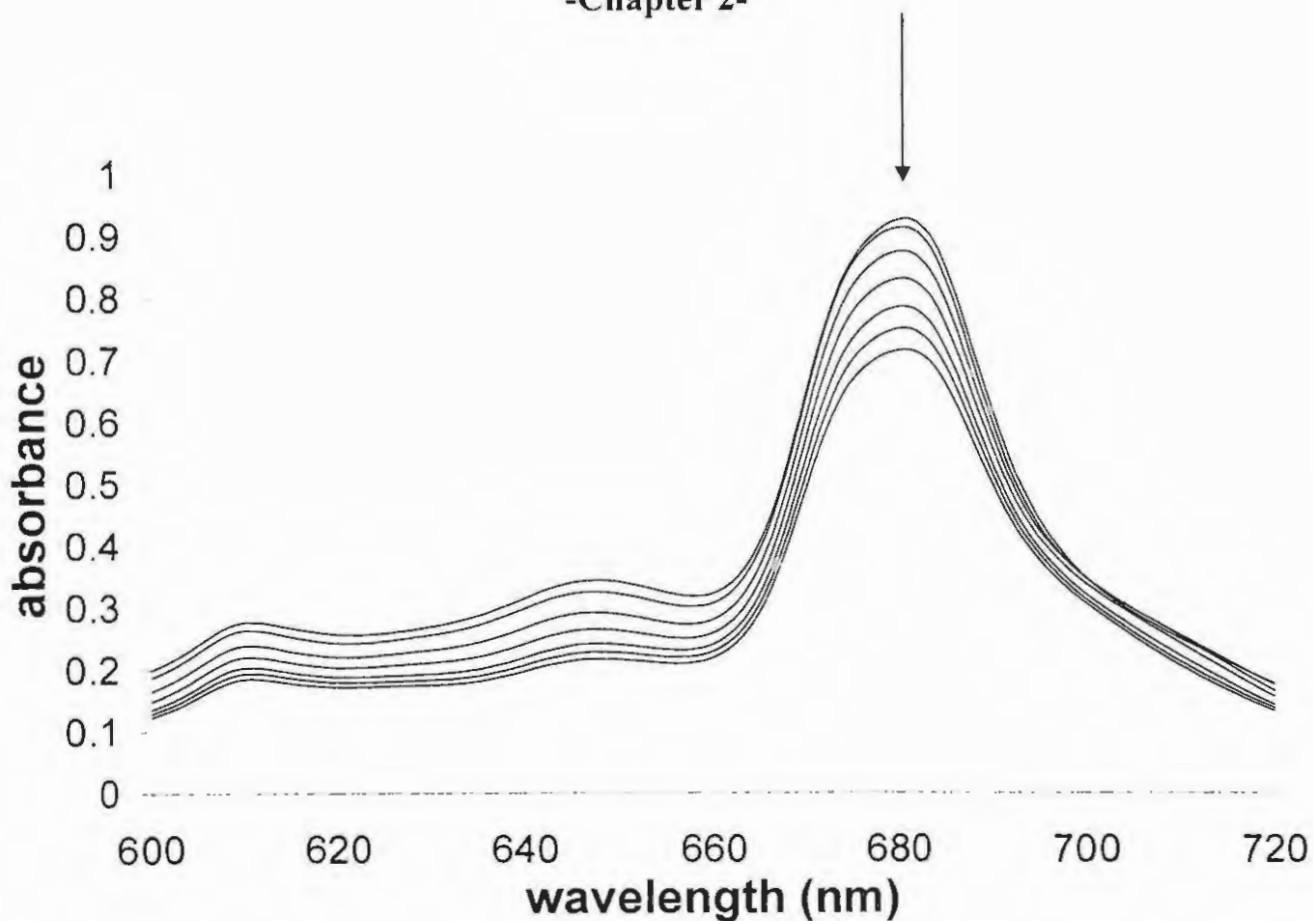


Fig. 28. The phthalocyanine photobleaching process in DMSO.

Fig. 29 compares the effect of solvent, oxygen, d^6 -DMSO and singlet oxygen quencher on the photobleaching process. Experiments were thus performed whereby the solutions were deaerated with N_2 gas or saturated with O_2 in order to study the role of oxygen in the mechanism for photobleaching and photo-assisted axial ligand exchange in the complexes. 2,4-Ditertbutylphenol ($1 \times 10^{-2} \text{ mol l}^{-1}$) and DABCO ($2 \times 10^{-3} \text{ mol l}^{-1}$) were used as radical and singlet oxygen scavengers.

-Chapter 2-

respectively. The increase of the photobleaching rate with increase in oxygen concentration, indicates that oxygen is involved in the process, as seen by comparing the kinetic curves for nitrogen, air and oxygen saturated solutions, Fig. 29. Inhibition of the photobleaching process in the presence of the singlet oxygen quencher, DABCO, and the increase in the photobleaching rate in d^6 -DMSO solution (Fig. 29) are in agreement with the involvement of singlet oxygen in the photooxidation of the phthalocyanine macrocycle in compound **55**.

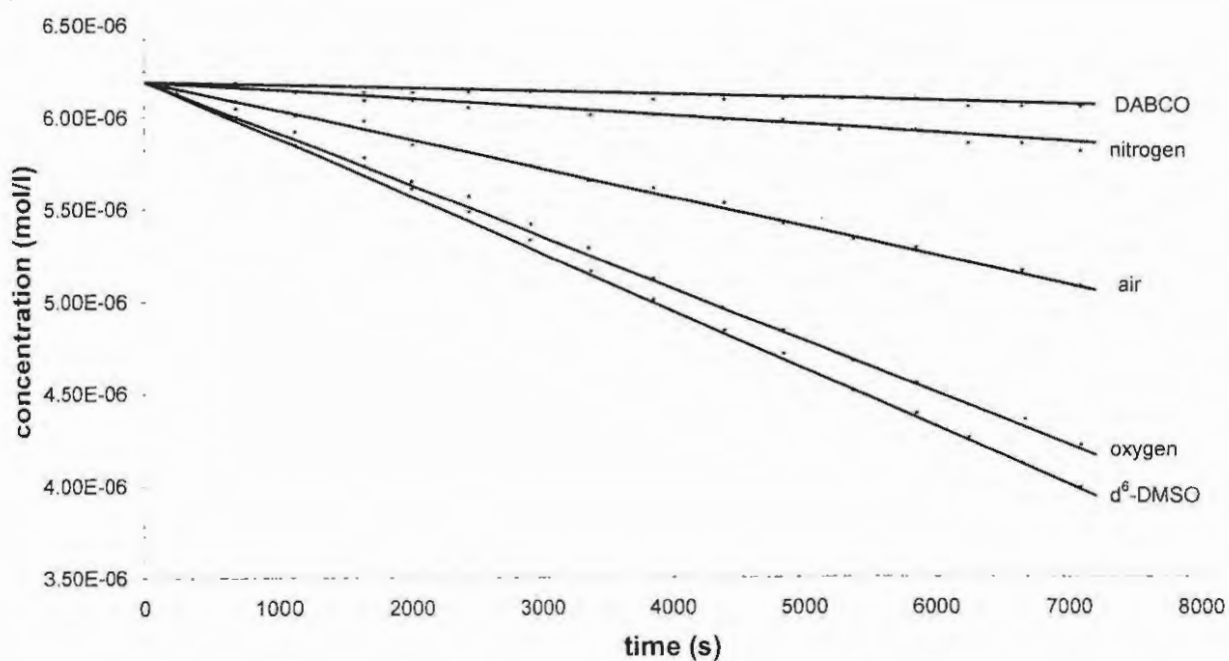


Fig. 29. Photobleaching kinetic curves for compound **55** in DMSO saturated with air, nitrogen or oxygen or in aerated d^6 -DMSO and in aerated DMSO in the presence of 0.02 mol l^{-1} DABCO.

-Chapter 2-

It has been found that the dihydroxyl derivative **55** in DMSO sensitizes formation of singlet oxygen with a quantum yield of 0.07 (Table 9). Thus the photobleaching of compound **55** in DMSO solution most likely proceeds mainly through a self-sensitized photooxidation by singlet oxygen. There has been some speculation in the literature about the singlet oxygen interaction with the phthalocyanine macrocycle. Schnurpfeil et al. suggest singlet oxygen cycloaddition to phthalocyanine pyrrole units resulting in the macrocycle destruction and formation of phthalimide (Fig. 30).¹³⁶

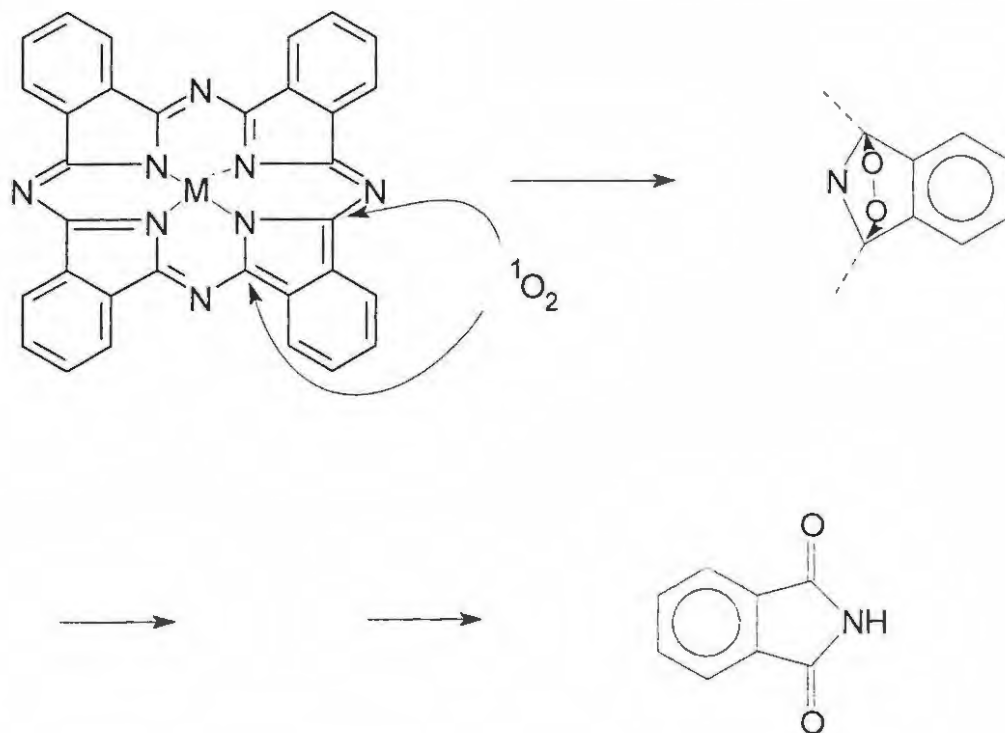


Fig. 30. Suggested photobleaching mechanism.

-Chapter 2-

2.4.3 Singlet oxygen quantum yields

Quantum yields of singlet oxygen photogeneration (Φ_{Δ}) of compounds **54** - **78** are presented in Table 9, and were determined using Eq. 14, Section 1.8.1 and ZnPc as the standard.

Table 9. Singlet oxygen quantum yields of compounds **54** to **78** in DMSO.

Compound	Φ_{Δ} (± 0.02)
54	0.14
55	0.07
57	0.21
58	0.14
60	0.19
61	0.14
62	0.20
63	0.21
64	0.21
65	0.03
66	0.21
67	0.18
68	0.11
69	0.17
70	0.16
71	0.15
72	0.20
73	0.41
74	0.23
75	0.28
76	0.31
77	0.34
78	0.11

-Chapter 2-

No photobleaching or phototransformation of the sensitizer complexes was observed during the determination of singlet oxygen quantum yields, since these processes occur much slower than singlet oxygen production. (Fig. 31)

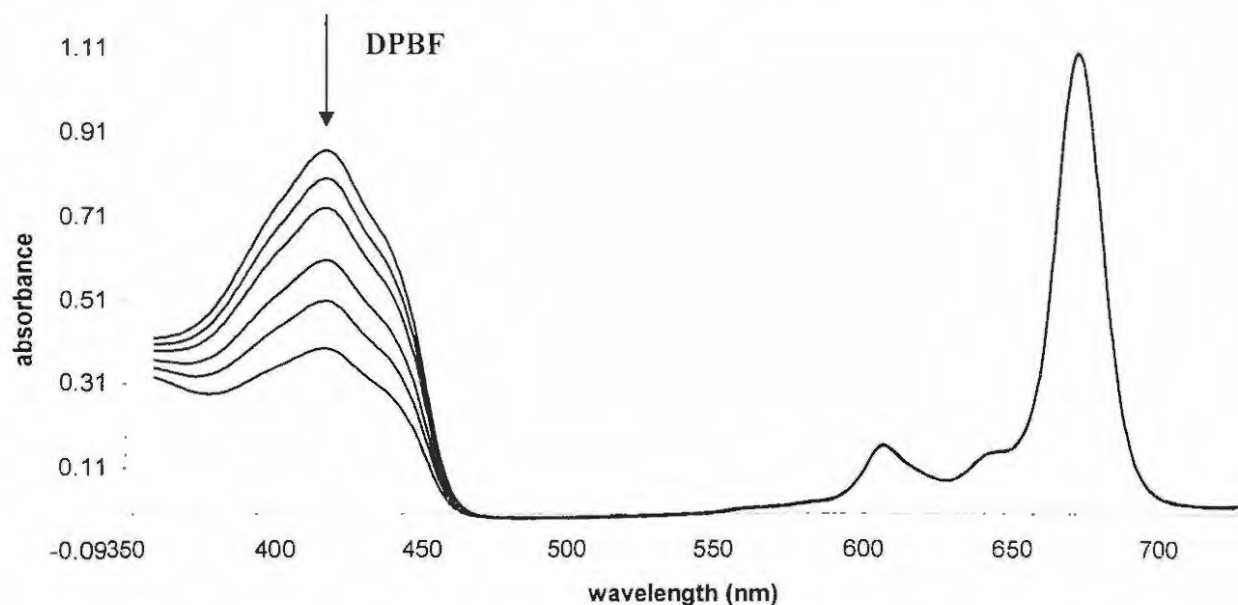


Fig. 31. UV-Visible spectra of DPBF degradation by singlet oxygen in DMSO.

The majority of the values in Table 9 are in the range 0.15 – 0.20 with a few compounds having lower values ($\Phi_{\Delta} = 0.07$ for **55** and $\Phi_{\Delta} = 0.03$ for **65**) or a higher value ($\Phi_{\Delta} = 0.41$ for **73**). Φ_{Δ} for compound **55** deviates from the other compounds due to its low solubility, possibly caused by hydrogen bond attraction between the axial hydroxyl groups. It is well known that intermolecular

-Chapter 2-

interactions between phthalocyanine rings result in decreased photochemical activity due to enhanced probability of radiationless decay of excited states. On the other hand, bulky hexyl substituents in the axial position of the silicon phthalocyanine **73** prevents association or aggregation of the rings, resulting in higher singlet oxygen quantum yields. This can be seen in Fig. 32 where the silicon phthalocyanine ring is depicted in the center with the hexyl groups forming a bulky axial substituent.

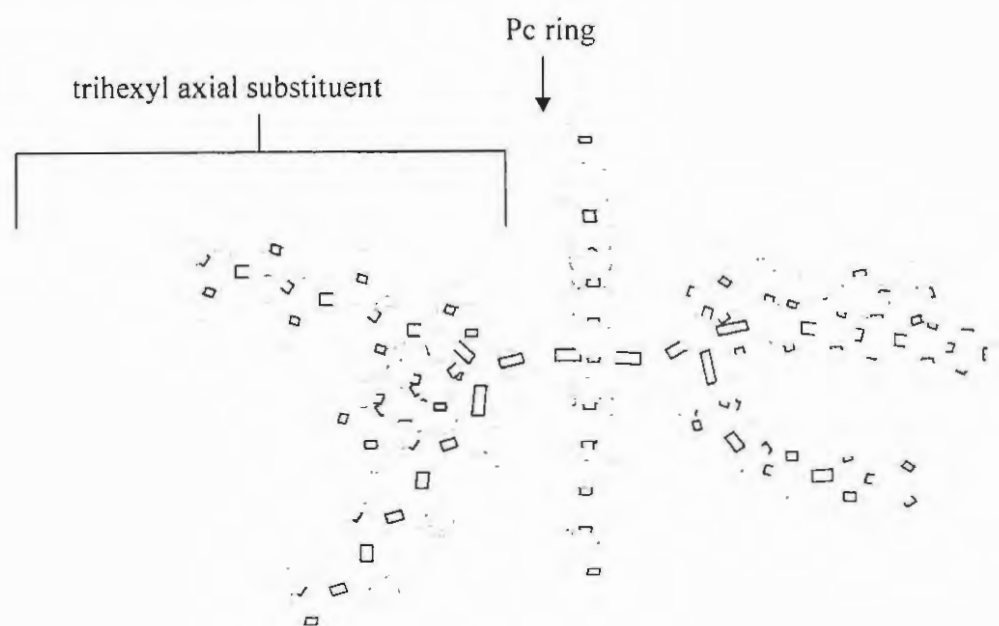


Fig. 32. Geometry optimized structure of hexyl substituents on compound **73**.

-Chapter 2-

Compound **65** has an extremely low value of $\Phi_{\Delta} = 0.03$, although it has good solubility and exists in monomeric form in DMSO. Amine-substituted compounds are known to be singlet oxygen quenchers.¹³⁷ Indeed, amines **68** and **61** also have low Φ_{Δ} values of 0.11 and 0.14 respectively, which may be explained by partial singlet oxygen quenching by the axial substituents. Compound **65**, however, exhibits a lower Φ_{Δ} value when compared to the rest of the amine-containing axial substituents. Compound **65** does not deviate only in singlet oxygen quantum yields, but as noted above, also in axial substituent phototransformation efficiency as well. Such behaviour indicates enhanced competitive degradation of the excited states of compound **65**, decreasing photochemical activity.

Generally, the peripherally substituted complexes in DMSO have decreased singlet oxygen quantum yields compared to their peripherally unsubstituted silicon phthalocyanine counterparts by a factor of approximately 2. The singlet oxygen quantum yield of the peripherally unsubstituted dichloro silicon phthalocyanine (Cl_2SiPc) using the relative method was found to be $\Phi_{\Delta} = 0.38$ which is in good agreement with that in the literature.¹³⁸ The corresponding octaphenoxy compound **54** has a substantially decreased value of $\Phi_{\Delta} = 0.14$.

-Chapter 2-

Since **54** is more soluble than Cl_2SiPc a difference in solubility cannot explain the higher Φ_Δ values of Cl_2SiPc . This is probably an effect of the ring structure. In the case of the oligomeric compounds **74** – **78**, however, aggregation is largely prevented by the linking groups as well as the terminal groups. An interesting trend is observed in the generation of singlet oxygen as seen in Fig. 33 where an increase in singlet oxygen generation is observed up to compound **77** (with 5 rings) and a drop is observed to **78** (with 9 rings).

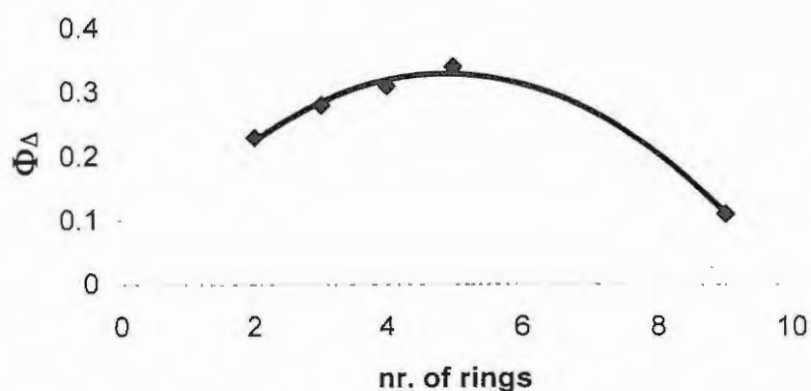


Fig. 33. Relationship of degree of oligomerisation with singlet oxygen quantum yield (Φ_Δ).

This phenomenon is probably as a result of various factors such as the increase in aggregation behaviour and the change in geometry of the molecules (as seen in the above mechanisms), which has been shown in this work to be important in the photochemical behaviour of these compounds.

-Chapter 2-

2.5 Photophysical properties

The photophysical properties of selected octaphenoxy silicon phthalocyanines are shown in Table 10. The properties shown are the fluorescence quantum yield, fluorescence lifetime, triplet quantum yield and triplet lifetime with the singlet oxygen quantum yields for reference. The theoretical fluorescence lifetime refers to the use of the Strickler-Berg equation as explained in Section 1.9.2, Eq. 19.

Table 10. Photophysical data of compounds **54**, **55**, **62**, **65**, **72** and **73** in DMSO. Exp. = experimentally determined value. Th. = Theoretically determined value (Eq. 19).

Compound	λ_{triplet} (ϵ_t)	Fluorescence data			Triplet data	
		Φ_F	τ_F (ns)		Φ_T	τ_T (μs) (Φ_Δ)
			Exp.	Th.		
54	480	0.21	2.4	3.5	0.31	194 (0.14)
55	480	0.18	1.9	3.0	0.30	179 (0.07)
62	475	0.02	1.8	1.7	0.29	260 (0.20)
65	490	0.03	3.5	3.2	0.43	271 (0.03)
73	480	0.29	3.6	3.3	0.40	311 (0.41)
72	485	0.34	4.0	3.6	0.41	356 (0.20)

2.5.1 Triplet lifetimes and quantum yields

Both the triplet lifetimes and triplet quantum yields were determined by flash laser photolysis for selected compounds. The resultant data obtained was in the form of a transient spectrum (difference absorbance spectrum, Fig. 34).

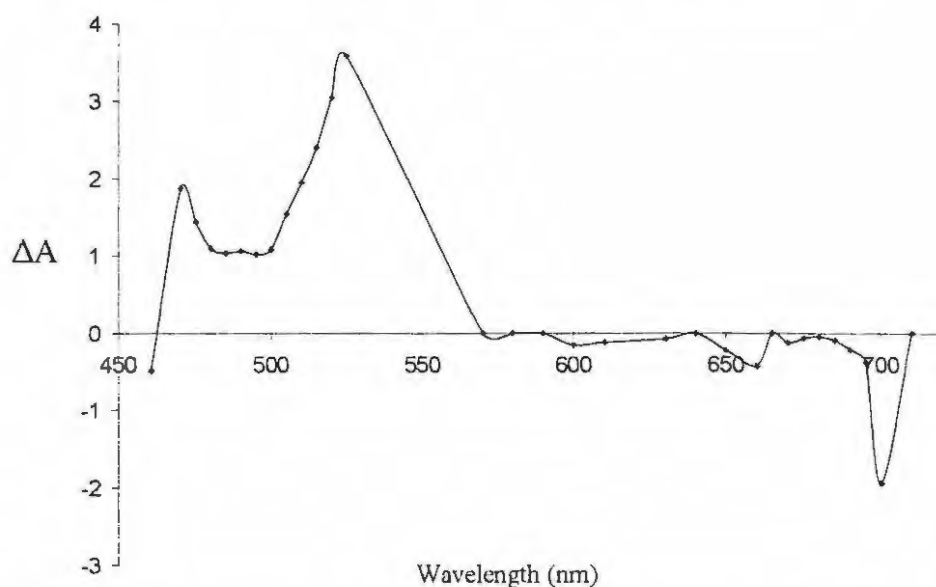


Fig. 34. Transient absorption spectrum of compound **72** in DMSO.

Each point on the transient spectrum was determined by the triplet decay at that specific point as shown in Fig. 35 for compound **72** at 480 nm. The peak at 480 nm has been assigned to the absorption spectra of the triplet state of MPc complexes.¹³³

-Chapter 2-

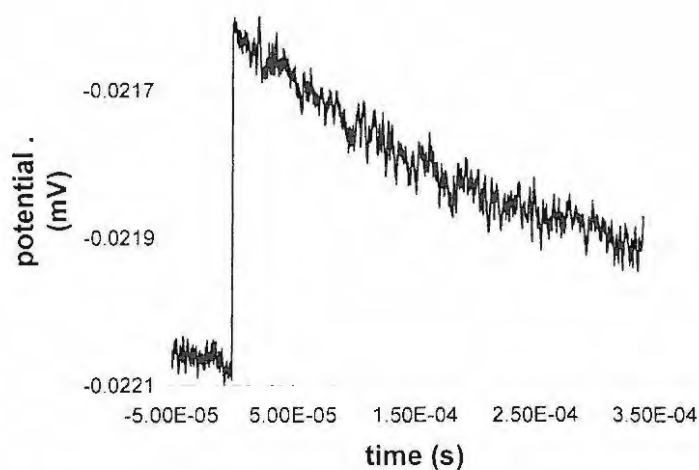


Fig. 35. Triplet decay observed at 480 nm for compound **72**.

The triplet lifetime was determined by the inverse of the gradient of a linear plot of the logarithm of the change in absorbance ($\ln A$) against time as explained in Section 1.9.3. The triplet decay at the triplet maximum was used for this calculation. The triplet state lifetimes (τ_T) vary according to the degree of aggregation of the molecules since compounds **54** and **55** have significantly lower values than the unaggregated (Section 2.3.2) **62**, **65**, **72** and **73**. The presence of the phenoxy groups on the periphery of the phthalocyanines also contributes to an increase in the triplet state lifetimes (179 – 356 μs) as compared to peripherally unsubstituted silicon phthalocyanines (100 – 200 μs).¹³⁹ This could indicate a lesser degree of triplet-triplet annihilation in the molecules due to an increase in intermolecular distancing in solution.

-Chapter 2-

The triplet quantum yields show variation (Table 10), and are not correlated to the singlet oxygen quantum yields of the respective compounds, an intramolecular quenching of the S_1 state is unlikely to contribute to Φ_{Δ} values due to the bis(aminophenoxy) **65** having the highest value. The relatively high triplet quantum yield of compound **65** while its singlet oxygen quantum yield is very low (Table 10) indicates that the aromatic amino groups quench singlet oxygen very effectively.

2.5.2 Fluorescence quantum yields

The fluorescence quantum yields of compounds **54**, **55**, **62**, **65**, **72** and **73** are somewhat surprising (Table 10), since low values are observed for **62** and **65**. These two molecules obviously demonstrate that fluorescence quenching is possible by the axial ligands, in fact naphthol is a known fluorescence quencher. Although compounds **62** and **65** have low fluorescence quantum yields these values are still sufficient for fluorescence imaging applications.

2.5.3 Fluorescence lifetimes

Fluorescence lifetimes were significantly lower for compounds **54**, **55** and **62** than compounds **65**, **72** and **73**. The aggregated nature of compounds **54** and **55** are most probably responsible for their lower values and the naphthoxy axial group in

-Chapter 2-

62 probably quenches the fluorescence to a degree. Using a modified Strickler-Berg equation (Eq. 19, Section 1.9.2) and the respective absorbance and emission spectra of compounds 54, 55, 62, 65, 72 and 73 a remarkably accurate prediction of the fluorescence lifetime is obtained for the unaggregated molecules 62, 65, 72 and 73 in DMSO with a systematic 10% error. Compounds 54 and 55 are understandably overestimated, as the theoretical calculation does not hold for aggregated molecules.

2.6 Cyclic Voltammetry

Cyclic voltammetry was recorded on selected compounds 54, 55 and 57-61. Fig. 36 shows a typical cyclic voltammogram of the complexes in DMF on a glassy carbon electrode (GCE) and dichloromethane on a gold (Au) electrode. The electrolyte used was tetrabutylammonium hexafluorophosphate (TBAHP) and the ferrocenium ferrocene Fc^+ / Fc couple was used as a reference. One oxidation couple and two reduction couples were observed within the potential range shown in Fig. 36. Both oxidation and reduction in SiPc complexes occur at the phthalocyanine ring, the central Si(IV) metal is redox inactive, hence the couples observed for complexes under discussion in this work are due to ring-based reductions and oxidation. The separation between the anodic and cathodic peaks (ΔE) for both reduction couples ranged from 70 to 156mV at a scan rate of 100

-Chapter 2-

mVs^{-1} , and the ratio of the cathodic to anodic peak currents (i_{pc}/i_{pa}) was found to be near unity at these scan rates. ΔE was found to be 60 mV for the internal standard, the ferrocinium/ferrocene. These data suggests quasi-reversible to irreversible one-electron transfer for each reduction couple. ΔE values were found to increase with scan rate, confirming the irreversible nature of the couples.

For all the complexes, the peak currents for the reduction processes showed an exponential dependence on the square root of the scan rate in DMF and in CH_2Cl_2 (Fig. 37) implying that electron transfer is not governed only by diffusion. The deviation from linearity observed in Fig. 37 suggests the presence of kinetic inhibition due to slow electron transfer or coupled chemical reactions.

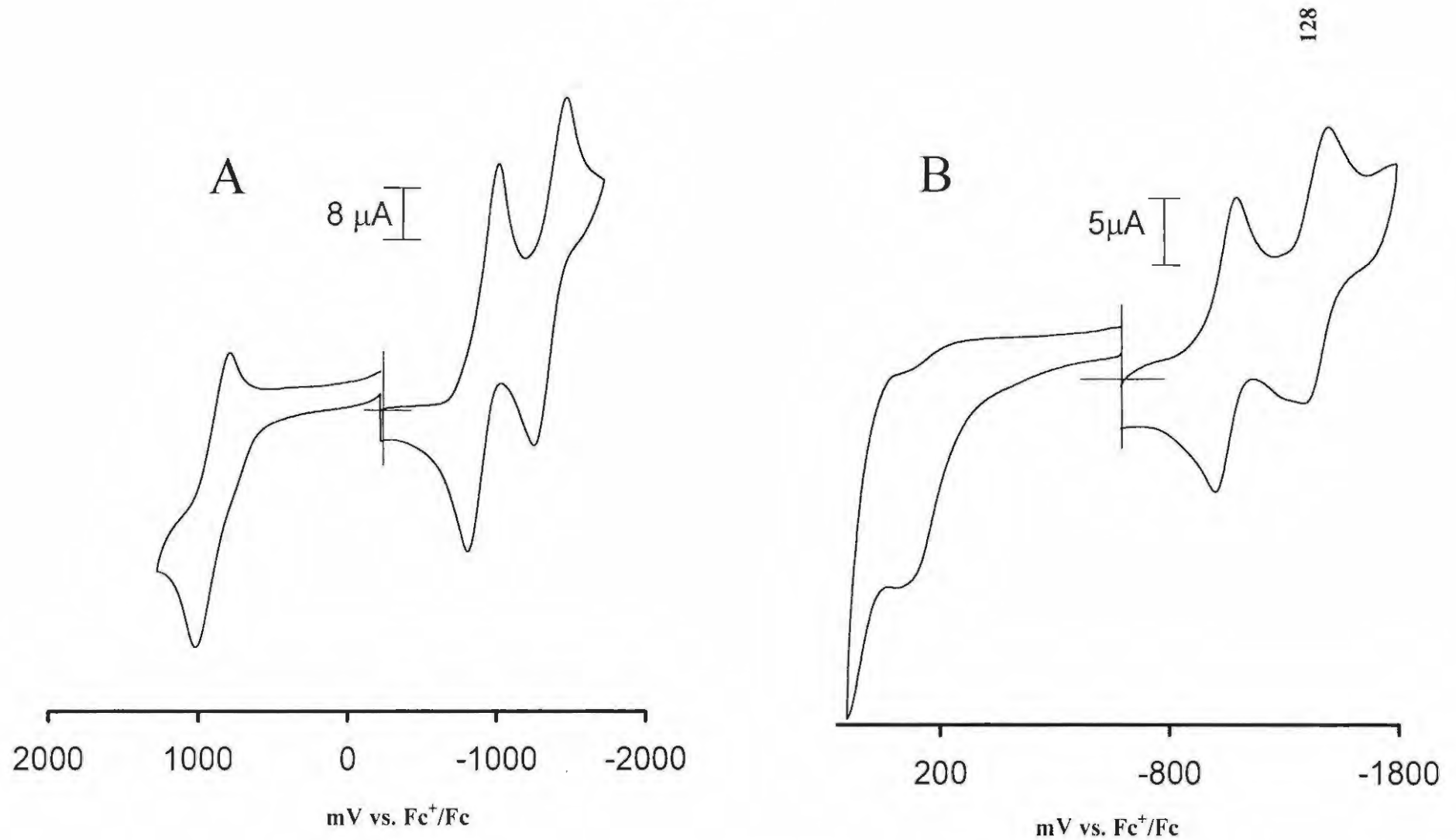


Fig. 36. Cyclic voltammograms (2nd scans) of complex 61 in A) CH₂Cl₂ and B) DMF. Electrolyte = 0.1 m dm⁻³ TBAHP. Scan rate = 100 mV s⁻¹.

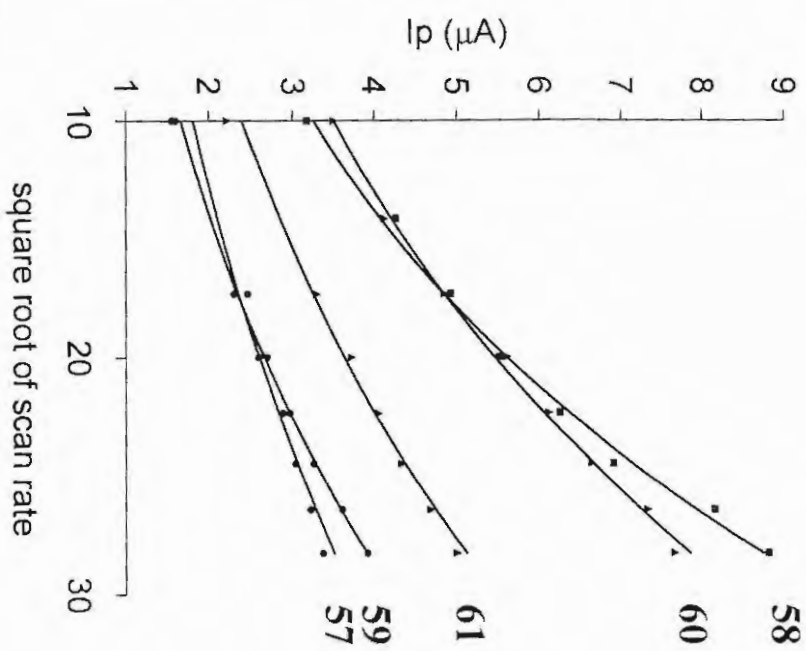
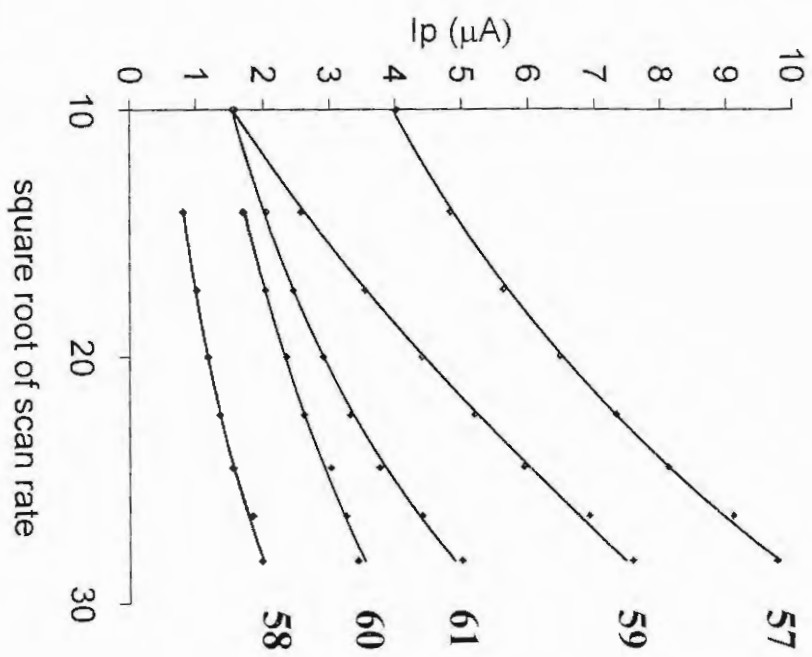


Fig. 37. The dependance of currents on the square root of scan rate for compounds **57** to **61** in a) DMF and b) CH_2Cl_2 . The currents plotted are for the first reduction couple (cathodic currents). Electrolyte = 0.1 mol dm^{-3} TBAHP.

-Chapter 2-

Examples of voltammograms obtained on repetitive scanning of the complexes on a glassy carbon electrode are shown in Figs 38 and 39. Typically cyclic voltammograms were obtained by scanning 10 times consecutively; three different types of behaviour were recognized. Firstly most of the compounds (55 and 57 to 60) displayed a decrease in their peak currents and then stabilized after a few scans.

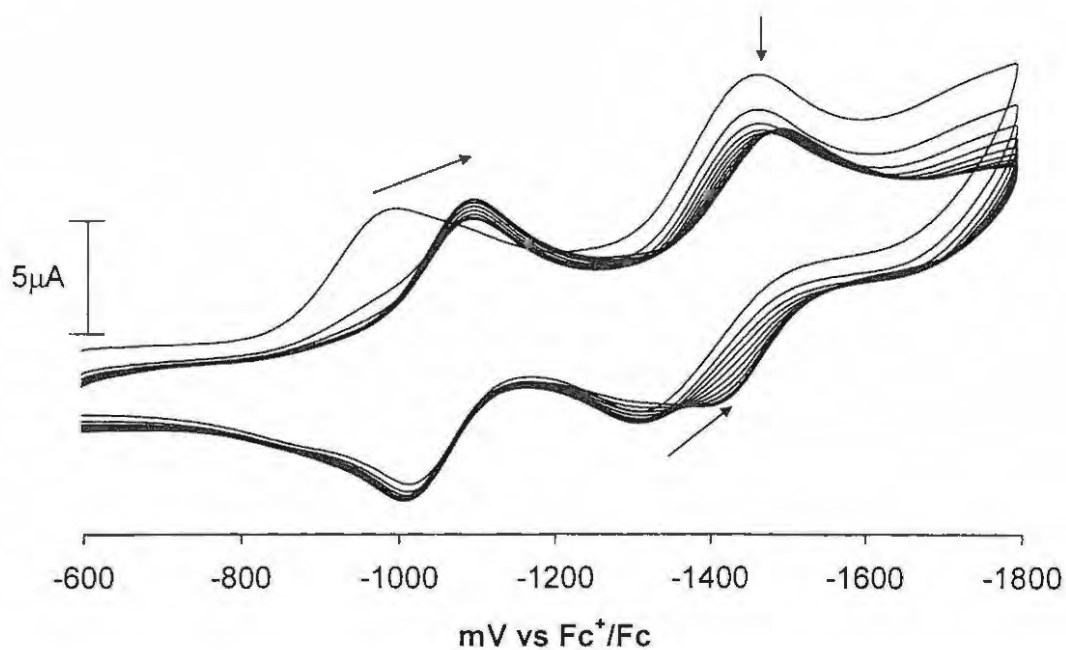


Fig. 38. Repetitive scanning of a solution of 61 in DMF. Electrolyte = 0.1 mol dm⁻³ TBAHP. Scan rate = 100 mV s⁻¹.

-Chapter 2-

This behaviour may be attributed to the orientation of the molecules onto the electrode surface. Aromatic systems are known to physisorb onto glassy carbon surfaces and this effect may cause a decrease in the peak currents, with the physisorbed molecules being responsible for the cyclic voltammograms obtained with time. The second type of voltammogram obtained was that for compound **61** wherein the first reduction peak showed a marked shift in peak potential to more negative values after the first scan. The reversibility of the second reduction couple improved after the first scan and in addition this couple shifted to a more negative potential. Fig. 38. There is also a slight decrease in currents for the second reduction couple, before stable currents are obtained. The shifting in potentials after the first scan suggests that a different complex is formed on the electrode, probably due to polymerization of the compound. The third type of voltammogram (compound **54**) showed an increase in currents for all peaks. Fig. 39, probably due to electrodeposition of the complex onto the electrode. This behaviour was observed only for **54**. The behaviour discussed above was observed on GCE and not on Au, because of the functional groups on the surface of GCE.

-Chapter 2-

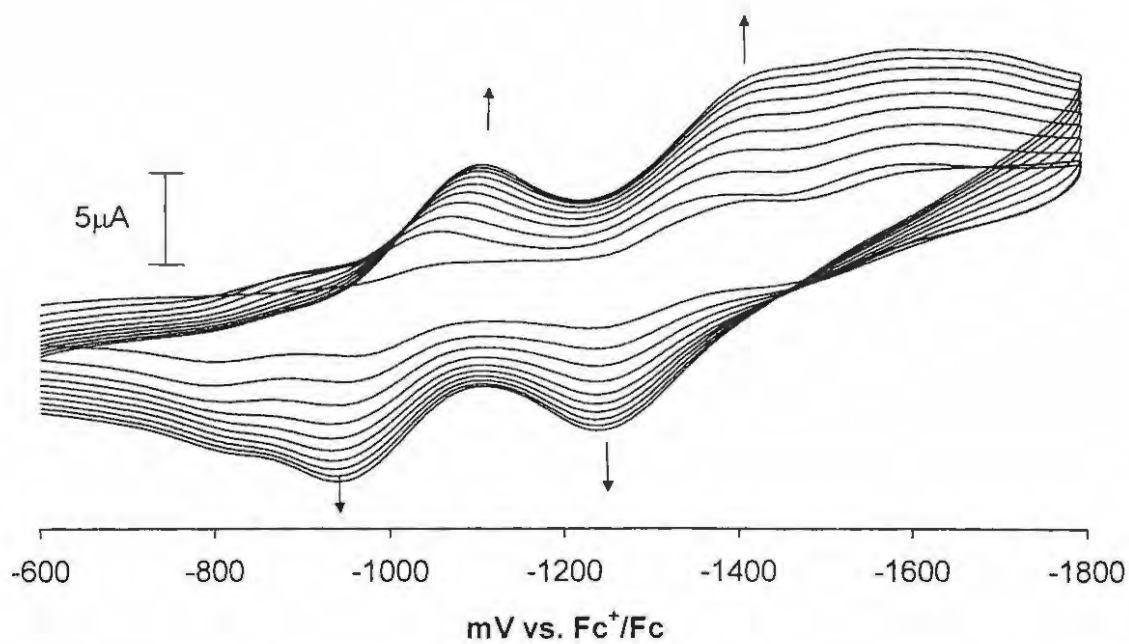


Fig. 39. Repetitive scanning of a solution of **54** in DMF. Electrolyte = 0.1 mol dm^{-3} TBAHP. Scan rate = 100 mV s^{-1} .

The increase in peak currents for **54** has a logarithmic relation to the number of scans (Fig. 40).

-Chapter 2-

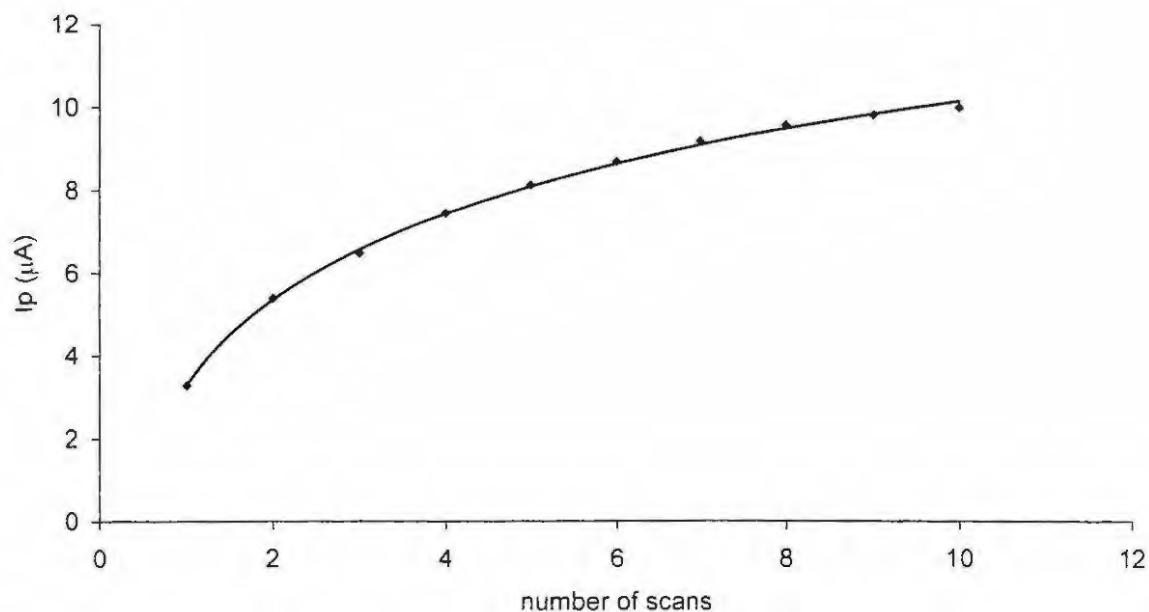


Fig. 40 The variation of current with scan number for compound **54** dissolved in DMF. Electrolyte = 0.1 mol dm^{-3} TBAHP. Scan rate = 100 mVs^{-1} .

The establishment of constant current after many scans signals complete coverage of the electrode. The differences in the behaviour of the complexes on repetitive scanning show that the axial ligands impart different properties onto the phthalocyanine complex. The nature of the products formed on the cyclic voltammetry scale following reduction of the complexes determine the ultimate behaviour of the phthalocyanine complexes upon repetitive scanning. For example, electrodeposition of compound **54** onto the electrode suggests that the product formed following reduction of this complex is less soluble than the parent

-Chapter 2-

compound, hence electrodeposition occurs. The proposed polymerization of compound **61**, may be due to the formation of highly reactive radical species upon reduction which attack neighbouring molecules, resulting in the polymerization.

For all the compounds in DMF, the oxidation couple showed more enhanced anodic currents when compared to cathodic currents, regardless of the scan number. This behaviour was observed when DMF was employed on a gold or on GC electrodes. However using dichloromethane as a solvent, i_{pc}/i_{pa} was found to be near unity for the oxidation couple, Fig. 36. The differences in the behaviour of the oxidation couple in DMF when compared to CH_2Cl_2 could be a result of the mild reducing nature of DMF. ΔE values for the oxidation couple were found to range from 90 to 200 mV for all complexes, suggesting quasi-reversible to irreversible behaviour. The peak currents for the oxidation process were also found to vary exponentially with the square root of scan rate as shown in Fig. 37 for the reduction process, again suggesting slow electron transfer. Oxidation is expected to occur more readily for SiPc complexes containing electron donating ligands. Complexes **58** and **60** were found to be more readily oxidized in dichloromethane, compared to the rest, reflecting a comparatively larger electron donating nature of the axial ligands. These two complexes were also more difficult to reduce in dichloromethane, Table 11. Due to the electron withdrawing nature of the chloride ligand, compound **54** was the easiest to reduce, though

-Chapter 2-

correspondingly was not the most difficult to oxidize. Compound **61** was more difficult to oxidize in dichloromethane than the rest of the complexes. The reduction couples were found to be separated by ~0.3 to 0.5 V in agreement with the separation reported for ring-based reduction processes in main group metal phthalocyanines¹³⁹. The separation between the first oxidation and the first reduction couples has been reported to be approximately 1.60 V for main group metal phthalocyanines.¹⁴⁰ The separation was found to be between 1.6 and 1.7 V for all the complexes except compound **61**, whose separation was found to be 1.8 V.

Table 11. Cyclic voltammetric data for all the silicon phthalocyanines containing 0.1M TBAHFP (all data represents $E_{1/2}$ /mV (vs Fc^+/Fc)).

Compound	1 st reduction		2 nd reduction		Oxidation	
	DMF	CH ₂ Cl ₂	DMF	CH ₂ Cl ₂	DMF	CH ₂ Cl ₂
54	-1011	-847	-1322	-1121	+603	+747
55	-968	-931	-1444	-1369	+388	+841
57	-870	-958	-1352	-1345	-	+733
58	-790	-988	-1263	-1397	+602	+626
59	-822	-889	-1342	-1296	-	+790
60	-829	-989	-1291	-1457	+314	+650
61	-1031	-929	-1450	-1371	+366	896

-Chapter 2-

The electrochemical data revealed some interesting aspects of the effect of axial ligands on the electronic nature of the silicon octaphenoxyphthalocyanine molecule, although no trend was observed in terms of oxidation potential and the ability of these molecules to generate singlet oxygen or to photodegrade by an oxidative mechanism.

Experimental

3.1 Equipment

UV-visible spectra were recorded on a Varian 500 UV/visible/NIR spectrophotometer. IR spectra (KBr pellets) were recorded on a Perkin-Elmer spectrum 2000 FTIR spectrometer. ^1H -nuclear magnetic resonance (NMR, 400 MHz) spectra were obtained in CDCl_3 using the Bruker EMX 400 NMR spectrometer.

3.2 Materials

Dimethylformamide (DMF), pyridine, dimethylsulfoxide (DMSO), 1,3-diphenylisobenzofuran (DPBF), diazabicyclooctane (DABCO), benzaldehyde, 1-naphtol, 2-naphtol, triphenylsilanol, trihexylsilanol, triethanolamine, methylsulphonic acid, succinic anhydride, 4-nitrophenol, 4-aminophenol, p-toluene sulphonic acid, terephthalic acid, propionic acid, phenol, hydroquinone, silicon tetrachloride, tetrahydronaphthalene, 1-chloronaphthalene, phthalonitrile, 4,5 dichlorophthalic acid, formamide, thionyl chloride, acetic anhydride, magnesium sulphate, potassium carbonate, isonicotinic acid and aminoethanol were used as supplied (Sigma-Aldrich). Zinc phthalocyanine (ZnPc), used as a standard was a gift from Dr. V. Derkacheva, from the Organic Intermediates and Dyes Institute in Moscow.

- Chapter 3 -

3.3 Electrochemical methods

Electrochemical data were collected with the BioAnalytical Systems (BAS) model 100 B/W electrochemical workstation. For cyclic voltammetry, a glassy carbon electrode (GCE, 3.0 mm diameter) was used as a working electrode in DMF solutions. In experiments employing dichloromethane as a solvent, a gold electrode (1.6 mm diameter) was employed as a working electrode. Platinum wire auxiliary and Ag wire pseudo-reference electrodes were employed for all electrochemical experiments. Ferrocene was employed as an internal standard, and tetrabutyl ammonium hexafluorophosphate (TBAHP) (0.1 mol dm^{-3}) as an electrolyte. Prior to cyclic voltammetry scans the glassy carbon or gold electrodes were polished with alumina ($< 10 \text{ nm}$) on a Buehler felt pad, followed by washing with deionised water and rinsing with methanol. For cyclic voltammetry studies concentrations were of the order of $10^{-3} \text{ mol dm}^{-3}$.

3.4 Photochemical methods

The photochemical experiments were carried out in a spectrophotometric cell of 1-cm pathlength. The experiments were carried out in air (i.e. without deoxygenating or bubbling of oxygen). Typically a 2 ml DMSO solution of the silicon octaphenoxy derivatives ($0.5 - 1 \times 10^{-5} \text{ mol l}^{-1}$) was introduced to the cell and photolysed in the Q band region of the dye with a General Electric

- Chapter 3 -

Quartz line lamp (300W). A 600 nm glass cut off filter (Schott) and a water filter were used to filter off ultraviolet and far infrared radiation. An interference filter (Intor, 670 nm with a bandwidth of 20 nm) was placed in the light path before the sample. To measure the light intensity, a power meter may be used and gives a value in $\text{J s}^{-1} \text{cm}^{-2}$. This value may then be converted into photons $\text{s}^{-1} \text{cm}^{-2}$ by dividing the energy of the wavelength of interest ($E = hc/\lambda$) into the value read off the light meter. The light intensity was thus measured and found to be 5×10^{16} photons $\text{s}^{-1} \text{cm}^{-2}$. The wavelength of the interference filter was chosen such that it was close to the Q band absorption of the phthalocyanine. Experiments were also performed whereby the solutions were deaerated with N_2 gas or saturated with O_2 in order to study the role of oxygen in the mechanism for photobleaching and photo-assisted axial ligand exchange in silicon octaphenoxy derivatives. 2,4-Ditertbutylphenol ($1 \times 10^{-2} \text{mol l}^{-1}$) and DABCO ($2 \times 10^{-3} \text{mol l}^{-1}$) were used as radical and singlet oxygen scavengers respectively. d_6 -DMSO was also used for hydrogen abstraction and singlet oxygen information.

- Chapter 3 -

3.4.1 Singlet oxygen quantum yields determination

To determine singlet oxygen quantum yields the relative method using ZnPc as reference and DPBF as scavenger of singlet oxygen were used. To avoid chain reactions induced by DPBF in the presence of singlet oxygen the concentration of DPBF was lowered to $\sim 3 \times 10^{-5} \text{ mol l}^{-1}$. These conditions resulted in first order kinetics being observed. The typical procedure was as follows. DMSO solutions containing the $(X)_2\text{SiOPPc}$ derivative (absorbance below 1 at the irradiation wavelength) and DPBF ($3 \times 10^{-5} \text{ mol l}^{-1}$) were prepared in the dark. Experiments were carried out in air without bubbling oxygen using a 2.0 ml sample of solution and this was irradiated in the Q band region. DPBF absorption decay at 417 nm was then followed. The light intensity and amount of absorbed photons were also obtained as mentioned above. The values of Φ_{Δ} were calculated with the Eq. 14 as explained in Chapter 1:

$$\Phi_{\Delta}^{\text{MPc}} = \Phi_{\Delta}^{\text{ZnPc}} \frac{(C_0 - C_t)^{\text{MPc}} (\alpha t)^{\text{ZnPc}} [\text{DPBF}]^{\text{ZnPc}}}{(C_0 - C_t)^{\text{ZnPc}} (\alpha t)^{\text{MPc}} [\text{DPBF}]^{\text{MPc}}} \quad \dots \text{Eq. 14}$$

The initial DPBF concentrations are kept the same for the ZnPc reference and the samples. Fig. 41 illustrates the setup used for photobleaching as well as singlet oxygen determinations the error in these calculations are $\pm 15\%$.

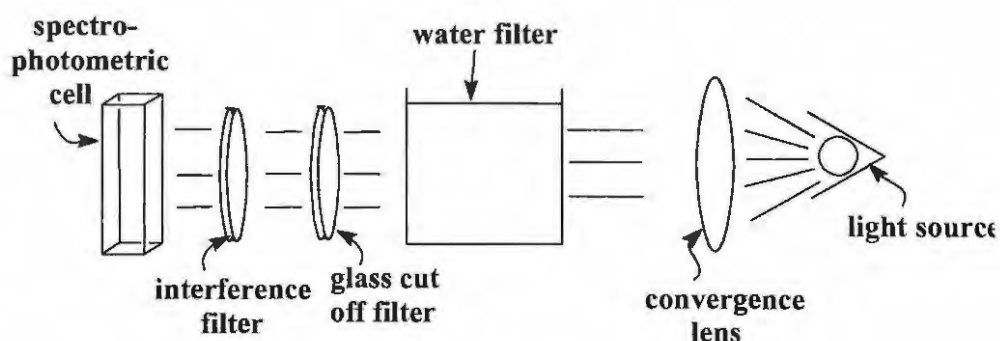


Fig. 41 Equipment setup for photochemical experiments

3.5 Photophysical determinations

Absorption and Fluorescence spectra were performed on a Perkin Elmer Lambda 15 and SPEX fluoromax spectrophotometers, respectively. Fluorescence decay measurements were made using the time-correlated single-photon method.¹⁴¹ The excitation source was a frequency-doubled, mode-locked Nd-Yag laser coupled to a synchronously pumped cavity-dumped dye laser with excitation at 640 nm. Detection was via a microchannel plate photomultiplier (Photek) and the instrument response time was up to 300 ps. The transient absorption spectra and decay kinetics were recorded using a laser flash-photolysis system. The excitation pulse was provided by an Nd-YAG laser (in frequency doubled mode, providing 160mJ, 8ns pulses of laser light at 0-10Hz), pumping a lambda-Physik FL2002 dye laser. Single laser pulse energies used ranged from 0.001 to 2 mJ. A 75 W xenon arc lamp provided the analyzing light. The kinetic curves were

- Chapter 3 -

averaged over 1-8 laser pulses by a Tektronix 2221A oscilloscope and then transferred to a PC via an in-house computer program. Fluorescence (Φ_F) and triplet (Φ_T) quantum yields were calculated by a comparative method using zinc phthalocyanine (0.18). Triplet extinction coefficients were calculated using the singlet depletion method.¹⁴² The laser flash photolysis system is schematically presented in Fig. 42.

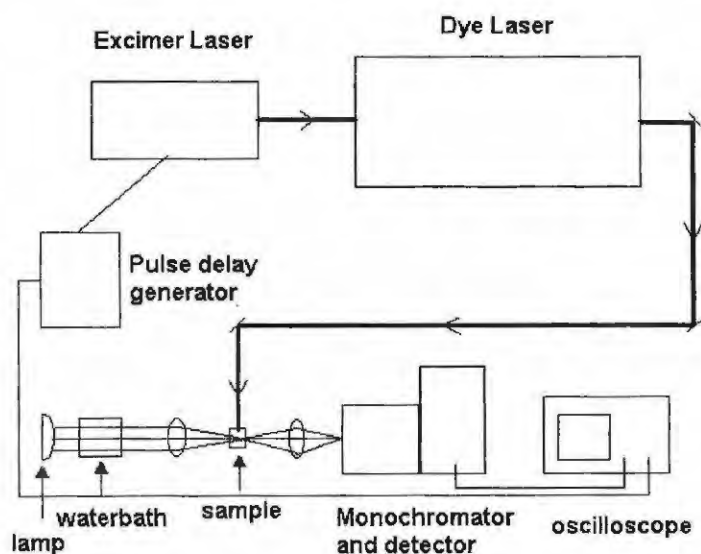


Fig. 42. The laser flash photolysis system for photophysical determinations.

3.5.1 Geometry optimization

Hyperchem Pro 6 was used to determine the optimum structure of compound 73 using the restricted hartree-fock semi-empirical PM3 method. The Newton-

- Chapter 3 -

Raphson optimization method was used. No configuration interaction calculations were performed.

3.6 Synthesis

3.6.1 Phthalonitriles synthesis¹¹⁰

4, 5-Dichlorophthalic anhydride (48) [Scheme 20, page 57]

A mixture of 4,5-dichlorophthalic acid 47 (30.0g, 0.13 mol) and acetic anhydride (50 ml) was heated under weak reflux for 5h while slowly distilling off of acetic acid being allowed. The reaction mixture was cooled, filtered and the filtrate was washed with petroleum ether to yield the 4,5-dichlorophthalic anhydride 48 (22.2g, 80%)

4,5-Dichlorophthalimide (49) [Scheme 20, page 57]

4,5-dichlorophthalic anhydride 48 (20.0g, 0.09 mol) was heated while stirring in formamide (30 ml) for 3h under reflux. After cooling, filtration and washing with water the light yellow powder was air dried to yield the 4,5 dichlorophthalimide 49 (14.5g, 75%).

4,5-Dichlorophthalamide (50) [Scheme 20, page 57]

4,5 Dichlorophthalimide 49 (14g, 0.07 mol) was stirred in 25 % aqueous ammonia solution (300 cm³) for 24h before a further 100 cm³ 25 % aqueous

- Chapter 3 -

ammonia solution was added. After 24 hours the yellowish product was filtered off and washed with water (3 x 200 ml) to yield the 4,5-dichlorophthalamide **50** (14.6g, 90 %); $\delta_{\text{H}}(\text{CDCl}_3)$ 8.42 (1H, d, Ar-H) 8.24 (1H, dd, Ar-H), 7.89 (1H, d, Ar-H). $\nu_{\text{max}}/\text{cm}^{-1}$ (KBr) 3340 (NH₂), 1679 (C=O), 1615 (NH₂).

4,5-Dichlorophthalonitrile (51) [Scheme 20, page 57]

Freshly distilled thionyl chloride (70 cm³, 0.07 mole) was added while stirring at 0°C to dry dimethylformamide (100 cm³) in a nitrogen atmosphere. After 2 hours, dry 4,5-dichlorophthalamide **50** (14g, 0.06 mol) was added. The mixture was stirred for 5h at 0°C and then at room temperature overnight before it was added to ice water (approx. 500 cm³), filtered and washed with water (6 x 100 cm³). After recrystallizing twice from methanol light yellow 4,5-dichlorophthalonitrile **51** was obtained (7.2 g, 61.0 %); $\delta_{\text{H}}(\text{CDCl}_3)$ 8.69 (1H, d, Ar-H), 8.62 (1H, dd, Ar-H), 8.11 (1H, d, Ar-H). $\nu_{\text{max}}/\text{cm}^{-1}$ (KBr) 2242 (CN), 1542 (NO₂), 1359 (NO₂)

4,5-Diphenoxyphthalonitrile (52) [Scheme 20, page 57]

A mixture of 4,5-Dichlorophthalonitrile **51** (0.80g, 4.06 mmol) and phenol (2.35g, 25 mmol) was added to dry DMSO (9ml) at 90°C under nitrogen. Dry K₂CO₃ (1.10g, 8 mmol) was added every 5 minutes until 8 portions had been

- Chapter 3 -

added (8.80g). The mixture was allowed to cool to room temperature and then added to ice-water (80 ml). The product **52** was filtered and recrystallized from methanol. Yield: 0.75g, 59%). $\delta_{\text{H}}(\text{CDCl}_3)$: 7.53 (4H, t, Ar-H), 7.36 (2H, t, Ar-H), 7.33 (2H, s, Ar-H), 7.15 (4H, d, Ar-H). $\nu_{\text{max}}/\text{cm}^{-1}$ (KBr) 2231 (CN), 1209 (Ar-O).

4,5-Diphenoxy-diiminoisoindoline (53) [Scheme 21, page 59]

The dicyanobenzene **52** (0.75g, 2.40 mmol) was added to a mixture of dry methanol (7 ml) and sodium methoxide (0.013 g). Anhydrous ammonia gas was bubbled through the stirred suspension for 1 hour. The suspension was then refluxed for 6h with continued addition of ammonia gas. The mixture was filtered and the green product **53** precipitated from methanol with water (20 ml), filtered and dried at 60°C *in vacuo* (0.61g, 72%). $\nu_{\text{max}}/\text{cm}^{-1}$ (KBr) 1692 (C=NH).

3.6.2 Silicon phthalocyanines synthesis

Octaphenoxypthalocyanininato (dichloro) silicon (54) [Scheme 22, page 61]

A mixture of the diiminoisoindoline **53** (0.62g, 1.98 mmol) and dry quinoline (2 ml) was stirred at room temperature for 10 minutes. SiCl_4 (0.2 ml, 2.8 mmol) was added and the mixture refluxed for 2 hours under nitrogen. 6 mol

- Chapter 3 -

dm⁻³ hydrochloric acid (20ml) was then added to the mixture. The resulting product was filtered and then Soxhlet extracted with methanol until the extracts were clear, yielding a pure product after drying at 110°C overnight (0.45g, 67%). Anal. Calcd. for C₈₀H₄₈Cl₂N₈O₈Si: C,71.27; H,3.59; N, 8.31. Found: C,68.91; H,3.24; N,7.71. $\delta_{\text{H}}(\text{CDCl}_3)$: 9.21 (8H, s, 3,6-Pc), 7.50 (16H, t, Ar-H), 7.30 (24H, m, Ar-H). $\nu_{\text{max}}/\text{cm}^{-1}$ (KBr): 1203 (Ar-O).

Octaphenoxyphthalocyaninato (dihydroxy) silicon (55) [Scheme 23, page 63]

Compound **54** (0.20g, 0.15 mmol) was refluxed in a 1:1 mixture of pyridine and 25% ammonium hydroxide (20 ml) for 10 hours. The mixture was filtered and the precipitate washed with water. Upon drying at 110°C overnight the pure dihydroxy compound **55** (0.18g, 92%) was obtained. Anal. Calcd. for C₈₀H₅₀N₈O₁₀Si: C,73.27; H,3.85; N, 8.55. Found: C, 69.10; H, 3.44; N, 7.90. $\nu_{\text{max}}/\text{cm}^{-1}$ (KBr): 3393 (OH), 1207 (Ar-O), 850 (Si-O). This compound is to insoluble for ¹H-NMR determination.

For the axially ligated silicon octaphenoxy complexes **57** to **73** see Scheme 24, page 67 and Fig. 16, page 70

- Chapter 3 -

Octaphenoxyphthalocyaninato (bis(4-carboxybenzene)acetato) silicon (57)

A solution of the dichloro compound **54** (15mg, 0.011mmol) in DMF (2 ml) was heated to 160°C was added terephthalic acid (0.17g, 1 mmol) was added. The solution was refluxed for 1hour and allowed to cool. Water (10 ml) was added and the suspension was filtered and washed with water. The resulting product was extracted with chloroform. The green chloroform solution was dried with magnesium sulphate, filtered and the chloroform removed by distillation under reduced pressure to yield the product (16.1mg, 91%). Anal. Calcd. for C₉₆H₅₈N₈O₁₆Si: C,71.72; H,3.64; N, 6.97. Found: C, 70.55; H, 3.21;N, 6.71. $\delta_{\text{H}}(\text{CDCl}_3)$: 8.96 (8H, s, 3,6-Pc), 7.50 (16H, t, Ar-H), 7.31 (24H, m, Ar-H), 6.95 (4H, d, Ar-H), 5.18 (4H, d, Ar-H). $\nu_{\text{max}}/\text{cm}^{-1}$ (KBr): 1687 (CO), 1205 (Si-O).

Octaphenoxyphthalocyaninato bis(isonicatinato) silicon (58)

To a solution of the dichloro compound **54** (15mg, 0.011mmol) in DMF (2ml), isonicotinic acid (0.12g, 1mmol) was added and the solution was refluxed for 1 h. The solution was allowed to cool and 10 ml of water was added. The precipitate was washed with water and then extracted with chloroform. The chloroform solution was dried with anhydrous magnesium sulphate and the chloroform removed under reduced pressure to yield the product (15.4mg, 92%). Anal. Calcd. for C₉₂H₅₆N₁₀O₁₂Si: C,72.62; H,3.71; N,

- Chapter 3 -

9.21. Found: C, 72.18; H, 3.81; N, 8.74. $\delta_{\text{H}}(\text{CDCl}_3)$: 8.98 (8H, s 3,6-Pc), 7.61(4H, d, Ar-H), 7.51 (16H, t, Ar-H), 7.33 (24H, m, Ar-H), 4.97(4H, Ar-H). $\nu_{\text{max}}/\text{cm}^{-1}$ (KBr): 1686 (CO), 1203 (Si-O).

Octaphenoxyphthalocyaninato bis(propionato) silicon (59)

Propionic acid was added to a refluxing solution of **54** (20mg, 0.015mmol) in DMF. After one hour of refluxing the solution was allowed to cool to room temperature. Water (10 ml) was added and the mixture filtered. The precipitate was washed with water and then dissolved in chloroform, which was dried with magnesium sulphate and removed under reduced pressure to yield compound **59** (20 mg, 93%). Anal. Calcd. for $\text{C}_{86}\text{H}_{58}\text{N}_8\text{O}_{12}\text{Si}$: C,72.56; H,4.11; N, 7.87. Found: C, 72.87; H, 3.97; N, 7.63. $\delta_{\text{H}}(\text{CDCl}_3)$: 8.99 (8H, s, 3,6-Pc), 7.50 (16H, m, Ar-H), 7.32 (24H, m, Ar-H), -0.8 (4H, q, $-\text{CH}_2$), -1.1 (6H, t, $-\text{CH}_3$). $\nu_{\text{max}}/\text{cm}^{-1}$ (KBr): 1691 (CO), 1204 (Ar-O), 864 (Si-O).

Octaphenoxyphthalocyaninato bis(nitrophenoxy) silicon (60)

Nitrophenol (2g) was heated to 160°C and the dihydroxy compound **55** (20 mg, 0.015 mmol) was added. The solution was stirred for 30 minutes and allowed to cool. The resulting solid was Soxhlet extracted with water until no more yellow nitrophenol was observed yielding the product (22 mg, 93 %).

- Chapter 3 -

Anal. Calcd. for $C_{92}H_{56}N_{10}O_{14}Si$: C, 71.13; H, 3.63; N, 9.02. Found: C, 68.82; H, 4.06; N, 9.04. $\delta_H(CDCl_3)$: 8.94 (8H, s, 3,6-Pc), 7.53 (16H, t, Ar-H), 7.32 (24H, m, Ar-H), 6.59 (4H, d, Ar-H), 2.44 (4H, d, Ar-H). ν_{max}/cm^{-1} (KBr): 1515 (NO₂), 1340 (NO₂), 1202 (Ar-O), 862 (Si-O).

Octaphenoxyphthalocyaninato bis(dimethylaminoxy) silicon (61)

The dihydroxy compound **55** (20 mg, 0.015 mmol) was added to a refluxing solution of dimethylaminoethanol (3 ml) and allowed to reflux for 1 hour. The solution was cooled to room temperature and 10 ml of water was added. The mixture was filtered and the precipitate (product) washed with water. The product was then dissolved in chloroform and the chloroform removed under reduced pressure to give a yield of 21 mg, 93 %. Anal. Calcd. for $C_{88}H_{68}N_{10}O_{10}Si$: C, 72.71; H, 4.71; N, 9.64. Found: C, 70.53; H, 4.81; N, 8.77. $\delta_H(CDCl_3)$: 9.00 (8H, s, 3,6-Pc), 7.48 (16H, t, Ar-H), 7.28 (24H, m, Ar-H), 0.58 (12H, s, CH₃), -0.85 (4H, t, α -CH₂), -2.0 (4H, t, β -CH₂). ν_{max}/cm^{-1} (KBr): 1301 (CN), 1202 (Ar-O), 863 (Si-O).

The axial ligation of the complexes **62** to **73** was achieved by the following general procedure. To a solution of compound **54** or **55** in DMF (1 ml per 0.1 g) was added a 6 molar excess of the appropriate ligands for the formation of compounds **62** to **73**. The solution was refluxed for 30 min and the reaction

- Chapter 3 -

mixture quenched by addition of water (until complete precipitation). The precipitates were worked up in three different ways after quenching with water as follows:

1) Excess ligands present following the synthesis of compounds **62**, **63**, **64**, **65**, **66**, and **67** were removed by dissolving the precipitate (containing both the unreacted acidic axial ligand compounds and the phthalocyanine) in chloroform and extracting with a 10% NaOH solution. The last step removed the base-soluble reagents completely as could be witnessed by clear colour changes in the aqueous layers. Compound **65** was additionally washed with a 1M HCl solution. The chloroform layer was then evaporated off to yield compounds **62**, **63**, **64**, **65**, **66**, and **67** all in quantitative yields (excess of 95%).

2) Excess ligands from the synthesis of **68**, **70** and **71** were removed by dissolving the respective precipitates in chloroform and washing with water (removing all the water-soluble acidic reagents), the chloroform was again evaporated off to give **68**, **70** and **71** in quantitative yields (greater than 95%).

3) Compounds **69**, **72** and **73** were isolated from their respective precipitates by TLC using chloroform as an eluent to give the following yields for **69** (82%), **72** (57%) and **73** (60%). Compound **69** actually showed three products

- Chapter 3 -

after the reaction and these were the phthalocyanine (green), the anhydride (colourless) and also the succinic acid (colourless). These three products separate well chromatographically. In the following data the common infrared bands at $\sim 850\text{ cm}^{-1}$ due to the Si-O and at $\sim 1200\text{ cm}^{-1}$ due to the aromatic ether bonds are omitted.

Octaphenoxyphthalocyaninato bis(1-naphthoxy) silicon (62)

Anal. Calcd. for $\text{C}_{100}\text{H}_{62}\text{N}_8\text{O}_{10}\text{Si}$: C, 76.81; H, 4.01; N, 7.19. Found: C, 76.22; H, 3.77; N, 7.0. $\delta_{\text{H}}(\text{CDCl}_3)$ 9.00 (8H, s, 3,6-Pc), 7.51 (16H, m, Ar-H), 7.29 (24H, m, Ar-H), 7.05 (2H, d, Ar-H), 6.93 (4H, m, Ar-H), 6.43 (2H, d, Ar-H), 6.21 (2H, d, Ar-H), 2.79 (2H, s, Ar-H). $\nu_{\text{max}}/\text{cm}^{-1}$ (KBr) 1600 (C-H).

Octaphenoxyphthalocyaninato bis(2-naphthoxy) silicon (63)

Anal. Calcd. for $\text{C}_{100}\text{H}_{62}\text{N}_8\text{O}_{10}\text{Si}$: C, 76.78; H, 4.01; N, 7.19. Found: C, 76.94; H, 4.33; N, 6.89. $\delta_{\text{H}}(\text{CDCl}_3)$ 8.98 (8H, s, 3,6-Pc), 7.47 (16H, m, Ar-H), 7.30 (24H, m, Ar-H), 7.04 (4H, t, Ar-H), 6.92 (4H, m, Ar-H), 6.44 (2H, d, Ar-H), 6.18 (2H, d, Ar-H). $\nu_{\text{max}}/\text{cm}^{-1}$ (KBr) 1600 (C-H)

Octaphenoxyphthalocyaninato bis(*p*-formylphenoxy) silicon (64)

- Chapter 3 -

Anal. Calcd. for $C_{92}H_{56}N_8O_{12}Si$: C, 74.08; H, 3.76; N, 7.54 Found: C, 74.12 ;H, 3.49; N, 7.88. $\delta_H(CDCl_3)$ 9.14 (2H, s, CHO), 8.96 (8H, s, 3,6-Pc), 7.50 (16H, t, Ar-H), 7.32 (24H, m, Ar-H), 6.26 (4H, d, Ar-H) 2.54 (4H, d, Ar-H). ν_{max}/cm^{-1} (KBr) 1707 (CHO).

Octaphenoxyphthalocyaninato bis(*p*-aminophenoxy) silicon (65)

Anal. Calcd. for $C_{92}H_{60}N_{10}O_{10}Si$: C, 74.04; H, 3.97; N, 9.38 Found: C, 73.58 ;H, 3.48 ; N, 9.49. $\delta_H(CDCl_3)$ 9.02 (8H, s, 3,6-Pc), 7.51 (16H, t, Ar-H), 7.32 (24H, m, Ar-H), 5.04 (4H, d, Ar-H), 3.22 (4H, s, NH_2), 2.26 (4H, d, Ar-H). ν_{max}/cm^{-1} (KBr) 3325 (NH_2), 1621 (NH_2), 1254 (NH_2).

Octaphenoxyphthalocyaninato bis(phenoxy) silicon (66)

Anal. Calcd. for $C_{92}H_{58}N_8O_{10}Si$: C, 75.47; H, 4.04; N, 7.73 Found: C, 74.87 ; H, 4.15; N, 7.66. $\delta_H(CDCl_3)$ 8.98 (8H, s, 3,6-Pc), 7.49 (16H, t, Ar-H), 7.28(24H, m, Ar-H), 5.76 (4H, d, Ar-H), 5.65 (4H, t, Ar-H), 2.41 (2H, d, Ar-H). ν_{max}/cm^{-1} (KBr) 1601 (C-H).

Octaphenoxyphthalocyaninato bis(*p*-hydroxyphenoxy) silicon (67)

Anal. Calcd. for $C_{92}H_{58}N_8O_{12}Si$: C, 73.88; H, 3.93; N, 7.48 Found: C, 74.21 ; H, 3.48; N, 7.88. $\delta_H(CDCl_3)$ 8.97 (8H, s, Ar-H), 7.49 (16H, t, Ar-H), 7.29

- Chapter 3 -

(24H, m, Ar-H), 5.12 (4H, d, Ar-H) 3.48 (2H, s, OH), 2.27 (4H, d, Ar-H).
 $\nu_{\max}/\text{cm}^{-1}$ (KBr) 3620 (OH).

Octaphenoxyphthalocyaninato Bis(diethanolamino-2-ethoxy) silicon (68)

Anal. Calcd. for $\text{C}_{92}\text{H}_{76}\text{N}_{10}\text{O}_{14}\text{Si}$: Calc.C, 70.17; H, 4.86; N, 8.92 Found: C, 69.94 ;H, 4.55; N, 8.78. $\delta_{\text{H}}(\text{CDCl}_3)$ 9.04 (8H, s, 3,6-Pc), 7.53 (16H, t, Ar-H), 7.30 (24H, m, Ar-H), 0.95 (8H, t, CH_2), 0.5 (8H, t, CH_2), -1.21 (4H, t, CH_2), -2.20 (4H, t, CH_2). $\nu_{\max}/\text{cm}^{-1}$ (KBr) 3638 (OH).

Octaphenoxyphthalocyaninato bis(succinoyl) silicon (69)

Anal. Calcd. for $\text{C}_{88}\text{H}_{58}\text{N}_8\text{O}_{16}\text{Si}$: Calc: C, 69.86; H, 3.91; N, 7.37 Found: C, 70.11; H, 3.58; N, 7.15. $\delta_{\text{H}}(\text{CDCl}_3)$ 9.05 (8H, s, 3,6-Pc), 7.51 (16H, t, Ar-H), 7.32 (24H, m, Ar-H), -0.91 (4H, t, CH_2), -2.10 (4H, t, CH_2). $\nu_{\max}/\text{cm}^{-1}$ (KBr) 1685 (CO).

Octaphenoxyphthalocyaninato bis(methanesulfonyl) silicon (70)

Anal. Calcd. for $\text{C}_{82}\text{H}_{54}\text{N}_8\text{O}_{14}\text{S}_2\text{Si}$: C, 67.14; H, 3.68; N, 7.59 Found: C, 66.78; H, 3.77; N, 7.77 $\delta_{\text{H}}(\text{CDCl}_3)$ 8.98 (8H, s, Ar-H), 7.57 (16H, t, Ar-H), 7.34 (24H, m, Ar-H), 0.28 (3H, s, CH_3).

- Chapter 3 -

Octaphenoxyphthalocyaninato bis(*p*-toluenesulphonyl) silicon (71)

Anal. Calcd. for $C_{94}H_{62}N_8O_{14}S_2Si$: C, 69.69; H, 3.89; N, 6.92 Found: C, 69.41; H, 3.47; N, 6.75. $\delta_H(CDCl_3)$ 8.49 (8H, s, 3,6-Pc), 7.48 (40H, m, Ar-H), 7.21 (8H, m, Ar-H), 2.95 (6H, s, CH_3). ν_{max}/cm^{-1} (KBr) 1605 (C-H).

Octaphenoxyphthalocyaninato bis(triphenylsiloxy) silicon (72)

Anal. Calcd. for $C_{116}H_{78}N_8O_{10}Si_3$: Calc.C, 76.18; H, 4.31; N, 6.12 Found: C, 76.10; H, 4.25; N, 6.01. $\delta_H(CDCl_3)$ 8.92 (8H, s, 3,6-Pc), 7.54 (16H, t, Ar-H), 7.30 (24H, m, Ar-H), 6.81 (6H, m, Ar-H), 6.53 (12H, m, Ar-H), 4.88 (12H, m, Ar-H). ν_{max}/cm^{-1} (KBr) 1044 (Si-O-Si).

Octaphenoxyphthalocyaninato bis(tri-*n*-hexylsiloxy) silicon (73)

Anal. Calcd. for $C_{116}H_{126}N_8O_{10}Si_3$ C, 74.21; H, 6.78; N, 6.02 Found: C, 74.78, H, 6.49; N, 5.85 $\delta_H(CDCl_3)$ 9.02 (8H, s, 3,6-Pc), 7.49 (16H, t, Ar-H), 7.29 (24H, m, Ar-H), 0.91 (12H, t, CH_2), 0.73 (18H, d, CH_3), 0.51 (12H, t, CH_2), -1.20 (12H, t, CH_2), -2.41 (12, t, CH_2). ν_{max}/cm^{-1} (KBr) 1051 (Si-O-Si)

- Chapter 3 -

See Fig. 17, page 78 for the oligomeric complexes 74 - 78

Oligomer 74

To a refluxing solution of the phthalocyanine **54** (5.1 mg) in dry DMF (4 ml) under nitrogen was added terephthalic acid (0.31 mg) previously completely dissolved in dry DMF (1 ml). The reaction was monitored by TLC and upon completion p-hydroxybenzaldehyde (0.1g) was added to the DMF solution and reflux was continued for 30 min. The reaction mixture was allowed to cool and water was added to quench the solution. After filtration the precipitate was washed with a 10% NaOH solution until the phenol and acid were washed out completely. A final wash with water and drying at 60°C under vacuum delivered the impure product, which was then further purified by preparative TLC using chloroform. (2.1 mg, 38%). Anal. Calcd. C, 73.82; H, 3.74; N, 7.57), Found. C, 74.11; H, 3.61; N, 7.51. $\delta_{\text{H}}(\text{CDCl}_3)$ 9.16 (2H, s, CHO) 9.00 (16H, s Ar-H); 7.51 (32H, t, Ar-H); 7.29 (48H, m, Ar-H); 6.31 (4H, d, Ar-H); 2.87 (4H, d, Ar-H); 2.57 (4H, d, Ar-H); $\nu_{\text{max}}/\text{cm}^{-1}$ (KBr) 1690 (CO)

Oligomer 75

To a refluxing solution of the phthalocyanine **54** (4.8 mg) in dry DMF (4 ml) under nitrogen was added terephthalic acid (0.39 mg) previously completely dissolved in dry DMF (1 ml). The reaction was monitored by TLC and upon

- Chapter 3 -

completion p-hydroxybenzaldehyde (0.1g) was added to the DMF solution and reflux was continued for 30 min. The reaction mixture was allowed to cool and water was added to quench the solution. After filtration the precipitate was washed with a 10% NaOH solution until the phenol and acid were washed out completely. A final wash with water and drying at 60°C under vacuum delivered the impure product which was then further purified by preparative TLC using chloroform.

(1.9 mg, 36%); Anal. Calcd: C, 73.66; H, 3.71; N, 7.64), Found. C, 73.29; H, 3.60; N, 7.85. $\delta_{\text{H}}(\text{CDCl}_3)$ 9.15 (2H, s, CHO) 8.99 (16H, s, Ar-H); 8.97 (8H, s, Ar-H); 7.50 (48H, m, Ar-H); 7.30 (72H, m, Ar-H); 6.30 (4H, d Ar-H); 2.89 (8H, m, Ar-H); 2.58 (4H, d Ar-H); $\nu_{\text{max}}/\text{cm}^{-1}$ (KBr)1690 (CO)

Oligomer 76

To a refluxing solution of the phthalocyanine **54** (5.1 mg) in dry DMF (4 ml) under nitrogen was added terephthalic acid (0.47 mg) previously completely dissolved in dry DMF (1 ml). The reaction was monitored by TLC and upon completion p-hydroxybenzaldehyde (0.1g) was added to the DMF solution and reflux was continued for 30 min. The reaction mixture was allowed to cool and water was added to quench the solution. After filtration the precipitate was washed with a 10% NaOH solution until the phenol and acid were washed out completely. A final wash with water and drying at 60°C

- Chapter 3 -

under vacuum delivered the impure product which was then further purified by preparative TLC using chloroform. (1.8 mg, 32%); Anal. Calcd: C, 73.58; H, 3.69; N, 7.67, Found: C, 73.11; H, 3.55; N, 7.49. $\delta_{\text{H}}(\text{CDCl}_3)$ 9.15 (2H, s, CHO) 9.00 (16H, s, Ar-H); 8.98 (16H, s, Ar-H); 7.50 (64H, m, Ar-H); 7.30 (96H, m, Ar-H); 6.29 (4H, d, Ar-H); 2.87 (12H, m, Ar-H); 2.60 (4H, d, Ar-H); $\nu_{\text{max}}/\text{cm}^{-1}$ (KBr)1690 (CO).

Oligomer 77

To a refluxing solution of the phthalocyanine **54** (5.1 mg) in dry DMF (4 ml) under nitrogen was added terephthalic acid (0.50 mg) previously completely dissolved in dry DMF (1 ml). The reaction was monitored by TLC and upon completion p-hydroxybenzaldehyde (0.1g) was added to the DMF solution and reflux was continued for 30 min. The reaction mixture was allowed to cool and water was added to quench the solution. After filtration the precipitate was washed with a 10% NaOH solution until the phenol and acid were washed out completely. A final wash with water and drying at 60°C under vacuum delivered the impure product which was then further purified by preparative TLC using chloroform.

(1.9 mg, 34%); Anal. Calcd C, 73.53; H, 3.68; N, 7.69, Found. C, 73.44; H, 3.75; N, 7.81. $\delta_{\text{H}}(\text{CDCl}_3)$ 9.16 (2H, s, CHO) 8.99 (16H, s, Ar-H); 8.97 (16H,

- Chapter 3 -

s, Ar-H); 8.95 (8-H, s, Ar-H); 7.49 (80H, m, Ar-H); 7.29 (120H, m, Ar-H); 6.31 (4H, d, Ar-H); 2.89 (16H, m, Ar-H); 2.57 (4H, d, Ar-H); $\nu_{\max}/\text{cm}^{-1}$ (KBr)1690 (CO)

Oligomer 78

To a refluxing solution of the phthalocyanine 54 (5.0 mg) in dry DMF (4 ml) under nitrogen was added terephthalic acid (0.55 mg) previously completely dissolved in dry DMF (1 ml). The reaction was monitored by TLC and upon completion p-hydroxybenzaldehyde (0.1g) was added to the DMF solution and reflux was continued for 30 min. The reaction mixture was allowed to cool and water was added to quench the solution. After filtration the precipitate was washed with a 10% NaOH solution until the phenol and acid were washed out completely. A final wash with water and drying at 60°C under vacuum delivered the impure product which was then further purified by preparative TLC using chloroform.

(1.0 mg), 18%; Anal. Calcd Calc: C, 73.43; H, 3.66; N, 7.73. Found. C, 74.01; H, 3.64; N, 7.65. $\delta_{\text{H}}(\text{CDCl}_3)$ 9.15 (2H, s, CHO) 9.00 (16H, s, Ar-H); 8.98 (16H, s, Ar-H); 8.96 (40H, m, Ar-H); 7.50 (144H, m, Ar-H); 7.30 (216H, m, Ar-H); 6.30 (4H, d, Ar-H); 2.89 (32H, m, Ar-H); 2.57 (4H, d, Ar-H) $\nu_{\max}/\text{cm}^{-1}$ (KBr)1690 (CO)

- Chapter 3 -

3.4.3 Microwave synthesis

Microwave irradiations were carried out in a Defy DM206T microwave oven at 800W power.

The general procedure for the microwave syntheses was as follows:

Solid **54** (0.01g, 7.42 μmol) was thoroughly mixed in a sample vial with an appropriate amount (Table 3) of each of the solid or liquid compounds to be used as axial ligands using a spatula. The reagents for compounds **62**, **63**, **60**, **64** and **69** were placed in an alumina bath for irradiation while the reagents for compounds **61** and **68** were irradiated in the sample vials. The irradiation was done at 800W and the times are given in Table 3. After the reaction was complete (tlc) the mixtures were worked up as follows: For compounds **62**, **63**, **60** and **64** the compounds were purified by washing with 10% NaOH until no more naphthol or phenol could be detected. The residual solids were washed with water (3x10ml) and extracted into chloroform. The chloroform was dried with anhydrous MgSO_4 , filtered and the product was isolated by evaporation of the chloroform under reduced pressure. Compounds **61** and **68** were isolated by washing with water (3x20ml) to remove residual alcohols. The solid products were dried at 60°C under vacuum. For **69** it was necessary to separate the chloroform extract of the reaction mixture on preparative TLC

- Chapter 3 -

plates with chloroform as eluent. The yields of these reactions are given in Table 3.

-Chapter 4-

Conclusions and Future perspectives

Various axially substituted silicon phthalocyanines were easily prepared by various methods in high yield. A primary objective in the synthesis of these compounds was to obtain a high degree of isomeric purity and this was achieved by using disubstituted phthalonitriles that led to a phthalocyanine that was a single isomer. This isomeric purity was preserved upon attachment of the axial ligands as witnessed by the UV-visible spectra and the well-defined ^1H -NMR spectra. The synthesis of the oligomeric silicon phthalocyanines was surprisingly easy to achieve, but the yields were relatively low. This study revealed an interesting process of axial ligand exchange upon irradiation of the molecules in solution. This exchange may have implications for the silicon phthalocyanines *in vivo* as all the axial ligands were exchanged for hydroxyl groups. The geometry of the axial ligand bond to the silicon central metal was of importance in terms of the rate of axial ligand exchange. The dihydroxyl silicon phthalocyanine **55** photodegrades upon continued irradiation without a singlet oxygen quencher being present indicating the role of singlet oxygen in the degradation of this compound.

All the studied compounds generate singlet oxygen in oxygen-containing solutions. The peripheral phenoxy groups seem to halve the singlet oxygen quantum yields compared to peripherally unsubstituted silicon phthalocyanines but still generate enough singlet oxygen to be useful in PDT. Axial alkyl chains seem to enhance singlet oxygen generation as seen in this study and also

-Chapter 4-

by the work of Kenney et. al. wherein his PC-4 compound is a very useful PDT sensitiser.

There is no direct relation between the triplet quantum yields or the triplet lifetimes and the singlet oxygen quantum yields of these compounds. The triplet lifetimes, in fact, are almost twice as long as their peripherally unsubstituted counterparts and this is in contrast to the singlet oxygen quantum yield values. The fluorescence quantum yields are relatively high and thus may be valuable in tumour imaging applications. Fluorescence lifetimes showed excellent correlation between the theoretical Strickler-Berg equation and the experimentally determined fluorescence lifetimes. The only exceptions were the aggregated compounds **54** and **55**. Electrochemical characterisation of several of these compounds revealed redox potential dependence upon the nature of the axial ligands electron donating or electron withdrawing capabilities. Differing electrode surface interactions with these compounds led to 3 different types of electrochemical behaviour. In terms of the PDT application these compounds thus show excellent potential for use as sensitisers and also as imaging agents for tumour detection due to their excellent fluorescence properties. Future work on these compounds may entail further structure – activity correlation in terms of *in vivo* experimentation. Structural modifications may also be considered so that the axial ligand is used as a ‘magic bullet’ to target tumour cells more selectively.

- References -

- 1 Lever, A.B.P., *Adv. Inorg. Chem. Radiochem.*, **7**, 27 (1965)
- 2 Leznoff, C.C. in *Phthalocyanines; Properties and Applications (Vol. 1)*, Eds. Leznoff, C.C. and Lever, A.B.P., VCH, New York, p399 (1989)
- 3 Moser, F.H., Thomas, A.L., *The Phthalocyanines (Vol. 2)*, CRC Press, Florida, p1 (1983)
- 4 Braun, A. Tcherniac, *J. Ber. Deut. Chem. Ges*, **40**, 2709 (1907)
- 5 Byrne, G.T. Linstead, R.P. Lowe, *R. J. Chem. Soc.*, 1017, (1934)
- 6 Linstead, R.P., Lowe, A.R., *J. Chem. Soc.*, 1022 (1934)
- 7 Joyner, R.D., Cekada, J., Linck, R.G. and Kenney, M.E., *J. Inorg & Nuclear Chem.*, **15**, 387 (1960)
- 8 Lowery, M.K., Starshak, A.J., Esposito, J.N., Krueger, P.C. and Kenney, M.E., *Inorg. Chem.*, 128 (1964)
- 9 Kreuger, P.C. and Kenney, M.E., *J. Org. Chem.*, **28**, 3379 (1963)
- 10 Hanack, M. and Lang, M., *Adv. Mater*, **6**, 819 (1994)
- 11 Shutt, J.D., Batzel, D.A., Sudiwala, R.V. and Kenney, M.E., *Langmuir*, **4** 1240 (1988)
- 12 Wöhrle, D., in *Phthalocyanines: Properties and Applications (Vol. 1)*, Eds. Leznoff, C.C. and Lever, A.B.P., VCH, New York (1989)
- 13 Li, Z., and Lieberman, M., *Supramolecular Sci.*, **5**, 485 (1998)
- 14 Aoudia, M., Cheng, G., Kennedy, V.O., Kenney, M.E. and Rodgers, M.A.J., *J. Am. Chem. Soc.*, **119**, 6029 (1997)
- 15 Joyner, R.D., and Kenney, M.E., *Chem. Eng. News*, **40**, 42 (1962)
- 16 Haisch, P. and Hanack, M., *Synthesis*, 1251 (1995)
- 17 Kliesch, H., Weitemyer, A., Müller, S. and Wöhrle, D., *Liebigs. Ann.*, 1272 (1995)
- 18 Kohn, M., *J. Am. Chem. Soc.*, **73**, 480 (1951)

- References -

- 19 Hanack, M., Gul, A., and Hirsch, A., *Mol. Cryst. Liq. Cryst*, **187**, 365 (1990)
- 20 Derkacheva, V.M. and Luk'yanets, *Zh. Obshch. Khim.*, **50**, 2313 (1980)
- 21 Wöhrle, D., Schnurpfeil, G. and Knothe, G., *Dyes and Pigments*, **18**, 97 (1992)
- 22 Brach, P.J., Grammatica, S.J., Ossanna, O.A. and Weinberger, L., *J. Heterocyclic. Chem.*, **7**, 1403 (1970)
- 23 Pawlowski, G. and Hanack, M., *Synthesis*, 287 (1980)
- 24 Bryant, G.C., Cook, M.J., Ryan, R.G., and Thorne, A.J., *Tetrahedron*, **52**, 809 (1996)
- 25 Cook, M.J., *J. Mater. Chem.*, **6**, 677 (1996)
- 26 Metz, J., Schneider, O., and Hanack, M., *Inorg. Chem.*, **23**, 1065 (1984)
- 27 Rafaeloff, R., Kohl, F.J., Kreuger, P.C. and Kenney, M.E., *J. Inorg. Nucl. Chem.*, **28**, 899 (1965)
- 28 Joyner, R.D. and Kenney, M.E., *Inorg. Chem.*, **1**, 236 (1962)
- 29 Eaborn, C., in *Organosilicon compounds*, Academic Press, New York, N.Y., p100 (1960)
- 30 He, J., Larkin, H.E., Li, Y.S., Rihter, B.D., Zaidi, S.I.A., Rodgers, M.A.J., Mukhtar, H., Kenney, M.E., and Oleinick, N.L., *Photochem. Photobiol.*, **65**, 581 (1997)
- 31 Silver, J., Sosa-Sanchez, J.L., and Frampton, C.S., *Inorg. Chem.*, **37**, 411 (1998)
- 32 Chen, H.Z., Wang, M. and Yang, S., *J. Polym. Sci. A: Polym. Chem*, **35**, 959 (1997)
- 33 Shirk, J.S., Pong, R.G.S, Bartoli, F.J, and Snow, A.W., *Appl. Phys. Lett.*, **63**, 1880 (1993)
- 34 Mandal, B.K., Sinha, A.K., and Kamath, M., *J. Polym. Sci. A: Polymer Chemistry*, **34**, 643 (1996)
- 35 Owen, J.E., Kenney, M.E., *Inorg. Chem.*, **1**, 334 (1962)

- References -

- 36 Sounik, J.R., Norwood, R.A., Popolo, J., Holcomb, D.R. and Ghatani, S.S., *J. Appl. Polym. Sci.*, **53**, 677 (1994)
- 37 Gedye, R.N., Smith, F.E., and Westaway, K.C., *Tetrahedron Lett.*, **27**, 279 (1986)
- 38 Hwang, D.R., *J. Chem. Soc., Chem. Commun.*, 1799 (1987)
- 39 Patil, D., Mutsuddy, B. and Garard, R., *J. Microw. Power. Electromagn. Eng.*, **27**, 49 (1992)
- 40 Loupy, A., Petit, A., Ramdani, M., Yvanaeff, C., Majdoub, M., Labiad, B. and Villemin, D., *Can. J. Chem.*, **71**, 90 (1993)
- 41 Alvarez, C., Delgado, F., Garcia, O., Medina, S. and Marquez, C., *Synth. Commun.*, **21**, 619 (1991)
- 42 Chemat, F., Poux, M. and Berlan, J., *J. Chem. Soc. Perkin Trans.2*, 2597 (1994)
- 43 Villemin, D., and Labiad, B., *Synth. Commun.*, **20**, 3333 (1990)
- 44 Bram, G., Loupy, A., and Madjoub, M., *Tetrahedron*, **46**, 5167 (1990)
- 45 Villemin, D., and Alloum, A.B., *Synth. Commun.*, **21**, 63 (1991)
- 46 Villemin, D., Martin, B., and Garrigues, B., *Synth. Commun.*, **23**, 2251 (1993)
- 47 Jinchang, D., Hengjie, G., Jinzhu, W., and Caizhen, L., *Synth. Commun.*, **24**, 301 (1994)
- 48 Abenhaim, D., Ngoc-Son, C., Loupy, A., and Ba-Hiep, N., *Synth. Commun.*, **24**, 1199 (1994)
- 49 Villemin, D., and Martin, B., *J. Chem. Res. (S)*, 146 (1994)
- 50 Bram, G., Loupy, A., Madjoub, M., and Petit, A., *Chem. Ind (London)*, 396 (1991)
- 51 Pilard, J.F., Klein, B., Texier-Boullet, F., and Hamelin, J., *Synlett*, 219 (1992)
- 52 Shabaani, A., *J. Chem. Res.*, 672 (1998)

- References -

- 53 Ungurenasu, C., *Synthesis*, **10**, 1729 (1999)
- 54 Bown, S.G., *J. Photochem. Photobiol. B: Biol.*, **6**, 12 (1990)
- 55 Raab, O. *Z. Biol*, **39**, 524 (1900)
- 56 Auler, H. and Banzer, G. *Z. Krebsforsch*, **53**, 65 (1942)
- 57 Bellnier, D., Ho, K. and Pandey, R.K., *Photochem. Photobiol.*, **50**, 221 (1989)
- 58 Phillips, D., *Science Progress*, **77**, 300 (1993/94)
- 59 Kongshaug, M., Moan, J. and Brown, S.B., *Br. J. Cancer*, **59**, 184 (1989)
- 60 Reddi, E., Zhou, C., and Biolo, R., *Br. J. Cancer*, **61**, 407 (1990)
- 61 Kessel, D., *Photodynamic therapy of Neoplastic Diseases*, CRC Press, Vol II, p.117 (1990)
- 62 Morgan, J., Lottman, H. and Abbou, C.C., *Photochem. Photobiol.*, **60**, 486 (1994)
- 63 Klyashchitsky, B.A., Nechaeva, T.S. and Ponomaryov, G.V., *J. Controlled Release*, **29**, 16 (1994)
- 64 Chan, W.S., Marshall, J.F, *Cancer. Res.*, **48**, 3044 (1988)
- 65 Henderson, W.H., Dougherty, T.J., *Photochem. Photobiol.*, **55**, 147 (1992)
- 66 Kessel, D., Thompson, P., Saatio, K. and Nantwi, K.D., *Photochem. Photobiol.*, **45**, 787 (1987)
- 67 Edwards, L. Gouterman, M. *J. Mol. Spectr.*, **33**, 293 (1970)
- 68 Boyle, R.W., van Lier, J.E., *Synthesis*, 1079 (1995)
- 69 Phillips, D., *Photochemistry of sensitizers for PDT*. Proceedings of IUPAC Conference on Photochemistry, Prague (1994)
- 70 Atkins, P.W., *Physical Chemistry (5th Ed.)*, Oxford University Press, Oxford, p211 (1994)

- References -

-
- 71 Rosenthal, I. and Ben-Hur, E., in *Phthalocyanines; Properties and Applications*, Eds. Leznoff, C.C. and Lever, A.B.P., VCH, New York, p400 (1989)
- 72 Dougherty, T.J., Pottery, W.R., and Weishaupt, K.R., *Porphyrin Localization and Treatment of Tumours*, Liss, New York, (1984)
- 73 Kessel, D., *Photochem. Photobiol.*, **39**, 851 (1984)
- 74 Wegner, E.E., and Adamson, A.W., *J. Am. Chem. Soc.*, **88**, 394 (1966)
- 75 Gaspard, S., and Viovy, R., *J. Chem. Phys.*, **76**, 571 (1979)
- 76 Butler, J., Hodgson, B.W., Hoey, B.Y., Land, E.J., Lea, J.S., Lindey, E.J., Rushton, F.A.P., and Swallow, A.J., *Radiat. Phys. Chem.*, **34**, 633 (1989)
- 77 Kraljic, I., and Mohsni, S.E., *Photochem. Photobiol.*, **39**, 851 (1984)
- 78 Mosinger, J., and Micka, Z., *J. Photochem. Photobiol. A: Chemistry*, **107**, 77 (1997)
- 79 M.K. Boyd in *Organic Photochemistry*, Ed. V.Ramamurthy, K.S. Schanze. Marcel Dekker, Inc., New York (1997)
- 80 Spikes, J.D., *Photochem. Photobiol.*, **55**, 797 (1992)
- 81 Cox, G.S., Krieg, M., Whitten, D.G., *J. Am. Chem. Soc.*, **104**, 6930 (1982)
- 82 Mang, T.S., Dougherty, T.J., *Photochem. Photobiol.*, **45**, 501 (1987)
- 83 Potter, W.R., Mang, T.S., Dougherty, T.J., *Photochem. Photobiol.*, **46**, 96 (1987)
- 84 Hongying, Y., Fuyuan, W., and Zhiyi, Z., *Dyes and Pigments*, **43**, 109 (1999)
- 85 Barltrop, J.A. and Coyle, J.D., *Principles of Photochemistry*, John Wiley & Sons, p21 (1990)
- 86 Roth, N. J. L. and A. C. Craig, *J. Phys. Chem.*, **78**, 1154 (1974)
- 87 Ingle, J. D. Jr. and Crouch, S.R. in *Spectrochemical Analysis*, Prentice Hall, N. J. (1988)
- 88 Strickler, S.J., and Berg, R.A., *J. Chem. Phys.*, **37**, 814 (1962)

- References -

- 89 Ware, W. R. and B. A. Baldwin, *J. Chem. Phys.*, **40**, 1703 (1964)
- 90 Lacey, J.A., Phillips, D., Milgrom, L.R., Yahioğlu, G. and Rees, R.D., *Photochem. Photobiol.*, **67**, 97 (1998)
- 91 Jacques, P., Braun, A.M., *Helv. Chim. Acta*, **64**, 1800 (1981)
- 92 Bensasson, R., Goldschmidt, C.R., Land, E., and Truscott, T.G., *Photochem. Photobiol.*, **28**, 277 (1978)
- 93 Bensasson, R., Goldschmidt, C.R., Land, E., Truscott, T.G., *Photochem. Photobiol.*, **28**, 281 (1978)
- 94 Wang, J., *Analytical Electrochemistry*, 1st Ed., VCH, New York 1 (1994)
- 95 Nyokong, T., *S. Afr. J. Chem.*, **48**, 23 (1995)
- 96 Nyokong, T., *Polyhedron*, **12**, 375 (1993)
- 97 Fu, Y., Fu, G. and Lever, A.B.P., *Inorg. Chem.*, **33**, 1038 (1994)
- 98 Ferraudi, G., in Leznoff, C.C. and Lever, A.B.P., *Phthalocyanines, Properties and Applications (Vol. 1)*, VCH, New York, p311 (1989)
- 99 Limson, L.J., Ph.D. Thesis, Rhodes University, Grahamstown (1998)
- 100 Wheeler, B.L., Nagasubramanian, G., Bard, A.J., Schechtman, L.A., Dininny, D.R. and Kenney, M.E., *J. Am. Chem. Soc.*, **106**, 7407 (1984)
- 101 Gaspard, S. and Maillard, P., *Tetrahedron*, **43**, 1083 (1987)
- 102 Wöhrle, D., Gitzel, J., Okuro, I. and Aono, S., *J. Chem. Soc. Perkin Trans. 2*, 1172 (1985)
- 103 Leznoff, C.C., Hu, M., McArthur, R., Qin, Y., van Lier, J.E., *Can. J. Chem.*, **72**, 1992 (1994)
- 104 Duggan, P.J. and Gordon, P.F., *Chem. Abstr.*, **105**, 72642 (1987)
- 105 Homborg, H., and Murray, K.S., *Z. Anorg. Allg. Chem.*, **149**, 517 (1984)
- 106 Sugimoto, H., Higashi, T., and Mori, M., *J. Chem. Soc., Chem. Commun.*, 622 (1983)

- References -

-
- 107 Turek, P., Andre, J.J., Giraudeua, A., and Simon, J., *Chem. Phys. Lett.*, **134**, 471 (1987)
- 108 Cook, M.J., Dunn, A.J., Howe, S.D. and Thomson, A.J., *J. Chem. Soc., Perkin Trans. I*, 2453 (1988)
- 109 Kovshev, E.I. and Luk'yanets, E.A., *J. Gen. Chem. USSR*, **42**, 1584 (1972)
- 110 Kobayashi, N., in Leznoff, C.C. and Lever, A.B.P., *Phthalocyanines, Properties and Applications (Vol. 2)*, VCH, New York, p117 (1993)
- 111 Wöhrle, D., Eskes, M., Shigehara, K. and Yamada, A., *Synthesis*, 194 (1993)
- 112 Silver, J., Sosa-Sanchez, J.L. and Frampton, C.S., *Inorg. Chem.*, **37**, 411 (1998)
- 113 Sounik, J.R., Holcomb, D.R., *J. Appl. Polym. Sci.*, **53**, 677 (1994)
- 114 Lowery, M.K., Starshak, A.J., Esposito, J.N., Krueger, P.C. and Kenney, M.E., *Inorg. Chem.*, 128 (1963)
- 115 Joyner, R.D. and Kenney, M.E., *Inorg. Chem.*, **1**, 236 (1962)
- 116 Kraus, G.A. and van der Louw, S.J., *Synlett*, 726 (1996)
- 117 Krueger, P.C. and Kenney, M.E., *Inorg. Chem.*, **28**, 3379, (1963)
- 118 Macdonald, I.J. and Dougherty, T.J., *J. Porphyrins Phthalocyanines*, **5**, 105 (2001)
- 119 Ochsner, M., *Eur. J. Med. Chem.*, **31**, 939 (1996)
- 120 Shabaani, A., *J.Chem.Res.*, 672 (1998)
- 121 Ungurenasu, C, *Synthesis*, **10**, 1729 (1999)
- 122 Kobayashi, N., Sasaki, N., and Konami, H., *Inorg. Chem.*, **36**, 5674 (1997)
- 123 Decrau, R., Julliard, M. and Giorgi, M., *Acta.Cryst.*, **C55**, 1717 (1999)
- 124 Mandal, B.K., Sinha, A.K. and Kamath, M., *J. Polym. Sci. A.*, **34**, 643 (1996)

- References -

- 125 Krueger, P.C. and Kenney, M.E., *Inorg. Chem.*, **28**, 3379, (1963)
- 126 Lukyanets, E., *J. Porphyrins Phthalocyanines*, **3**, 424 (1999)
- 127 Zhang, X., Xu, H., *J. Chem. Soc. Faraday Trans.*, **89**, 3377 (1993)
- 128 Joyner, R.D. and Kenney, M.E., *Inorg. Chem.*, **1**, 236 (1962)
- 129 Li, Z., Lieberman, M., *Supramolecular Sci.*, **5**, 485 (1998).
- 130 Mortimer, C.T., *Reaction heats and bond strengths*, Pergamon press, New York, p185 (1962)
- 131 Morrison, R.T., and Boyd, R.N., *Organic Chemistry(4th Ed.)*, Allyn and Bacon, London (1983)
- 132 Pelmeshnikov, A., Stzandh, H., Pettersson, L., Leszezynski, J., *J. Phys. Chem. B.*, **107** 5779 (2000)
- 133 Ferraudi, G., in *Phthalocyanines: Properties and Applications (Vol.1)*, eds. Leznoff, C.C. and Lever, A.B.P., VCH, New York, p 320 (1989)
- 134 Kuznetsova, N.A., Kaliya, O.L., *Russ. Chem. Rev.*, **42**, 36 (1998).
- 135 Boyd, M.K. in *Organic Photochemistry*, Ed. Ramamurthy, V., Schanze, V., Marcel Dekker, Inc., New York, p180 (1997)
- 136 Schnurpfeil, G., Sobbi, A., Spiller, W., Kliesch, H., Wöhrle, D., *J. Porphyrins Phthalocyanines*, **1**, 159 (1997)
- 137 Firey, P.A., Ford, W.E., Sounik, J.R., Kenney, M.E. and Rodgers, M.A.J., *J. Am. Chem. Soc.*, **110**, 7626 (1988)
- 138 Daziano, J., Steenken, S., Chabannon, C., Mannoni, P., Chanon, M.,Julliard, M., *Photochem. Photobiol.*, **64**, 712 (1996)
- 139 He, J., Larkin, H.E., Li, Y., Rihter, B.D., Zaidi, S.A.I., Rodgers, M.A.J., Mukhtar, H., Kenney, M.E., and Oleinick, N.L., *Photochem. Photobiol.*, **65**, 581 (1997)
- 140 Lever, A.B.P., Milaeva, E.R., Speier, G. in *Phthalocyanines: Properties and Applications, Vol. 3*. Leznoff, C.C., Lever, A.B.P. (eds)., VCH, New York, Ch. 5 (1993)

- References -

- 141 Latimer, P., Bannister, T.T. and Rabinowitch, E., *Science*, **124**, 585 (1958)
- 142 Seybold, P.G. and Gouterman, M., *J. Mol. Spectrosc.*, **31**, 1 (1971)

